Blocking murine chronic graft versus host disease at different biological phases

A Dissertation
SUBMITTED TO THE FACULTY OF
UNIVERSITY OF MINNESOTA
BY

Jing Du

IN PARTIAL FULFILLMENT OF THE REQUIREMENTS
FOR THE DEGREE OF
DOCTOR OF PHILOSOPHY

Dr. Bruce R. Blazar, M.D.

Sep 2017

Acknowledgments

I am deeply grateful to the University of Minnesota and the CMB PhD program for offering me the opportunity to study in this great place. It has been a wonderful learning experience.

I would like to thank all the current and past members in the Blazar lab. The time spend with all of you has been a substantial part of my life during the past 5 years. I will forever grateful for all the help, encouragement and inspiration you give me in every way you did! Katelyn Paz has been an excellent co-worker and friend. She is always generous with her support and encouragement. Govindarajan Thangavelu has been a great resource for my questions and he is always willing to share what he knows. The time we spent together will always be treasured in my memory: Ryan Flynn, Cameron McDonald Hyman, Rachelle Veenstra, Michelle Smith, Brent Koehn, Asim Saha, Dawn Reichenbach, Pat Taylor, Jemma Nicholls, Michael Loshi, Michael Zaiken, Melanie Schaechter, Randy Donelson and Colby Feser. You have all made my PhD experience rich and vivid.

I would like to express my deepest gratitude to my advisor Dr. Bruce Blazar. He has been an excellent role model for me to learn from. He is extremely knowledgeable, efficient, and always willing to help. He has been patiently helping me grow and become a better researcher.

I cannot thank enough for the people who are there to make sure everything runs smoothly. LeAnn Micek, thanks for taking care of the whole lab so that we can focus on research. Lisa Hubinger, thanks for gathering and passing all those helpful information to me and rescuing me from things like late registration and picking up wrong courses. Jamie Panthera, thanks for taking good care of our lab animals and always keep the inventory up to date.

I would like to thank my research committee, Dr. Bruce Walcheck, Dr. Jeffrey Miller, Dr. Michael Murtaugh, for contributing your wisdom and time to my research projects.

I would like to thank my families, including my mother, father, sister, brother in law and my nieces for always giving me your unconditional support and encouragement through all my difficult times. Although being more than 6,000 miles away, you always find a way to let me feel your love, care and support.

Finally, I'd like to thank my husband and best friend Pan Liu. Thanks for being an awesome person and wonderful husband. Without you, I could not have completed this.

Dedication

This dissertation is dedicated to the memory of my father Ronggui Du.

Abstract

Allogeneic hematopoietic stem cell transplantation (aHSCT) is the only curative option for many otherwise incurable diseases such as hematopoietic malignancies and genetic disorders. However, chronic Graft-Versus-Host Disease (cGVHD) is commonly seen in long-term survivors of aHSCT and has become the leading cause of non-relapse mortality. Little improvement has been made to the clinical management of cGVHD in several decades, which relies on systemic immunosuppression that is often associated with complications. This is expected to change with updated understanding of cGVHD pathogenesis brought by the development of several new murine models. It is broadly accepted that cGVHD development undergoes 3 biological phases: 1. Tissue damage and innate immune activation leading to donor T cells activation, 2. Compromised immune tolerance and disturbed immune reconstitution leading to autoimmunity, 3. Aberrant tissue repair and autoantibody deposition leading to activation of pro-fibrotic pathways. In this study, we sought to explore approaches to block cGVHD through the inhibition of each biological phase of cGVHD. First, we demonstrated that donor T cells allo responses is dependent on a Ca^{2+} dependent inositol trisphosphate 3-kinase B (Itpkb) – an enzyme downstream of T cell receptor activation and functions through regulation of intracellular Ca^{2+} level. Blocking Itpkb by genetic ablation or pharmacological inhibition completely blocked or attenuated cGVHD in 2 different cGVHD models with complementary clinical manifestations. Second, we demonstrated that the deregulated immune balance could be restored by infusion of a potent regulatory cell population, the invariant Nature Killer T cells (iNKTs). iNKT infusion expanded Treg population in a

CXCR5 and IL-4 dependent manner and restored the T follicular helper/regulatory balance. Third, we demonstrated that pulmonary fibrosis as a result of end organ damage during cGVHD could be reversed by Pirfenidone, a drug approved by FDA for idiopathic pulmonary fibrosis. The effect was associated with reduced macrophage infiltration and TGF-β production. Finally, to identify cGVHD biomarkers for cGVHD early diagnosis and treatment, we conducted full spectrum proteomic analysis of serum samples from the well-established murine multi-organ system cGVHD model with bronchiolitis obliterans syndrome (BOS). Using high throughput, discovery-based Mass Spectrometry (MS) technique, we identified 4 potential biomarkers of cGVHD, of which CCL15 proved druggable and was verified in highly characterized and previously reported patient cohorts. Collectively, this work identifies several potential therapeutic targets and a verified biomarker that may improve cGVHD clinical management and diagnosis. In addition, this work provides new insights into cGVHD pathogenesis.

Table of Contents

List of Abbreviations

APC	Antigen Presenting Cell
aHSCT	Allogenic hematopoietic stem cell transplantation
BAFF	B-cell Activating Factor
BCR	B-cell Receptor
BM	Bone Marrow
BMT	Bone Marrow Transplant
BO	Bronchiolitis Obliterans
Btk	Bruton's Tyrosine Kinase
CRK	CRK proto-oncogene, adaptor protein
CRKL	CRK like protein
CCL	Chemokine (C-C motif) ligand
CXCL	Chemokine (C-X-C motif) ligand
CCR	CC chemokine receptor
CXCR	CXC chemokine
Cy	Cyclophosphamide
FDA	Food and drug administration
GC	Germinal Center
GVHD	Graft-versus-Host disease
H-Y	Male Histocompatibility
Ig	Immunoglobulin
IL	Interleukin
INKT	invariant natural killer T
IP3	Inositol 1,4,5-trisphosphate
IP4	Inositol 1,3,4,5- tetrakisphosphate
ITK	Interleukin-2 Inducible Kinase
ITPKB	Inositol 1,4,5-trisphosphate 3-kinase B
KO	Knockout
LTβR	Lymphotoxin Beta Receptor

mAb	Monoclonal Antibody
MHC	Major Histocompatibility Complex
MiHA	Minor Histocompatibility Antigen
MS	Mass Spectrometry
PDGF	Platelet Derived Growth Factor
PD-1	Programmed Death Protein 1
PNA	Peanut Agglutinin
SRBC	Sheep red blood cell
Syk	Spleen Tyrosine Kinase
TBI	Total Body Irradiation
TCR	T cell receptor
Tfh	T Follicular Helper
TGF-β	Transforming growth factor beta
Th	T Helper
Treg	T Regulatory
WT	Wild Type

List of Tables

Chapter 5:

List of Figures

Chapter 1

Chapter 2

Chapter 3

Chapter 4

Chapter 5

Chapter 6

Chapter 1 Introduction

1.1 History of bone marrow transplantation and graft versus host disease

The origin of stem cell transplantation dates backed to 1950s and was closely linked with the development of techniques using radioactive materials. During the 1910s and 20s, radioactive compounds were becoming increasingly used in the workplace in a way that no protection was taken into consideration and used. Consequently, a higher incidence of leukemia and other diseases was observed in those workers. However, only a small number of people had been affected by the radiation and the cause of their deaths only became apparent much later after their death. Thus, doctors could not generate useful conclusions regarding why the diseases happen and how to prevent them. Later, the rapid progress on radiation research had ultimately led to the invention of nuclear bomb which caused thousands of death in Japan during world war II, not only from the blast of bomb explosion, but also from the intense nuclear radiation. Doctors and researchers had the unfortunate opportunity to observe tens of thousands of patients and gain a more comprehensive understanding of how "radiation sickness" progressed in humans and which regions of the body were most affected. Doctors had gradually realized that radiation exposures of the bones cause the loss of blood cells. This observation triggered the desire to restore bone marrow function in aplasia caused by radiation exposure in human.

At the same time, researchers were using animal models to understand the effect of radiation on health and disease. In a pivotal experiment, Jacobsen (1949) and colleagues

cite ref in bibliography documented that hematopoiesis was preserved in mice after lethal irradiation if the spleen was shielded. He further demonstrated a similar protective effect by shielding the femur, establishing that bone marrow and spleen are organs to produce and/or store blood cells. Lorenz (1951) and colleagues[1] later demonstrated that mice recovered from radiation injury when infused with bone marrow after a lethal dose of radiation. It was uncertain that whether the protective effect is from humoral or cellular factors. However, subsequent work established bone marrow as the source of "cellular elements" required for hematopoietic recovery. Ford et al[2] (1956) reported that lethally irradiated mice were protected by a subsequent marrow infusion, and Nowell et al[3] (1956) demonstrated the presence of rat cells in the marrow of irradiated mice that are protected against lethal irradiation by rat marrow. These studies established that bone marrow contains cells that have the ability of making blood cells, what we now know as the hematopoietic stem cells.

Accumulating studies in rodent models of bone marrow transplantation led to initial attempts at translating the discovery into the clinic. In 1957, Thomas ED reported temporary recovery after intravenous infusion of BM in patients receiving radiation and chemotherapy[4]. Later, he demonstrated hematopoietic recovery after autologous BM transplantation between identical twins following high dose radiation (1000 cGray)[5]. However, most bone marrow transplantations at that time were before the knowledge of histocompatibility antigen and HLA genotyping, and the grafts were mostly from siblings or un-related donors. Not surprisingly, almost all the early clinical transplantation efforts

in the late 1950s and early 1960s failed. In many cases the graft was rejected, and, if the graft was accepted, patients developed severe “secondary disease” that led to death. Billingham[6] (1959) and colleagues described an immune reaction characterized by rash, diarrhea after bone marrow infusion, which they called "Runt disease" or what is now known as Graft Versus Host Disease (GVHD), the result of an immune reaction of the engrafted lymphoid cells against the tissues of the host. Thus, the idea of BMT was almost abandoned by the doctors at that time. However, research on animals continued and researchers realized that procedures based on inbred mice cannot directly transfer to human. Research done on outbred animals such as dogs and primates eventually relighted the hope of using BMT to treat diseases. New methods of host immunosuppression and myelosuppression involving chemotherapeutic agents such as cyclophosphamide and busulphan, respectively, were developed. Techniques for isolating the grafts from peripheral blood and bone marrow were improved. Agents to combat graft rejection were further refined in the dog transplantation model.

In 1968 in Minnesota, the first successful allogeneic transplant was performed[7]. The donor was a sibling of the patient. By this time, it was known that genetic matching (known as HLA) is the key to a successful transplant. A sibling is the most likely person to be a good match as they inherited DNA from the same parents and can be fully matched for HLA antigens. Having a closely matched donor can help reduce the possibility of developing GVHD. However, many people do not have a sibling who is HLA-matched. In this situation, an HLA-matched unrelated donor can be used. The first

successful unrelated donor transplant took place in 1973 in New York when a young boy with a genetic immunodeficiency disorder received multiple marrow transplants from a donor identified as a match through a blood bank in Denmark[8]. In 1986, the National Bone Marrow Donor Registry was federally funded in Seattle. Stem cell transplantation has been increasingly performed each year world wide for a long list of different diseases[9–13]. However, GVHD, especially cGVHD continues to a significant burden for long-term survivors of transplant patients[14,15]

1.2 Murines models of cGVHD

Mice are the most widely used animals for many areas of biomedical researches. Compared with other research animals that are being used, mice have several advantages[16]. First, large number of mice with same genetic background can be maintained in similar environment in relatively low cost. This is desirable for getting solid repeatable conclusions. Second, gene-editing techniques on mice are more mature than other research animal species. Thus the use of genetically modified mice has been promoting researches in gene function study and facilitating certain assays (luciferase expressing mice). Third, the handling of mice is relatively easier than other animals so that lab personals can gain the ability of working on mice quickly. Studies conducted on mice have identified many factors that are responsible for the success or failure of a BMT. Murine model of cGVHD are generally categorized into the following types based on the phenotypes and underlying immunologic mechanisms: 1. Autoimmunity driven by B cell mediated autoantibody production leading to systemic lupus erythematosus (SLE)

like disease – the SLE model. 2. Pro-fibrotic pathways activation that result in sclerodermatous like disease - the Scl model. 3. Germinal center response driven systemic fibrosis with bronchiolitis obliterans (BO)- the BO model.

The SLE models mimic the autoimmune features of human cGVHD and have been useful in study both human lupus and cGVHD. In the SLE-cGVHD models, immune cells from MHC-mismatched donors are adoptively transferred to recipients. In a typical setting, parent peripheral immune cells are infused to non-irradiated F1 recipients. The resulting phenotype is predominated by the generation of autoantibodies directed against dsDNA, ssDNA and chromatin and immune-complex glomerulonephritis[17–20]. Involvement of lung has also been reported in several studies[21]. Mechanism that leads to autoantibody production is described as CD4 T cells activation by B cells as antigen presenting cell (APC) and B cell activation and maturation with the help of CD4 T helper cells. The role of CD8 T cells is much smaller in the pathogenesis of these models. Although the SLE models have contributed to the understanding of cGVHD pathogenesis, especially in the establishment the roles of B cells and autoantibodies, there are many shortcomings. For example, the use of peripheral blood cells rather than stem cells and the lack of conditioning regimen on recipients are obviously not mimicking human BMT, while these factors can have major effects on the outcome of BMT. In addition, although these models have the autoimmune features seen in cGVHD patients, the specificities of autoantibodies identified in human patients are a lot more heterogeneous, suggesting the more complex immunological mechanism are taking place in human.

The Scl model uses donor and recipient combination that differs only at the minor histocompatibility loci but is MHC matched. The most common strain combination is B10.D2 (H2d) into Balb/c (H2d) model. In a typical experiment, Balb/c recipients are conditioned by irradiation followed by transplanting B10.D2 bone marrow and un-fractioned splenocytes or purified T cells. Fur loss, skin thickening and scleroderma can be noticed 3-week post-BMT. Weight loss that is proportional to donor T cell dose usually accompanies skin disease, suggesting a systemic effect of the disease. Indeed, fibrotic change in the liver, lung and gastrointestinal track are also noticed[22].

Histologically, disease mice loss dermal fat and hair follicles are destroyed[22]. Different from the skin lesion caused by acute GVHD, skin thickening, but not cytotoxic epithelial injury, is the predominant manifestation of Scl GVHD, as the epidermis is intact, without significant numbers of apoptotic keratinocytes, a marker of cytotoxic injury[23]. Collagen deposition is increased and this is proceeded by influx of heterogeneous infiltrates of both lymphocytes and mononuclear cells including macrophages that express the M2 macrophage marker CD206[24].

Different from the SLE models that do not involve conditioning regimen, tissue damaged caused by pre-transplant conditioning plays an important role in the pathogenesis in the Scl models. Usually, recipients are irradiated by lethal dose of X-ray (700-1100 cGray). Damaged tissues release chemokines such as CCL2, CCL3 and CCL5 that recruit innate immune cells such as macrophages into the damage sites. At the same time damage

associated molecular patterns (DAMPs) released from damaged tissue activates innate immune cells and donor T cells, result in the release of pro-inflammatory cytokines such as IFN-γ, IL-1β and so on that further aggravates tissue damage. Macrophages play an important role in the development of skin scleroderma in these models. Markers of macrophage activation are increased after BMT, such as scavenger receptors MARCO and [spell out ScR-A] type I and II. MHCII molecules that are increased during antigen presentation are also increased during skin scleroderma[25]. In 2 different MHC mismatched models

(Colony Stimulating Factor (CSF) mobilized Balb/c graft to B6 recipient and B6 graft to B6D2F1 recipient) that also develop skin scleroderma as the major manifestation, Alexander et al proved that skin scleroderma is mediated by infiltrating macrophages that are donor derived and dependent on CSF-CSFR signaling M2 macrophages. Treatment with anti–CSF-1R monoclonal antibody reduced macrophage infiltration and pathology score[26].

The Scl-cGVHD models share many phenotypic features with the sclerodermatous form of human cGVHD, which is generally refractory to standard therapy. The incidence of sclerodermas cGVHD is estimated to be 3-10%, although both its incidence and severity could be increased as a result of more frequent unrelated donor transplants and the use of mobilized peripheral blood as stem cell source[27]. Although Scl-models generally parallel with a severe form of clinical cGVHD, one shortcoming of the Scl-cGHVD models is that they don't regenerate the autoimmune phenotypes seen in patients and B cells don't

seem to be required in the pathogenesis of the models. As a result, discoveries based solely on these models may not be readily translatable to human clinic.

Panoskaltsis-Mortari et al have developed a murine model that incorporates clinical relevant conditioning regimen and develops a wide spectrum of symptoms seen in patients[28,29]. In this model, B10.BR (H2k) recipients are conditioned with cyclophosphamide (120mg/kg body weight) and total body irradiation (830 Gy), followed by tail vein infusion of B6 donor T cell depleted bone marrow cells and ~70,000 purified T cells (Figure 1). Transplanted mice lose about 20% body weight at 8-weeks post BMT and have $\geqslant$80% total survival rate.

The phenotypic hallmark of this model is the development of multi-organ disease including lung, liver, tongue, spleen, thymus and colon. Fibrosis development in lung and liver can be detected as early as 4 weeks post-BMT and proceed to at least 12 weeks post-BMT. Importantly, fibrosis development in the lung results in BO, which is a late-stage complication of GVHD and happens to 6% of GVHD patients. The 5-year survival rate of BO is estimated by the National Institutes of Health to be only 10%. BO can be detected by in vivo lung function measurements using the FlexiVent measurement. This technique allows for the in vivo functional monitoring the development of disease and therapeutic effect of treatments, which is not available for other models.

The loss of pulmonary function and development of BO is mediated by donor T cells and B cells infiltration, antibody deposition, and macrophage infiltration in the peri-bronchiolar and peri-vascular area. Histologically, lungs of disease mice display peribronchiolar and perivascular cuffing and infiltration of the airway epithelium. The pathology appeared predominantly bronchiolar, with some alveolar involvement. Completely occluded bronchioles are observed in 20% of the animals in this model. The pattern of inflammation along with increased collagen deposition surrounding non-obliterated bronchioles was similar to the pathology that defines occluded bronchioles in humans[28]. In addition, TGF-β staining in these areas is also increased. TGF-β is a central player in fibrotic responses. Macrophages may be the main producer of TGF- β and the immunohistological staining of both co-localized with each other. Spontaneous germinal center reaction is the immunological hallmark of this model. Increased germinal center B cells frequency in spleen, enlarged germinal center and increased follicular help T cells and regulatory T cell ratio can been seen after 6 weeks post BMT.

This model incorporates clinical relevant pre-conditioning regimen including both cyclophosphamide and irradiation, which are commonly used in treatment protocols of blood malignancies. In addition, irradiation is commonly performed before BMT in human to enhance immune suppression and make niche for the coming donor bone marrow. In the Bo model, Cyclophosphamide exacerbates TBI-induced glutathione redox reactions in the recipients tissues, along with sublethal doses of donor T cells (to avoid aGVHD) favored the generation of cGVHD[30]. Thus, the BO model closely mimic

the pre-conditioning regimen used in human BMT. Another advantage of the BO model is that the mechanism of this model linked autoimmune and pro-fibrotic pathways, both of which are seen in human cGVHD. Using the BO model, mechanisms leading to cGVHD have been elucidated and potential drug targets and treatment methods have been identified. This includes methods that inhibit germinal center reactions such as lymphotoxin-β receptor (Lymphotoxin Beta Receptor) - immunoglobulin fusion protein, Tregs infusion and iNKTs infusion. Strategies that block B cell and T cell signaling pathways such as Ibrutinib drug targeting Bruton's tyrosine kinase (BTK) and IL-2 inducible T cell kinase (ITK) and GNF362 drug targeting Inositol-trisphosphate 3-kinase B (Itpkb) are effective in reversing cGVHD in the BO model. Pirfenidone that target the pro-fibrotic pathways show efficacy in the BO model. IL-21 is required for T follicular helper cells and germinal center B cells interactions and IL-17 is important for cGVHD pathogenesis, thus targeting Rho-associated kinase 2 (ROCK2), a regulator of IL-17 and IL-21 decreases cGVHD.

However, there are several points to take into consideration when translating experiment results from this model to human clinic. For example, the donor and recipient mouse strain in this model are MHC mismatched, while in human BMT, the majority cases are MHC matched and miHAs mismatched. The level of genetic disparities affects not only the disease severity, but also the mechanism as to how disease develops, since MHC molecule is crucial for antigen presentation. In addition, the targets of antibodies developed in this model are to be studied.

1.3 Pathogenesis of cGVHD

1.3.1 T cells

T cells play a continuous role in cGVHD pathogenesis. In the initiation stage, factors such as pre-transplant conditioning and previous aGVHD cause tissue damages and the subsequent release of pathogen associated molecular patterns (PAMPs) and damage associated molecular patterns (DAMPs). These molecules activate APCs such as macrophages, dendritic cells, and B cells. Activation of these cells results in the production of pro-inflammatory molecules that not only aggravate tissue injury, but also activate and shape donor T cells contained in the grafts as well as donor bone marrow derived T cells into different linages[31]. Various approaches that deplete donor T cells from grafts reduce the subsequent incidence and severity of chronic GVHD. These include positive selection of CD34 stem cells as well as methods to deplete T cells, such as targeting pan–T-cell antigens. T-cell depletion in vivo with antithymocyte globulin (ATG) administered in the peritransplant period reduces the incidence of cGVHD without affecting graft versus leukemia effect[32,33]. Early post-transplantation course of high-dose cyclophosphamide has been shown to reduce the incidence and severity of cGVHD[34].

Strategies that alter T cell trafficking, TCR or cytokine receptor signalings have also been explored[33]. Ibrutinib inhibits interleukin-2 (IL-2)–inducible kinase (ITK), which is highly expressed in T cells. In murine models, inhibition of both Bruton's tyrosine kinase (BTK) and ITK by ibrutinib contributed to the prevention of chronic GVHD[35]. Ruxolitinib, a

selective inhibitor of Janus kinase 1 (JAK1) and JAK2 mediate receptor-mediated signaling for a variety of proinflammatory cytokines, including interferon-γ and IL-6, and inhibition of this pathway has been shown to suppress activation and differentiation of dendritic cells as well as T cells. Inhibition of JAK1/JAK2 signaling with ruxolitinib has been shown to reduce cGVHD in murine models and human patients[36]. Targeting ROCK2 decreases cGVHD. ROCK2 is an enzyme that regulate IL-17 and IL21 by KD025 decreases cGVHD in multiple murine models[37].

During active cGVHD, T cell homeostasis is disturbed and the balance between different linages is disrupted. While aGVHD is considered as a Th1 dominant disease, the scenario of cGVHD is much more complicated. Th17 has been implicated in cGVHD pathogenesis[38]. In systemic sclerosis, a condition closely resembling scleroderma, the predominant clinical feature of cGVHD after aHSCT, fibrosis is mediated by Th17 cells infiltrating the skin and serum IL-17 levels positively correlate with disease severity[39]. Malard reported increased Th17 cells and Th17/Treg ratio in the liver biopsy of cGVHD patients[40]. An activated Th17 prone T cell subset (CD146+) is increased in a cohort of 20 aGVHD patients. In addition, $CD146^{-/-}$ donor T cells fail to induced cGVHD in the BO model[41].

1.3.2 B cells and antibodies

Several early observations on cGVHD patients pointed out that cGVHD may have autoimmune features: 1. several different types of auto-antibodies were identified from a

cohort of 40 cGVHD patients, including antibodies against both surface and intracellular antigens[42]; 2. IgM and complement were detected in the dermo-epidermal areas of cGHVD skin, but not or less in the healthy controls[43]; 3.Besides antibodies that target self-antigen, antibodies against allo-antigen have also been identified. Male HCT patients with female donors develop high titer H-Y antigen specific antibody responses 4-12 months after sex-mismatched transplantation in association with chronic GVHD[44]. The existence of circulating auto/allo-antibodies suggested a pathogenic role for B cells in cGHVD. Thus B cell targeting therapies have been extensively explored in cGHVD[45]. For example, anti-CD20 monoclonal antibody shows clinical and histological efficacies in 5 patients with refractory cGHVD[46]. Multiple phase II trials using rituximab therapy (anti-CD20 monoclonal antibody) have confirmed an important B cell role in chronic GVHD with overall rituximab response rates ranging 40-70% rate in steroid refractory cGVHD patients[47–49].

Although autoantibodies have been frequently associated with cGVHD, there have been discussions regarding the clinical significance of the autoantibodies. A cohort of 280 cGVHD patients were examined the presence of a broad array of autoantibodies in serum. Analysis shows that no significant associations were found between cGVHD activity and severity, and presence of autoantibodies[50], while another study of much smaller cohort suggested association between autoantibody and cGVHD[51]. To understand the role of antibody, Srinivasan et al transplanted mice with bone marrow from (m+s) IgMxJhD BALB/c donors. These mice are capable of generating membrane-bound IgM and

secreting IgM, but they produce and secrete >100-fold less antigen- specific IgG than similarly immunized wildtype (WT) controls. Recipients of bone marrow from these mice have significantly better pulmonary function, compared with recipients of WT bone marrow[29]. This experiment clearly showed that B cell's role in cGVHD is antibody dependent. In addition to this, Defu Zeng et al used an (Ig)Hmg1 DBA/2 mice whose B cells have normal APC and regulatory function, but cannot secrete antibodies, to prove antibody production is required for cGVHD development in the scleroderma model[52]. Adoptive transfer of cGVHD antibody to healthy mice resulted in cGVHD target tissue deposition of these antibodies[29], further supporting that antibodies play an active role in cGVHD pathogenesis. However, how these antibodies mediate cGVHD remain a question to be answered.

The differentiation of mature B cells is a dynamic and highly regulated process (illustrated in Figure 2) that includes both deletion of autoreactive B cells and positive selection of B-cell clones capable of recognizing a broad repertoire of foreign antigens. In the bone marrow, the first tolerance check point happens at the "immature B cell" stage where B cells start express functional B cell receptor IgM on the surface that can bind to antigens. If the IgM shows reactivity to self-antigen, B cells expressing that IgM will be removed from the repertoire by mechanisms such as clonal deletion, receptor editing and apoptosis[53]. In healthy individuals, B-cell development begins with the continuous production of precursor B cells in the bone marrow that are exported to the periphery as a large pool of transitional B cells. More than half of the developing B cells in the bone

marrow express autoreactive B-cell receptors (BCRs). These autoreactive B cells are usually deleted or anergized but failure of tolerance checkpoints can lead to escape from deletion of self-reactive B cells and the production of autoantibodies and autoimmune disease[54]. Auto-reactive B cells are highly B cell activating factor (BAFF) dependent. The low BAFF concentrations in B cell microenvironment are not enough to support autoimmune B cells survival in healthy individuals. However, in the setting of aHSCT and cGVHD, BAFF concentrations are significantly increased[55,56], while high levels of BAFF promote the differentiation and survival of auto-reactive B cells. In addition to increased BAFF level, the BM output of transitional and mature naive B cells are reduced during cGVHD as a result of pre-BMT conditioning, preventative immune suppression and occurrence of acute GVHD. Thus B cell reconstitution is generally slow. In contrast, patients who have normal numbers of naive and circulating transitional B cells after aHSCT are common in patients who do not go on to develop cGVHD. These observations suggest that increased BAFF/B cell ratio contributes to abnormal B-cell homeostasis characteristic of cGVHD. Thus treatments targeting B cell signaling and promoting bone marrow function recovery after BMT warrant further exploring.

In addition to elevated BAFF/B cell ratio, there is increasing evidence suggesting aberrant B cell signaling during cGVHD. B cells in cGVHD patients showed evidence of increased metabolic activity and survival, with enhanced signaling via the AKT and ERK pathways[57]. Signaling after BCR engagement by antigen entails phosphorylation and activation of the tyrosine kinase SYK (spleen tyrosine kinase), which subsequently

phosphorylates and activates the tyrosine-rich adapter protein B cell linker protein (BLNK) that is then recruited to the BCR signalosome. BLNK is central to downstream signaling, as it also acts as a docking protein for BTK, and other crucial BCR complex signaling molecules. Using anti-IgM as a surrogate for soluble antigen, Allen et al found that cGVHD B cells not only responded more robustly after exposure, but that this response was associated with increased protein levels of the proximal BCR machinery molecules SYK and BLNK[58]. The SYK inhibitor fostamatinib abrogated BCR activation and limit proliferative and survival advantage of human cGVHD B cells[58]. This finding was extended by Flynn et al, showing that SYK phophorylation is increased during murine cGVHD and is necessary in donor-BM-derived cells for the development and maintenance of cGHVD in the BO model. In addition, therapeutic pharmacologic inhibition of SYK decreases pathology in a murine BO model of cGVHD[59]. BTK is highly conserved Tec family kinase that propagates immune receptor-based signaling in B cells and is dispensable for antibody production. Blocking BTK by ibrutinib ameliorates cGVHD in both the scleroderma model and the BO model. These data suggest that BCR signaling after antigen engagement during post aHSCT B cell reconstitution is critical for persistence of auto-reactive B cells, and selective inhibition of BCR signaling may provide a new therapeutic target in patients with cGVHD. Indeed, ibrutinib was recently FDA approved as the only drug ever approved for treatment of steroid refractory GVHD.

In addition to a pathogenic role, B cells have beneficial role in cGVHD. Decrease of the frequency of a subset of IL-10 expressing B cells (Breg or B10 cells) has been correlated with human cGVHD[60,61]. The regulatory function of Breg cells has been demonstrated in mouse models of inflammation, cancer, transplantation, and particularly in autoimmunity[62,63].

1.3.3 Germinal center (GC) reactions

GCs are specialized regions found in secondary lymphoid organs in which activated B cells undergo diversification and affinity maturation that result in differentiation into both memory B cells and long-lived plasma cells that produce high-affinity, antigen-specific, class-switched antibodies. GCs are required for a sustained humoral immune reaction to allo-reactive antigens but also could result in the production of auto-reactive antibodies and a dysregulated autoimmune response[64]. In the BO model, enlarged GC and increased GC density were observed and disruption of GC reaction by lymphotoxin-β receptor immunoglobulin fusion protein could block disease. Flynn et al further demonstrated that follicular helper T cells (Tfh) and GC B cells frequencies are increased in cGVHD mice. In human, the levels of circulating Tfh cells are decreased in patients with active cGVHD, but these Tfh cells are activated and have increased functional ability to promote B-cell maturation and immunoglobulin secretion. This phenomenon is likely due to increased homing of Tfh in to second lymphoid organs, suggested by increased serum CXCL13[65]. Tfh migration to GC area by CXCR5 expression and the secretion of IL-21 is necessary for cGVHD development. Disruption of Tfh and GC B interaction by anti-

ICOS and anti-CD40 antibodies blocks cGHVD[66]. Patients with cGVHD frequently develop IgG antibodies directed at minor histocompatibility antigens in the recipient. In individual patients, these specific B-cell responses have been associated with clonal T-cell responses directed against different peptide epitopes contained within the same antigen[67,68]. These observations suggest that coordinated T- and B-cell responses in GC reactions are associated with cGVHD pathogenesis and identified several potential treatment targets for cGVHD.

The increased GC reactions may result from disturbed balance between Tfh and regulatory cells (Tfr). Tfr cells are effector subset of Tregs that originate from natural Treg precursors and express CXCR5, PD-1, ICOS, Bcl6 and Foxp3. The expression of CXCR5 directs them to migrate to GCs and suppress B cell responses[69]. McDonald-Hyman et al reported a decreased Tfr frequency in cGVHD mice. Treg infusion after disease establishment reverses cGVHD in CXCR5 dependent manner[70]. In vivo Treg expansion by iNKT infusion reversed cGVHD in the BO model[71]. These data suggested strategies restoring the balance between Tfh and Tfr in GC are promising for cGVHD treatment.

1.3.4 Macrophages, TGF-β and fibrosis

CD163+ macrophage infiltration of skin lesions after aHSCT was shown to be a significant predictive factor for refractory GVHD, as well as being a negative prognostic factor for overall survival[72]. The cumulative incidence of de novo–onset cGVHD was higher in patients with higher plasma soluble CD163 concentrations at day 80 than those

with lower concentrations. The use of granulocyte colony- stimulating factor (G-CSF)–mobilized stem cell grafts clinically has been associated with increased cGVHD[73]. This is likely due to the amplification effect of G-CSF on IL-17A production, which controls the infiltration of macrophages into skin and cutaneous fibrosis[74]. In a sclerodermatous cGVHD model, donor M2 macrophages infiltrating the skin were noticed and G-CSF treatment after transplantation exacerbated macrophage infiltration and cutaneous pathology. In addition, depletion of macrophages using an anti–CSF-1R mAb markedly reduced cutaneous and pulmonary cGVHD[26]. Increased CD68+ macrophages are associated with liver fibrosis in a humanized cGVHD mouse model[75]. These study collectively suggested that macrophage plays an active pathogenic role in cGVHD pathogenesis. However, how macrophages contribute to cGVHD pathogenesis is largely unknown. We recently reported co-localization of macrophage marker F4/80 and TGF-β in the peri-bronchiolar areas of cGVHD lungs in the BO model, the same area where extensive collagen deposition occurs. In addition, the percentage of latency associated peptide (LAP, correlate with TGF-β production) expressing lung macrophages as well as the expression level of LAP are increased during cGVHD[24]. Levels of TGF-β mRNA were found to be highest in skin biopsies of cGVHD patients when compared to patients with aGVHD[76]. T cells and macrophages in the cGVHD skin express TGF-β1 but not TGF-β2 or TGF-β3 mRNA[25]. In addition, macrophages express very high levels of Fc-γ receptors and are highly efficient at opsonization of antibody-coated targets, which in turn can generate very high levels of TGF-β. These data suggested that the interaction of allo-(and/or auto) antibody with tissue macrophages and production of TGF-β might be

the mechanism driving tissue fibrosis during cGVHD.

TGF-β ligands signal through cell surface serine/threonine kinase receptors, known as type I and type II receptors. Following ligand binding and receptor phosphorylation, the SMAD signaling circuitry becomes activated. The SMAD proteins are a family of transcription factors consisting of 8 members, SMAD1-8, which are further subdivided into 3 classes based on structural and functional properties. Receptor-regulated SMADs (R-SMADs), SMAD1, 2, 3, 5, and 8, are the only SMADs directly phosphorylated and activated by the kinase domain of type I receptors. Upon phosphorylation, R-SMAD form a complex with the common SMAD, SMAD4, resulting in nuclear accumulation of activated complexes. In the nucleus, R-SMAD–SMAD4 complexes cooperate with transcriptional coregulators that further define target gene recognition and transcriptional regulation. The inhibitory SMADs, SMAD6 and SMAD7 function to inhibit TGF-β signaling[77,78]. TGF-β has been recognized as a central player of fibrotic responses because of its abilities including by not limited to (1) promote epithelial and endothelial cells to acquiring mesenchymal phenotypes, (2) recruitment of circulating fibrocytes and bone marrow–derived progenitor cells to the lung, and (3) activation, migration, and proliferation of resident fibroblasts and their differentiation into activated myofibroblasts, which promotes excessive extracellular matrix (ECM) deposition and abnormal collagen accumulation[79,80]. Due to the regulative role of TGF-β on multiple immune cells, targeting TGF-β has been explored in many diseases including cancer and fibrosis[81]. Targeting TGF-β in cGVHD has been published by several groups. Administration of a neutralizing antibody against TGF-β prevented or reduced virtually all cutaneous

manifestations of chronic GVHD, including cellular infiltration, immune cell activation, thickening and fibrosis[23]. Early neutralization of TGF-β after BMT led to increased aGVHD, while late neutralization of TGF-β (days 14–42 post-transplant) led to decreased cGVHD scores and reduced pathophysiology in both the GI tract and the skin[82]. Additionally, blocking SMAD3 phosphorylation has been proposed as one way to alleviate cGVHD symptoms[83]. Results from multiple murine models suggested TGF-β can be a target for cGVHD treatment. Gene array analyses have shown that decreased expression of components of the TGF-β signaling pathway in donor CD4+ and CD8+ cells is correlated with increased incidence of cGVHD in recipients[84]. In a murine cGVHD model, recipient Tregs that survived irradiation suppress development of cGVHD[85], possibly through the production of TGF-β[86]. These study suggested that the role of TGF-β in cGVHD is time sensitive and context dependent. Localized inhibition of TGF-β to reduce fibrosis and minimize effect on Treg warrants further exploration.

Figure 1.

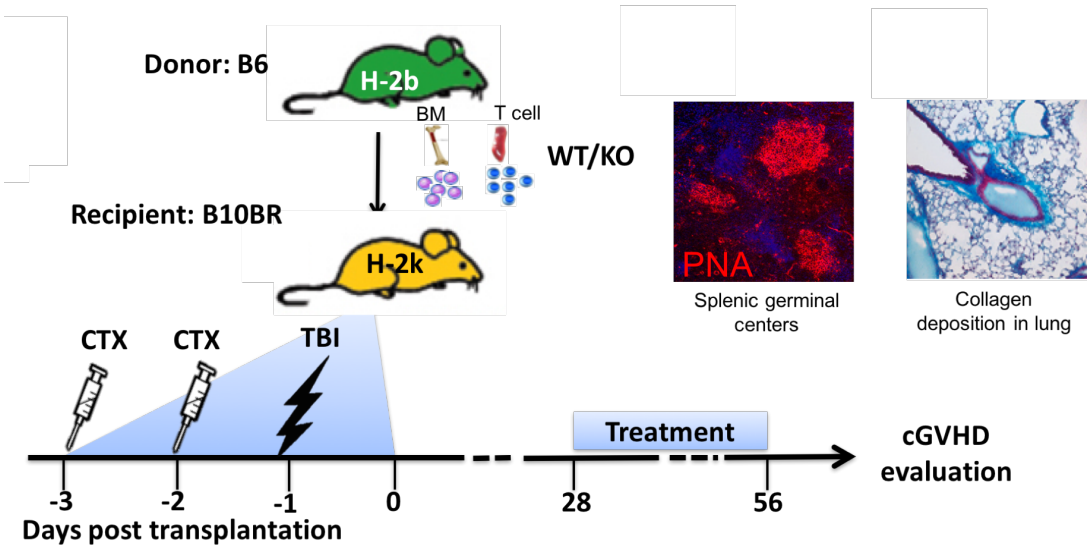

Figure 1. Schema of a BO model

B10.BR are conditioned by 2 doses of Cy (days -3 & -2) and total body irradiation (day-1). On day 0, conditioned B10.BR mice receive 10^7 B6 T-cell depleted BM without or with ~70,000 purified B6 T cells. Mice received BM with T cells will develop cGVHD with BO that can be detected on day 28. GC enlargement and collagen deposition in the lung can be detected around day 56. To evaluated therapeutic effect of a drug, mice are usually treated from day 28 to day 56 post transplantation.

Figure 2.

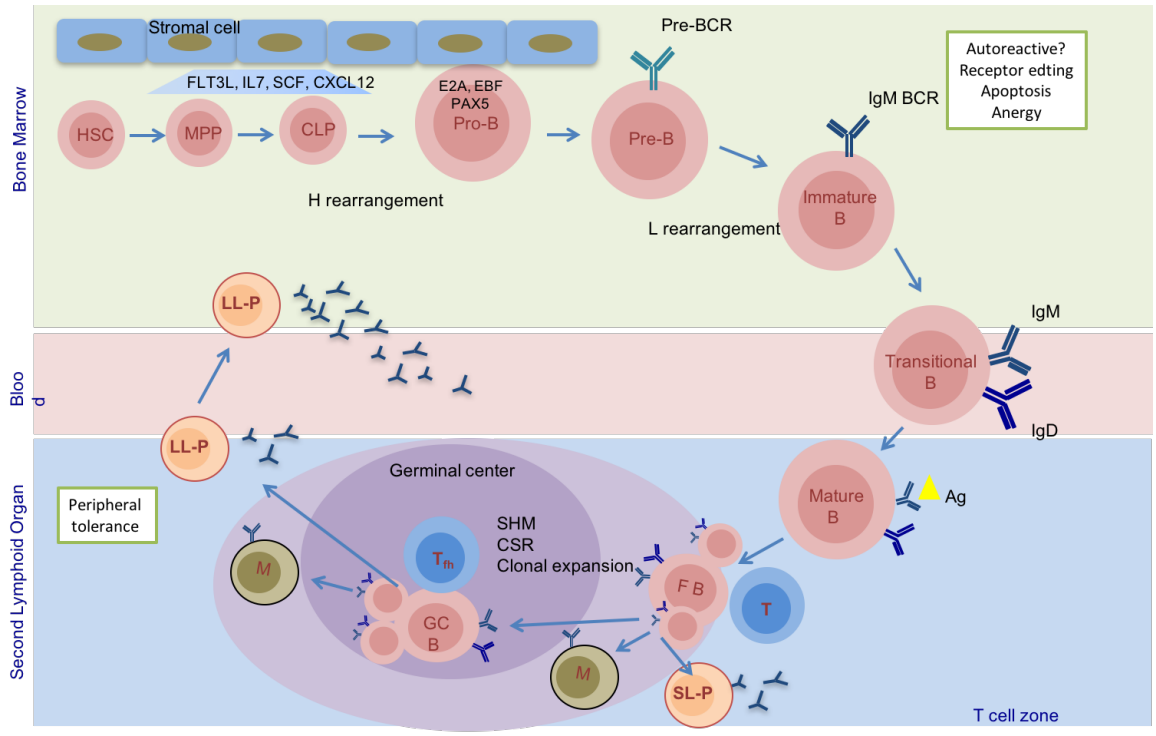

Figure 2. Development and differentiation of B cells

B cells originate from HSCs that have self renewal ability and the potential to generate all blood cells. HSCs differentiate into multi-potent progenitors (MPPs) and common lymphoid progenitors (CLPs) by interacting with bone marrow stromal cells. Signals that are important for early B cells development are FLT3L, SCF and CXCL12. BCR heavy chain rearrange starts at CLP and continue through Pro B cell stages. Expression of certain transcription factors combination such E2A, EBF and PAX5 by Pro B cell secures the progenitor cell a B cell fate. If a Pro B cell express a successful heavy chain, then the rearrangement stop and start to proliferate. The rearranged heavy chain can pair with a surrogate light chain and form a pre-BCR, which mark the B cell a pre-B cell. Pre B cell proceed to rearrange light chain. Once successfully assembling a light chain gene, the cell becomes an immature B cell that expresses a complete IgM and later an additional IgD on the cell surface. This stage of B cell is called transitional B cells, which migrate from the BM, through the blood into second lymphoid organs (SLO), where the transitional B cell meets its cognate antigen and become a mature B cell. Antigen binding mature B cells migrate to the B cell follicle in second lymphoid organ. At the border of B cell follicle and T cell zone, cognate T cell provides help to follicle B to undergo proliferation

and further differentiation. There are 3 fates for the follicle B cells. They can differential to memory B cell or short live plasma cell. The majority B cells will migrate to germinal center, where with the help of Tfh, they undergo somatic hyper mutation, class switch recombination and clonal expansion. Germinal center B cells will further differentiate into memory cell and long-lived plasma cell that secrete high affinity antibodies.

There are two check point to prevent B cell auto reactivity. The first one is in the BM, where BCR is tested for autoreactivity. Autoreactive B cell will be removed from the reptovire by mechanism such as receptor edition, apoptosis and anergy. Another check point in SLO has been proposed but the mechanism is largely unknown.

In cGVHD, the sites of both central and peripheral tolerance are target of disease, thus may compromise tolerance mechanism. The compromised tolerance mechanism together with an autoimmune prone milieu, facilitate B cell autoimmunity in cGHVD.

Chapter 2 Inositol kinase Itpkb is a novel therapeutic target for chronic graft versus host disease (cGVHD)

Abstract

Chronic graft versus host disease (cGVHD) is a common and life-threatening complication of allogeneic hematopoietic stem cell transplantation. cGVHD is mediated by donor T cells recognizing and attacking host tissues followed by activation of effector cells such as B cells to product pathogenic autoantibodies and macrophages to mediate fibrotic responses. Safer and more effective therapies are needed for cGVHD treatment. Inositol 1,4,5-trisphosphate 3-kinase B (Itpkb) is a Ca^{2+} dependent kinase downstream of lymphocyte receptor signaling that regulates T and B cell homeostasis and function by controlling the intracellular Ca^{2+} level, thus regulating apoptotic responses. Genetic deletion of Itpkb results in apoptosis. GNF362, a low molecular weight Itpkb inhibitor blocks T cell driven autoimmunity. In this study, we explore the role of Itpkb in cGVHD pathogenesis and hypothesize that cGVHD can be prevented by disrupting the Itpkb signaling pathway. We test the hypothesis in two preclinical cGVHD models with distinct clinical manifestations and pathophysiology, including a multi-organ system cGVHD mouse model that is characterized by bronchiolitis obliterans (BO) driven by spontaneous germinal center reactions and antibody deposition, and a scleroderma model that is characterized by macrophage infiltration and skin fibrosis. This study demonstrates that depleting Itpkb in donor T cells, but not in donor bone marrow blocked cGVHD lung disease and germinal center reaction in the BO model. In addition, pharmaceutical inhibition of Itpkb with GNF362 significantly reduced cGVHD manifestations in both models. These data identify Itpkb as an essential mediator of cGVHD pathogenesis and suggest Itpkb inhibition as a novel approach to treat cGVHD.

Introduction

cGVHD is the major obstacle for allogeneic hematopoietic stem cell transplantation (aHSCT) patients. Mortality caused by cGVHD is only second to relapse in long-term survivors of aHSCT. Although significance advance has been made in understanding the mechanisms of cGVHD pathogenesis, there has been limited change in the standard therapies of cGVHD, which rely mainly on systemic immune suppressions[87]. However, a significant portion of cGVHD patients do not respond to current standard therapies and the ones who respond are at higher risk of malignancy relapse and infection.

cGVHD is initiated by donor T cells activation and sustained by T and B cells interaction in germinal centers to produce high affinity self reactive autoantibodies[66–68]. Targeting T and B cell signaling has been explored in cGVHD treatment[49]. T and B cell receptor signaling pathways are tightly regulated by a number of mechanisms to ensure proper maturation, activation and function. Calcium (Ca^{2+}) signals in lymphocytes participate in the regulation of cell differentiation, gene transcription and effector functions[88]. An increase in intracellular levels of Ca^{2+} results from the engagement of immunoreceptors, such as the T-cell receptor, B-cell receptor and Fc receptors, as well as chemokine and co-stimulatory receptors[88]. In lymphocytes, receptor engagement activate phospholipase C-γ (PLC-γ), which hydrolyzes phosphatidylinositol-4,5-bisphosphate (PIP2) into diacylglycerol and inositol-1,4,5-trisphosphate (IP3), an essential second messenger mediating Ca^{2+} release from the endoplasmic reticulum. IP3-mediated depletion of endoplasmic reticulum Ca^{2+} stores triggers the opening of store-operated Ca^{2+} (SOC)

channels in the plasma membrane, leading to sustained increases in intracellular Ca^{2+}, which are required for cell cycle entry and gene expression[89]. The calcium-dependent inositol kinase, Itpkb phosphorylates the 3' position of the inositol ring to convert IP3 to inositol 1,3,4,5-tetrakisphosphate (IP4), thus act as an negative regulator of intracellular Ca^{2+} level[90]. Itpkb is implicated in autoimmune responses. During B cell development and maturation, Itpkb negatively regulate BCR signaling strength and control B cell selection and tolerance induction[91]. Mice lacking Itpkb had impaired B lymphocyte development and defective IgG3 antibody responses to a T lymphocyte–independent antigen[92]. Inhibition of Itpkb in mature T lymphocytes results in enhanced intracellular calcium levels following antigen receptor activation leading to T cell death. Deletion of Itpkb or treatment with Itpkb inhibitors blocks T-cell dependent antibody responses in vivo and prevents T cell driven arthritis in rats[92]. In this report, we study the role of Itpkb in the development of cGVHD in 2 complementary pre-clinical murine models including the germinal center response driven systemic model with BO and the scleroderma model.

Materials and methods

Mice

C57Bl/6 (B6; H2b), Balb/c (H2d) and B10.D2 (H2d) mice were purchased from the National Cancer Institute and used at 8-12 weeks old. B10.BR (H2k) mice were purchased from the Jackson Laboratory and used at 10-14 weeks old. $Itpkb^{fl/+}$ mice in B6 background were generated in the Genomic institute of the Novartis Research Foundation[93] and transferred to University of Minnesota. $Itpkb^{fl/fl}$ offspring from the

Itpkb$^{fl/+}$ parents were crossed with B6 mice that express CRE under the control of the triple mutant form of the human estrogen receptor; which does not bind its natural ligand (17β-estradiol) at physiological concentrations but will bind the synthetic estrogen receptor ligands 4-hydroxytamoxifen (OHT). Tamoxifen injections delete the Itpkb gene. Animal protocols were approved by Institutional Animal Care and Use Committee at the University of Minnesota.

Induction of cGVHD in vivo

For the BO cGVHD model, B10.BR mice were conditioned with intraperitoneal Cytoxan (Sigma, 120mg/kg/day, i.p., day-3&-2) and total body irradiation (8.3 Gray delivered by x-ray [list machine, dose rate) on day-1), followed by infusion of 10^7 B6 T cell depleted bone marrow (TCD-BM) only as non-cGVHD control, or plus 70,000 purified splenic T cells to induce cGVHD (day 0)[24]. For the scleroderma model, BALB/c mice were conditioned with TBI (7.75 Gray, day0), followed by infusion of 10×10^6 B10.D2 TCD-BM only or plus 1.8×10^6 CD4 and 0.9×10^6 CD8 T cells (day0) [22].

GNF362 Treatment

GNF362 was identified via high-throughput compound screening and optimized for drug-like properties using medicinal chemistry in Genomics Institute of the Novartis Research Foundation (GNF)[93]. GNF362 was formulated at 2mg/mL in 20% hydroxyl propyl-beta cyclodextrin in water. Mice were then dosed orally with GNF362 at 200 microgram dose

or vehicle twice daily from day 28-56 for the BO model and day 21-55 for the scleroderma model.

Pulmonary function tests: Pulmonary function tests were performed as described previously[28]. Briefly, Nembutal anesthetized mice were intubated and ventilated using the Flexivent system (Scireq). Pulmonary resistance, elastance and compliance were recorded and analyzed using the Flexivent software version 5.1.

Histopathology and immunostaining:

Lung, liver and skin were embedded in Optimal Cutting Temperature (OCT) compound, snap frozen in liquid nitrogen, and stored in -80°C. Lungs were inflated by 75% OCT prior to harvest. For trichrome staining 8 µm cryosections were fixed for overnight in Bouin's solution and stained with the Masson's trichrome staining kit (Sigma HT15). Collagen deposition was quantified as a ratio of blue area to total area by ImageJ.

For immunostaining, acetone fixed 8µm cryosections were stained with indicated markers. For macrophages staining, frozen sections of lung or skin were stained with anti CD68-ef660 (FA-11, eBioscience 50-0681). For immunoglobulin deposition, sections of lung were stained with goat anti-mouse Ig (BD 55401). Confocal images were acquired on an Olympus FluoView500 Confocal Laser Scanning Microscope

Flow Cytometry: For Tfh and GC B cells, single cell suspension of spleens was obtained and stained with fixable viability dye, fluorchrome-labeled anti-CD4 (RM4-5, BD), anti-CXCR5 (SPRCL5, eBioscience), anti-PD-1 (J43, eBioscience), anti-CD19 (eBio1D3, eBioscience), anti-GL7 (GL-7, eBioscience) and anti-Fas (J02, BD). GC B cells were defined as Fas and GL7 double positive CD19 B cells. Tfh cells were defined as PD1 and CXCR5 high CD4 T cells. Cells were analyzed on BD LSRFortessa.

Statistical analysis: GraphPad Prism 6 was used to conduct the statistical analysis. Groupwise comparisons were made by unpaired student T-test. Error bars indicated means +/- standard error of the mean (SEM). Significance: *P<0.05; **P<0.01; ***P< 0.001; ****P<0.0001.

Results and discussion:

Itpkb in donor T cells is required to cause cGVHD in the BO model

Itpkb functions downstream of TCR and BCR signaling pathways and negatively regulate intracellular Ca^{2+} level, thus regulates lymphocytes development, differentiation and function[88]. Itpkb inhibition blocked T cell dependent antibody production in a rat arthritis model[93]. Thus we determined to test whether Itpkb depletion or blockade can affect the antibody driven fibrosis in the BO model. Since the cGVHD is initiated by donor T cell allo-responses and sustained by donor BM derived B cells and macrophages, we transplanted mice with $Itpkb^{-/-}$ or WT BM alone or with $Itpkb^{-/-}$ or WT T cells. To deplete the Itpkb gene, $Itpkb^{fl/fl}$-CRE mice were treated with Tamoxifen for 5 days and rested for

a week before BM and T cells harvesting. Pulmonary function tests indicated that recipients of WT BM and Itpkb$^{-/-}$ T cells did not develop lung fibrosis - the phenotypic hallmark of the BO model, suggesting itpkb is required in donor T cells to cause cGVHD. This result correlate with previous report showing Itpkb is required for T cell activation and function, and loss of it triggers T cells apoptosis[93]. In contrast to the effects in donor T cells, Itpkb expression in BM is dispensable for cGVHD progression, as recipients of Itpkb$^{-/-}$ BM and WT T cells still developed lung disease as severe as mice received WT BM and WT T cells (Figure 1A). We further examined lung and liver by Masson's trichrome staining and immunofluorescent staining to look at collagen and Ig deposition, which are apparent in cGVHD[29]. Itpkb$^{-/-}$ donor T cells recipients did not show extensive collagen deposition in the peri-bronchiolar and peri-vascular areas in lung and liver, while there was no difference between the groups receiving WT or Itpkb$^{-/-}$ BM and WT T cells (Figure 1B&C). Ig deposition in lung was also absent when donor T cells lack Itpkb (Figure 1D). In contrast, Ig deposition was present in the mice receiving Itpkb$^{-/-}$ BM and WT T cells. These results suggest that Itpkb signaling is required in donor T cells to initiate cGVHD and point out a difference in the requirement of Itpkb by lymphocytes during different stages of cGVHD: donor T cells rely on Itpkb to become activated and proliferate to initiate cGVHD in the early stage of disease, while donor BM derived B cells and T cells can function without Itpkb to sustain cGVHD pathogenesis.

cGVHD pathogenesis is dependent on spontaneous GC reactions and the production of auto/allo reactive antibodies; thus we examined the effect of loss of Itpkb signaling in

donor T cells on GC reactions. About a 2 fold increase of GC reaction magnitude was seen during cGVHD, demonstrated by increased splenic GC B cell frequency (Figure 2B), Tfh (Figure 2C) cell frequency and Tfh/Tfr (Figure 2d) ratio. However these increases were absent in mice receiving Itpkb$^{-/-}$ donor T cells, suggesting a failure of inducing autoimmune response by Itpkb$^{-/-}$ donor T cells. This result correlates with the previous result showing lack of pulmonary disease in the Itpkb$^{-/-}$ donor T cells recipients.

Therapeutic pharmacologic inhibition of Itpkb decreases cGVHD in 2 preclinical murine cGVHD models with distinct clinical manifestations.

Having demonstrated the requirement for Itpkb in donor T cells to cause cGVHD, we next sought to determine whether drug treatment in mice with established cGVHD would be similarly efficacious as Itpkb deletion in donor T cells. GNF362 is a highly selective, orally potent low molecular weight (LMW) inhibitor that binds to the ATP-binding pocket of Itpkb[93]. GNF362 has been show to reduce T cell dependent arthritis in a rat model. To reverse established cGVHD in the BO model, mice were treated with oral GNF362 from day 28 until the end of experiment, as we previously determined that cGVHD is consistently present by day 28 as measured by pulmonary function tests. GNF362 treated mice had significantly improved pulmonary function compared to vehicle treated mice (Figure 3A). We further examined whether this was associated with effects on GC reactions. Surprisingly, even though pulmonary disease was alleviated by GNF362, the frequencies of cells participating GC reactions stayed mostly untouched (Figure 3B-E).

Previously we've shown that macrophage infiltration in the lung is involved in cGVHD pathogenesis[24,26]. To understand the therapeutic effect of GNF362 on cGVHD, we examined macrophage infiltration in the lung. Macrophages infiltrated the lung of cGVHD mice. GNF362 blocked macrophage infiltration in the treatment group (Figure 3F). These results suggest that therapeutic administration of GNF362 reversed cGVHD through effect on macrophage infiltration. Itpkb loss on HSCs resulted in the expansion of granulocyte monocyte progenitor but did not alter the number of peripheral monocyte count[94]. In a competitive in vivo setting, Itpkb-/- versus WT BM derived macrophages showed significantly reduced ability to repopulate the periphery[95]. However, no study has addressed the effect of Itpkb loss on macrophage migration and function in an inflammatory environment. Ca^{2+} signal act as second messenger in Fc receptor, chemokine receptor and toll like receptor in macrophage[88]. Our observation suggests that itpkb may regulate macrophage migration in an inflammatory environment.

In order to determine whether the effect of Itpkb inhibition by GNF362 attenuates murine sclerodermatous cGVHD, we used a miHA mismatched murine model involving lethally irradiated recipients. In the model, Balb/c recipients were lethally irradiated and infused with purified T cells from B10.D2 recipients. Skin scleroderma accompanied with loss of activity is the major clinical manifestation of this model. GNF362 treatment from day 21-55 significantly improved clinical score (Figure 4A) as well as skin score (Figure 4B&C). Previously we've shown that M2 macrophages infiltration is apparent in the skin of the sclerodermatous mice. Here, we show that GNF362 treatment significantly reduced

macrophage infiltration (Figure 4D, quantified in Figure 4E). We further looked at the effect of GNF362 on cytokine production of T cells and showed that GNF362 significantly reduce IFN-γ production from T cells. These results suggested that GNF362's therapeutic effect in the scleroderma model is associated with reduced macrophage infiltration and T cell IFN-γ production.

Taken together, this study identified Itpkb as a key enzyme for donor T cells to initiate cGVHD. Therapeutic inhibition of Itpkb reversed lung disease in the BO model and ameliorated skin disease in the scleroderma model. These results highlight Itpkb as a potential therapeutic target for cGVHD therapy.

Figure legends:

Figure 1. Itpkb is required in donor T cells but not BM to cause cGVHD

Conditioned B10.BR mice were transplanted with WT or Itpkb$^{-/-}$ BM with or without 70,000 WT or Itpkb$^{-/-}$ donor T cells. (A) Pulmonary function was evaluated at around 8 weeks post transplantation. (B-D) Lungs and livers were taken for trichrome staining and immune stainng. (B) Collagen deposition in the lung was assessed by trichrome staining that identifies collagen in blue. Percent of collagen deposition area was quantified by Fiji software. (C) Liver collagen deposition staining and quantification. (D) Immunofluorescence staining of Ig deposition in the lung. Results shown are representative from 2 independent experiments with similar results.

Figure 2. Itpkb expression in donor T cells is required for the development of spontaneous germinal center reaction

Splenocytes were harvested at 6-8 weeks post transplantation and were stained with markers for GC B cells (A), Tfh (B) cells and Tfr (C) cells. Ratio of Tfh/Tfr was calculated in (D). GC B cells are $CD19^{+}Fas^{+}GL7^{+}$ population. Tfh cells are $CD4^{+}Foxp3^{-}CXCR5^{+}PD1^{hi}$ population. Tfr cells are $CD4^{+}Foxp3^{+}CXCR5^{+}PD1^{hi}$ population. Results shown are representative from 2 independent experiments with similar results.

Figure 3. GNF362 reversed cGVHD lung disease associated with inhibition of macrophage infiltration but without altering germinal center reactions

Transplanted mice were treated with GNF362 or vehicle from 4 to 8 weeks post transplantation. (A) Pulmonary function test was performed around week 8. (B-E) Germinal center responses were assessed by measure the frequencies of GC B cells (B), Tfh (C), Tfr (D) and Tfh/Tfr ratio (E). GC B cells are $CD19^{+}Fas^{+}GL7^{+}$ population. Tfh cells are $CD4^{+}Foxp3^{-}CXCR5^{+}PD1^{hi}$ population. Tfr cells are $CD4^{+}Foxp3^{+}CXCR5^{+}PD1^{hi}$ population. (F) Macrophages in the lung were staining by CD68-FITC. Quantification was done by Fiji software by measuring the percentage of positive staining areas. Results shown are representative from 3 independent experiments with similar results.

Figure 4. GNF362 reversed skin scleroderma caused by cGVHD

Conditioned Balb/c mice were transplanted with B10.D2 BM only or with 2.7×10^{6} purified T cells (CD4:CD8=2:1). GNF362 treatment (200 microgram per oral, twice

daily) started at around day21. (A) Clinical manifestations of cGVHD were assessed by giving scores to weight loss, activity, posture and fur condition. Healthy mice receive score 0. (B) Skin scores was assessed by measuring the area of skin with fur loss or sclerodermatous lesion. Intact skin was given score 0. (C) Photograph of mice in BM only group, vehicle treated cGVHD group and GNF362 treated group. (D) Macrophage marker CD68 and M2 macrophage marker CD206 were used to staining the skin of transplanted mice. (E) Quantification of macrophage in skin by Fiji software. (F-G) Lymph nodes were harvested on day 55 post transplantation and lymphocytes were stimulated in vitro. IFN-γ production was evaluated by flow cytometry. Results shown are representative from 2 independent experiments with similar results.

Figures

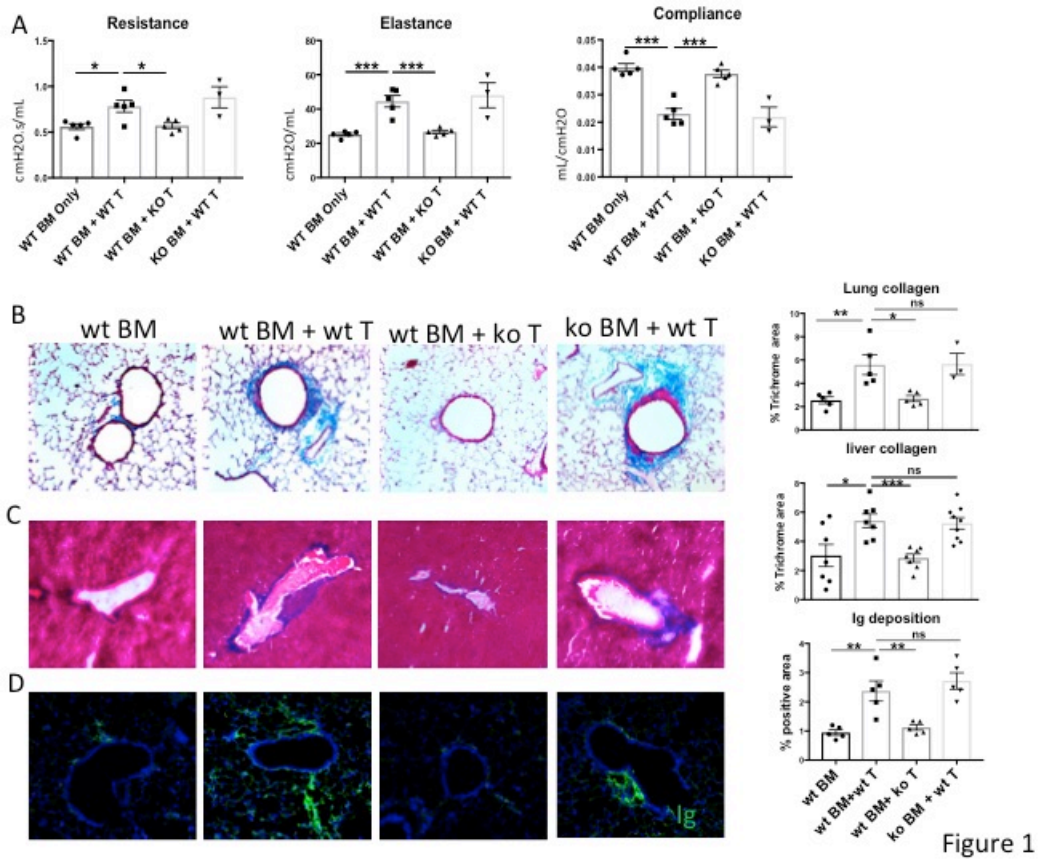

Figure 1

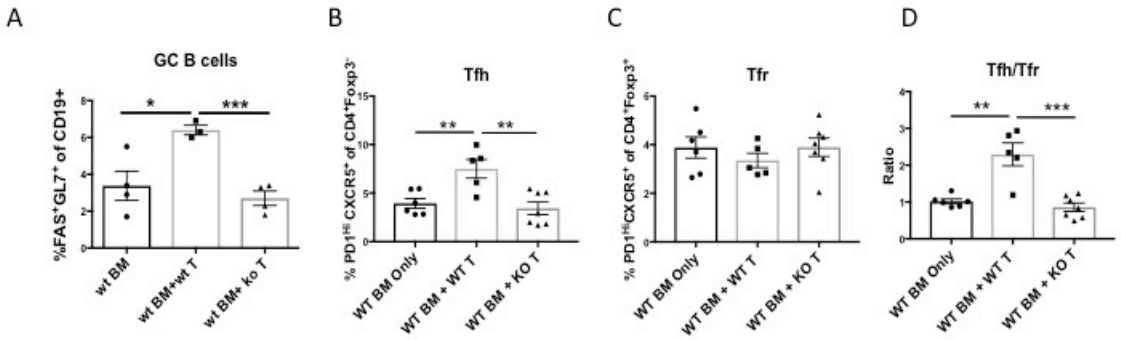
A
GC B cells
%FAS+GL7+ of CD19+
*
***
wt BM
wt BM+wt T
wt BM+ ko T
B
Tfh
% PD1HI CXCR5+ of CD4+Foxp3-
**
**
WT BM Only
WT BM + WT T
WT BM + KO T
C
Tfr
% PD1HiCXCR5+ of CD4+Foxp3+
WT BM Only
WT BM + WT T
WT BM + KO T
D
Tfh/Tfr
Ratio
**
***
WT BM Only
WT BM + WT T
WT BM + KO T

Figure 2

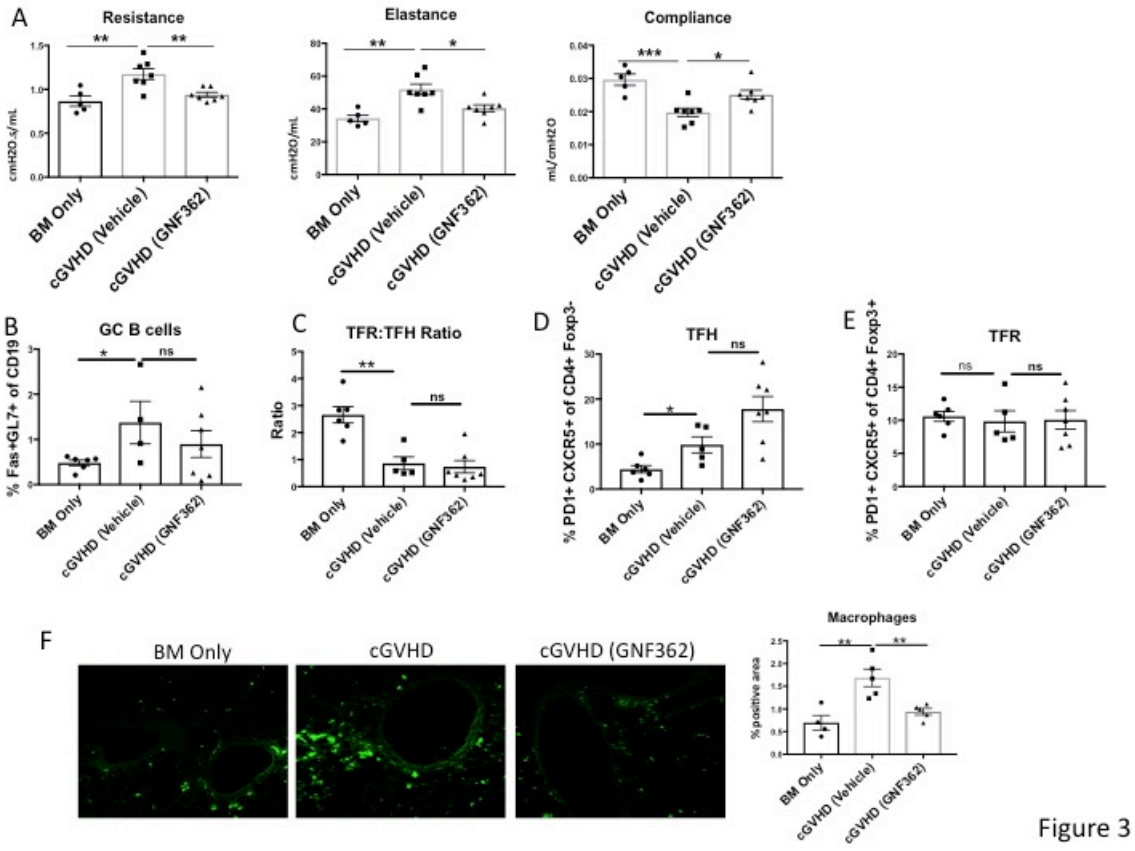
A
Resistance
Elastance
Compliance
cmH2O·s/mL
cmH2O/mL
mL/cmH2O
BM Only
cGVHD (Vehicle)
cGVHD (GNF362)
B
GC B cells
% Fas+GL7+ of CD19
C
TFR:TFH Ratio
Ratio
D
TFH
% PD1+ CXCR5+ of CD4+ Foxp3-
E
TFR
% PD1+ CXCR5+ of CD4+ Foxp3+
F
BM Only
cGVHD
cGVHD (GNF362)
Macrophages
% positive area

Figure 3

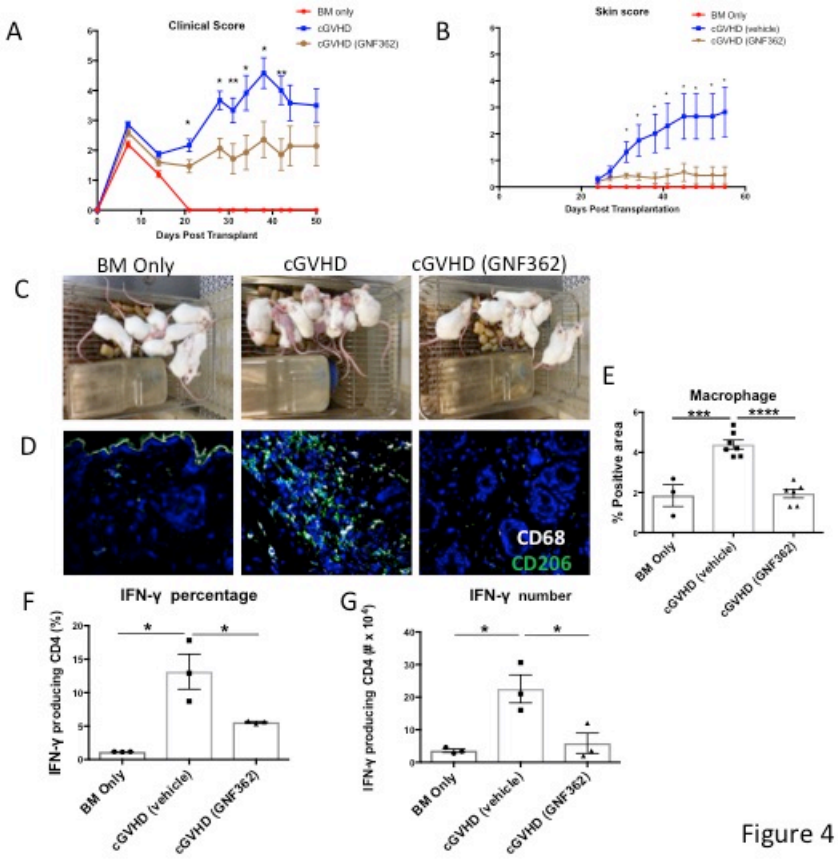
A
Clinical Score
BM only
cGVHD
cGVHD (GNF362)
Days Post Transplant
B
Skin score
BM Only
cGVHD (vehicle)
cGVHD (GNF362)
Days Post Transplantation
C
BM Only
cGVHD
cGVHD (GNF362)
D
CD68
CD206
E
Macrophage
% Positive area
BM Only
cGVHD (vehicle)
cGVHD (GNF362)
F
IFN-γ percentage
IFN-γ producing CD4 (%)
BM Only
cGVHD (vehicle)
cGVHD (GNF362)
G
IFN-γ number
IFN-γ producing CD4 (# x 10⁶)
BM Only
cGVHD (vehicle)
cGVHD (GNF362)

Figure 4

Chapter 3 Invariant Natural Killer T cells Ameliorate Murine Chronic GVHD by Expanding Donor Regulatory T cells

Originally published by the American Society of Hematology in the journal Blood
Jing Du, Katelyn Paz, Govindarajan Thangavelu, Dominik Schneidawind, Jeanette Baker, Ryan Flynn, Omar Duramad, Colby Feser, Angela Panoskaltsis-Mortari, Robert S. Negrin and Bruce R. Blazar
Blood. 2017 Jun 8;129(23):3121-3125.

Abstract

Chronic graft-versus-host-disease (cGVHD) can cause multi-organ system disease typically with autoimmune-like features, resulting in high mortality and morbidity due to treatment limitations. Invariant natural killer T cells (iNKTs), a small population characterized by expression of a semi-invariant T-cell receptor, rapidly produce copious amounts of diverse cytokines upon activation that exert potent immune regulatory function. Here, we show that iNKTs are significantly reduced in a cGVHD murine model that recapitulates several aspects of autoimmunity and organ fibrosis observed in cGVHD patients. Low iNKT infused doses effectively prevented and, importantly, reversed established cGVHD, as did third-party iNKTs. iNKTs suppressed the autoimmune response by reducing the germinal center (GC) reaction, associated with an increase in total Tregs and follicular Tregs (Tfr) that control the GC reaction along with pathogenic antibody production. Treg depletion during iNKT infusions completely abolished iNKT efficacy in treating cGVHD. iNKT cell IL-4 production and GC migration were critical to cGVHD reversal. In vivo stimulation of iNKT cells by alpha-galactosyl-ceraminde was effective in both preventing and treating cGVHD. Together, this study demonstrates iNKT deficiency in cGVHD mice and highlights the key role of iNKTs in regulating cGVHD pathogenesis and as a potentially novel prophylactic and therapeutic option for cGVHD patients.

Introduction

cGVHD is the major cause of non-relapse morbidity and mortality that lacks effective and safe therapies[87]. Preclinical models have elucidated autoimmunity as the key of cGVHD pathogenesis, where dysregulated GC and extra-follicular B-cell responses can lead to the production of autoantibodies that initiate fibrotic responses[66]. While Tregs can treat established murine cGVHD[70], clinical Treg production can be challenging and sustaining Treg persistence likely requires an IL-2 source that is suppressed by Tregs. Thus, we have explored an alternative immune regulatory population, iNKT cells, that are not exquisitely IL-2 sensitive and are highly effective in limited cell numbers in preventing acute GVHD (aGVHD)[96–98]. iNKT cells have immune regulation function[99], conferred by the rapid production of immune regulatory cytokines such as IL-4 and IL-10[100,101] and promote Treg expansion perhaps through a myeloid cell intermediate[97,102]. iNKT deficiency has been linked to autoimmune diseases (e.g. type 1 diabetes, rheumatoid arthritis and lupus)[103–105]. Donor graft iNKTs content and their capacity to expand have been associated with GVHD risk[106–108]. Total lymphoid irradiation and anti-thymocyte globulin conditioning in allo-HSCT patients results in an increase in the ratio of host iNKTs to conventional CD4+/CD8+ T cells which can reduce aGVHD in murine models and patients[109,110]. Here, we used a murine model of cGVHD induced by GC reaction that results in antibody production, deposition and triggering of monocytes/macrophages to cause systemic fibrosis, to evaluate the role of iNKT in preventing and treating cGVHD.

Materials and Methods

Mice and bone marrow (BM) transplantation

C57BL/6 (B6) (Charles River), B10.BR (JAX®), CXCR5$^{-/-}$ and IL4$^{-/-}$ on B6 background (JAX®) and B6.Foxp3.Luci.DTR-4 mice (gift from Professor Günter Hämmerling) were housed in a pathogen-free facility and used with IACUC approval. To induce cGVHD, B10.BR mice were given cyclophosphamide and total body irradiation pre-transplant and B6 bone marrow (BM) only (no cGVHD) or with 75,000 purified T-cells (cGVHD)[66].

iNKT isolation and Treg depletion

iNKT cells were FACS-sorted from CD1d-PBS57 tetramer enriched B6 splenocytes[98] to high purity (>95%) and maintained cytokine-producing function (not shown). iNKTs were infused at 50,000 or 100,000 doses at the indicated times. Where stated, Tregs were depleted in B6.Foxp3.Luc-DTR-4 mice by diphtheria toxin (DT) (0.1 microgram/mouse) injections before and after iNKTs infuson (d.-2,-1,1& 2).

cGVHD evaluation

cGVHD was evaluated by pulmonary functional tests (PFTs) and trichrome staining[29,66]. Lung hydroxyproline quantification was per manufacturer's instructions (Sigma MAK008). GC reaction was evaluated by immunofluorescence staining and flowcytometry[66]. Bioluminescent imaging (BLI) was performed using IVIS Spectrum.

Results and discussion

Therapeutic iNKT cell infusion reversed established cGVHD

To examine whether the iNKT pool in cGVHD is deficient, we analyzed splenic iNKTs from early phase cGVHD mice (d28) and naïve donor and host strain mice. cGVHD mice have a significantly lower splenic iNKTs than naïve mice and BM controls (Fig.1A-B). Thus, we explored adoptive iNKT transfer to treat cGVHD. Donor iNKTs were infused to cGVHD on d28&42 post-transplantation. iNKTs (50,000 or 100,000 cells) reversed lung cGVHD measured by PFTs (Fig.1C). Total lung hydroxyproline (Fig.1D), collagen deposition around peribronchial and perivascular areas (Fig.1E&F) were reduced (50,000 cells) or completely reversed (100,000 cells, this dose was used for subsequent studies). iNKT cells form a 3rd strain (Balb/c) reversed cGVHD as well as iNKT from donor strain (Fig.1G). iNKT infusion reduced GC area (Fig.1H&J) and increased Tfr density (Fig.1I&K). Flow cytometry analysis of d55 splenocytes confirms that iNKT reduces GC B and increases Tfr frequency (Fig.1L&M). Thus, donor iNKT reversal of established cGVHD was likely due to increased Tfr frequencies

iNKT reversed cGVHD through donor Treg expansion

Due to the reduced Treg frequency observed in both cGVHD patients[111] and our murine model[70], and reversal of cGVHD in murine model with Treg infusion[70], we examined whether iNKT reversed cGVHD through Treg expansion. Donor B6.Foxp3.Luci.DTR-4 mice[112] permitted both tracking expansion and eliminating Foxp3 expressing Tregs, iNKT increased Foxp3 signal intensity by 2-fold (Fig.2A&B). Peri-infusion donor Treg

depletion completely abrogated iNKT-mediated protection as indicated by PFTs (Fig.2C), confirming a Treg dependent mechanism.

Infused CD45.1 iNKT cells were detected in GC areas 5d after infusion (Fig.2D). To test whether GC migration and IL4 production are required for iNKT's protective function in cGVHD, iNKTs from CXCR5$^{-/-}$ or IL4$^{-/-}$ mice were infused. Neither CXCR5$^{-/-}$ nor IL4$^{-/-}$ iNKTs were able to reverse cGVHD (Fig.2E). Taken together with the high Tfr frequency conferred by iNKT infusion, these data point to in-situ Tfr expansion in GC area by iNKT through IL4 dependent mechnism as a key mechanistic underpinning of iNKT-mediated cGVHD therapy.

Pharmacologic activation of iNKT is effective in preventing and reversing cGVHD

To determine the potential of iNKT in preventing cGVHD, donor iNKTs were given on d1&14 (prophylaxis) or on d28&42 (therapy). PFTs showed that prophylactic infusion completely blocked cGVHD, resulting in modestly more robust protection compared with therapeutic infusion (Fig.2F). Prophylactic iNKT efficacy may be advantageous due to the expansion of host radio-resistant Tregs or donor Tregs in the graft that suppress inflammation and tissue damage, preventing cGVHD initiation, as well as easier disease prevention than reversal. In support of this latter hypothesis and further demonstrating the potential iNKT therapeutic benefits, we demonstrated the efficacy of RGI2001, a liposomal formulation of a-galactosylceramide, in both treating and to an even greater extent in preventing cGVHD (Fig.2G).

Because aGVHD is a critical risk factor for cGVHD[87], managing aGVHD can significantly reduce cGVHD incidence. iNKT infusion (25,000-100,000 cells) protected mice from aGVHD in a dose-dependent manner through Treg expansion[97]. These data and ours suggest that iNKT cells infusion protects from both aGVHD and cGVHD, which we speculate is due to the fact that both diseases are associated with an inadequate Treg pool and hence T effector/Treg ratio[111,113]. The fact that iNKT infusion is useful for both aGVHD and cGVHD offers the possibility for optimal treatment of patients with dual acute and chronic GVHD components[114].

Compared to Treg infusion, iNKT infusion required fewer cells (100,000 iNKT versus 500,000 Treg in the same model) to reach optimal effect[70,115]. Additionally, iNKT cells have inherent anti-viral and anti-tumor abilities[116] that are desirable for cGVHD patients. iNKT cells are persistent in host, as they can be detected in spleen, liver and lung at least 2 weeks after infusion (not shown). A detailed migration/expansion profile of iNKT cells in cGVHD mice is to be studied. In summary, this study provides evidence that iNKT infusion and expansion are promising prophylactic and therapeutic options for cGVHD patients.

Acknowledgements:

The following funding sources contributed to this work: National Institutes of Health National Cancer Institute grants P01 CA142106-06A1, 5P01-CA047741-20, P01-

CA049605; National Heart, Lung, and Blood Institute grants P01 HL075462， R01 HL126530 and K08HL107756; National Institute of Allergy and Infectious Diseases grants P01 AI 056299, and T32 AI 007313; and Leukemia and Lymphoma Society translational research grants 6458-15 and 6462-15.

Authorship:

Contribution: J.D. designed the experiments and wrote the paper; J.D., K.P., G.T., D.S., J.B., R.F., O.D. and C.F. performed experiments, discussed results and edited the paper. A.P.-M performed histologic analyses. R.S.N. and B.R.B contributed to experimental design, discussed results, and edited the paper.

Conflict-of-interest statement:

The authors declare competing financial interests as a pending patent on iNKT cell infusion to treat cGVHD.

Figure Legends

Figure 1. Therapeutic iNKT cell infusion reversed established cGVHD

B10.BR mice were conditioned by 2 doses of cyclophosphamide (120mg/kg body weight, ip) on d-3 and d-2 of transplantation. On d-1, B10.BR mice were irradiated (830 Gy by x-ray) then infused with T-cell depleted (TCD) BM only or with 75,000 purified T cells to induce cGVHD. (A-B) On d28 after transplantation, splenocytes were harvested from BM only mice and cGVHD mice and naïve mice of donor and recipient strains. Cells were stained with fluorochrome conjugated PBS57-CD1D tetramer, anti-CD4, anti-TCR-β and viability dye. iNKT cells were identified by $CD4^+$ TCR-β^+PBS57-$CD1D^+$ live cells. (A) Gating of iNKT cells. Cells were gated on live $CD4^+$ T cells. (B) Frequency of iNKT is significantly reduced in cGVHD mice. (C-D) On d28 and d42 post-transplantation, FACS sorted CD45.1 B6 iNKTs were infused to some cGVHD mice at a lower (50K) or higher (100K) dose. (C) Pulmonary function tests (PFTs) including resistance, elastance and compliance, were performed on d56 post transplantation. iNKT infusion significantly improves the pulmonary function. (D) Hydroxyproline was measured in the lungs of mice from Fig. 1C. iNKT infusion at the 100k cell dose significantly reduces hydroxyproline. (E) Trichrome staining that identifies collagen was performed on cryosections of lungs. (F) Collagen deposition was quantified by measuring the blue area of the Trichrome staining by Fiji software. iNTK infusion significantly reduce collagen deposition in the lung. (G) cGVHD was established previously described. Mice received Balb/c iNKT cells on d28 and 42. Balb/c iNKT cells reverse cGVHD. (H) Cryosections of spleen (d56) were stained with fluorochrome conjugated

anti-CD4 (FITC), anti-Foxp3 (eFluor660) and peanut-agglutinin (PNA) (CY3) and imaged by Olympus FV1000 system. Dotted lines delineate GC areas by PNA staining. (I) Follicular Tregs were identified as $CD4^{+}Foxp3^{+}$ cells within the GC areas. (J) Average GC size is decreased by iNKT. (K) Follicular Treg density is increased by iNKT. (L-M) Splenic GC B cells and follicular Tregs frequencies were determined by flow cytometry. iNKT infusion decreases GC B and increases follicular Treg frequencies. Unpaired student T-test was used when comparing 2 groups. Data shown are representative of 2 independent experiments with 5-8 mice per group. Significance: *P<0.05; **P<0.01; ***P< 0.001; ****P<0.0001.

Figure 2. iNKT reversed cGVHD through donor Treg expansion and prevent the onset of cGVHD

(A-C) cGVHD was established as per Fig 1, except that BM and T cells were harvested from B6.Foxp3.Luci.DTR-4 mice. Group 1 and 2 are BM only and cGVHD control as described before. Groups 3 - 5 are cGVHD mice that received diphtheria toxin (DT) (Group 3), iNKT infusion on d28 and d42 (Group 4) or iNKT infusion and DT (Group 5). (A) On d43, mice were imaged by Spectrum In Vivo Imaging system. (B) Quantification of the BLI signal shows depletion of Tregs by DT and expansion of Tregs by iNKT infusion. (C) PFTs were assessed as described in Fig 1. Treg depletion by DT injection completely abolishes iNKTs efficacy. (D) iNKT cells (white arrow) were identified by CD45.1+ in GC area. (E) Mice were transplanted as per Figure 1. iNKT cells from wildtype, $CXCR5^{-/-}$ or $IL4^{-/-}$ mice were infused to transplanted mice on d28 and 42. iNKT

cells from CXCR5$^{-/-}$ or IL4$^{-/-}$ mice lost the ability to reverse cGVHD. (F) cGVHD mice were infused with B6 iNKTs either on d1 and d14 (prophylaxis) or on d28 and d42 (therapy). Prophylatic iNKT infusion completely blocks cGVHD. (G) Prophylatic or therapeutic RGI2001(2.5 microgram/mouse) was given to transplanted mice. PFTs suggest RGI2001 prevents and reverses cGVHD. 5-8 mice per group were analyzed for each assay. Significance: *P<0.05; **P<0.01; ***P< 0.001; ****P<0.0001.

Figures

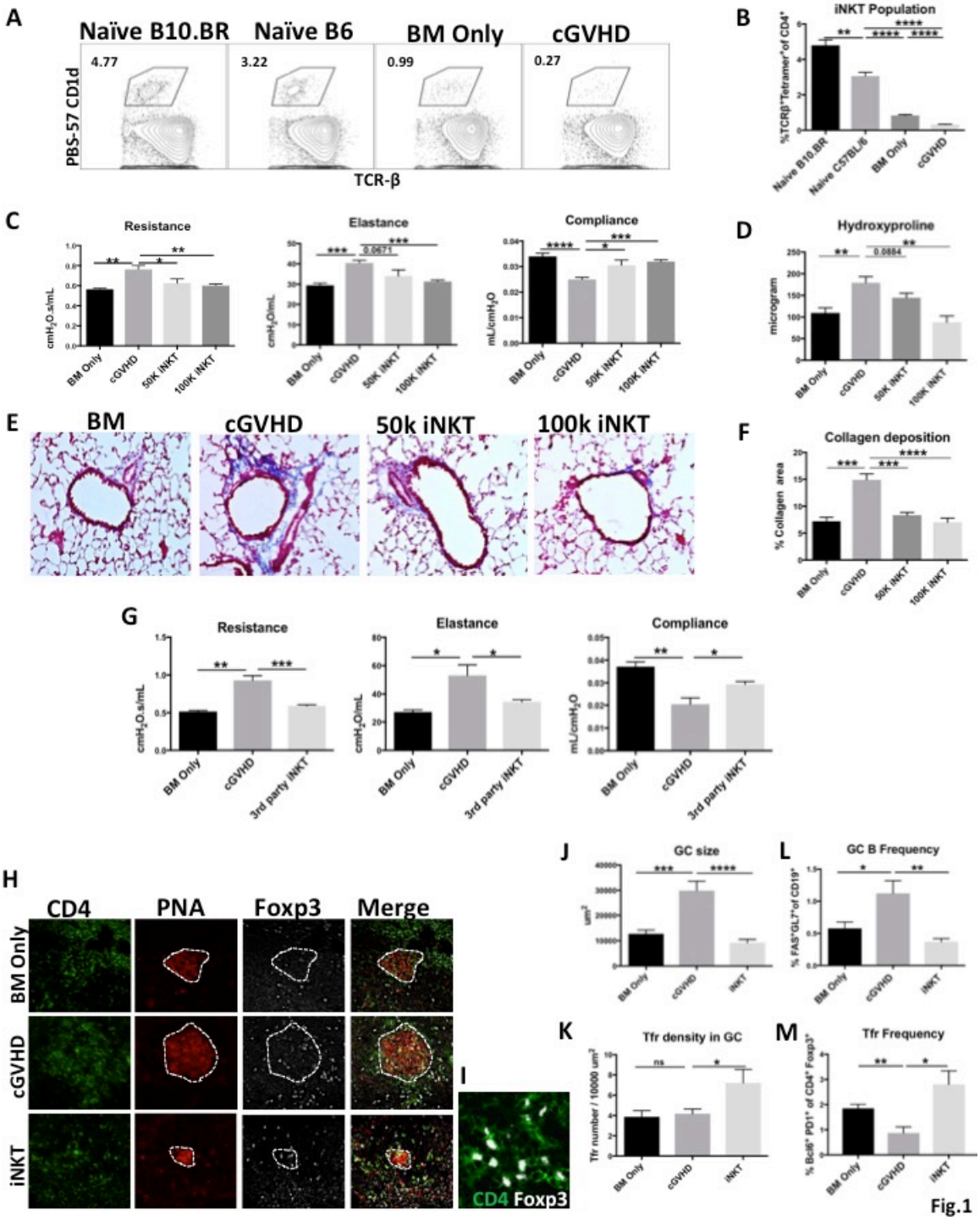

Fig.1

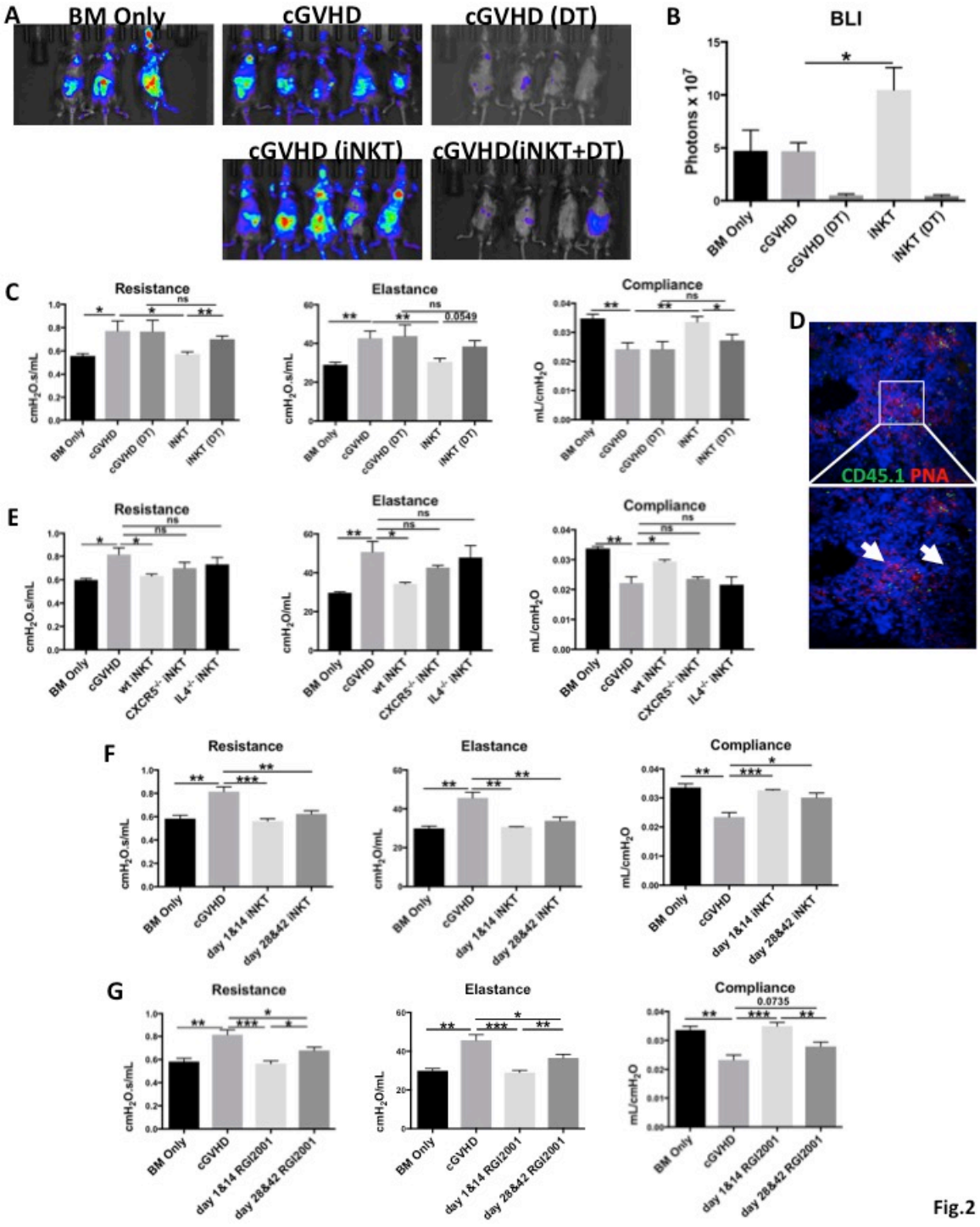
A
BM Only
cGVHD
cGVHD (DT)
cGVHD (iNKT)
cGVHD(iNKT+DT)
B
BLI
Photons x 10^7
BM Only
cGVHD
cGVHD (DT)
iNKT
iNKT (DT)
C
Resistance
Elastance
Compliance
cmH2O.s/mL
cmH2O/mL
mL/cmH2O
0.0549
D
CD45.1 PNA
E
Resistance
Elastance
Compliance
BM Only
cGVHD
wt iNKT
CXCR5-/- iNKT
IL4-/- iNKT
F
Resistance
Elastance
Compliance
BM Only
cGVHD
day 1&14 iNKT
day 28&42 iNKT
G
Resistance
Elastance
Compliance
0.0735
BM Only
cGVHD
day 1&14 RGI2001
day 28&42 RGI2001

Fig.2

Chapter 4 Pirfenidone Ameliorates Murine Chronic GVHD Through Inhibition of Macrophage Infiltration and TGF-β Production

Originally published by the American Society of Hematology in the journal Blood
Jing Du, Katelyn Paz, Ryan Flynn, Ante Vulic, Tara M. Robinson, Katie E. Lineburg, Kylie A. Alexander, Jingjing Meng, Sabita Roy, Angela Panoskaltsis-Mortari, Michael Loschi, Geoffrey R. Hill, Jonathan S. Serody, Ivan Maillard, David Miklos, John Koreth, Corey S. Cutler, Joseph H. Antin, Jerome Ritz, Kelli P. MacDonald, Timothy W. Schacker, Leo Luznik and Bruce R. Blazar
Blood. 2017 May 4;129(18):2570-2580.

Abstract

Allogeneic hematopoietic stem cell transplantation is hampered by chronic graft-versus-host disease (cGVHD) resulting in multi-organ fibrosis and diminished function. Fibrosis in lung and skin leads to progressive bronchiolitis obliterans (BO) and scleroderma, respectively, for which new treatments are needed. We evaluated pirfenidone, a FDA approved drug for idiopathic pulmonary fibrosis, for its therapeutic effect in cGVHD mouse models with distinct pathophysiology. In a full MHC-mismatched, multi-organ system model with BO, donor T cell responses that support pathogenic antibody production are required for cGVHD development. Pirfenidone treatment beginning one month post-transplant restored pulmonary function and reversed lung fibrosis, which was associated with reduced macrophage infiltration and TGF-β production. Pirfenidone dampened splenic germinal center B cell and T follicular helper cell frequencies that collaborate to produce antibody. In both a minor histocompatibility antigen-mismatched as well as a MHC-haploidentical model of sclerodermatous cGVHD, pirfenidone significantly reduced macrophages in the skin, although clinical improvement of scleroderma was only seen in one model. In vitro chemotaxis assays demonstrated that pirfenidone impaired macrophage migration to MCP-1 as well as IL-17A, that has been linked to cGVHD generation. Taken together, our data suggest that pirfenidone is a potential therapeutic agent to ameliorate fibrosis in cGVHD.

Introduction

cGVHD is a significant barrier of allogeneic hematopoietic stem cell transplantation (allo-HSCT) due to its high incidence and severity. Fibrosis affecting skin and internal organs is the predominant clinical feature of cGVHD. Bronchiolitis obliterans (BO) and scleroderma with their respective fibrotic bronchiolar and cutaneous changes[87] are two of the most devastating outcomes for cGVHD patients. Systemic immune suppression is the recommended treatment for cGVHD, although such treatment is not always effective in controlling disease and does not alleviate established fibrosis[117]. Additionally, systemic immune suppression can be associated with high infection and relapse rates[118]. New therapies that reverse fibrosis without compromising immune function are urgently needed. Several preclinical models have been developed to study cGVHD pathogenesis and test potential interventions[21,119–121]. For example, we have developed a murine model that uses full MHC-mismatched donors and recipients (B6→B10.BR) and incorporates a clinically relevant pre-transplantation conditioning regimen of high dose cyclophosphamide and total body irradiation (TBI) leading to the development of systemic fibrosis affecting the lung, liver and GI tract but not the skin. Studies from this model pointed to autoimmunity as the key of cGVHD pathogenesis, where induced germinal center (GC) reactions support the production of autoantibodies that are deposited in target organs causing fibrosis[26,29,66]. Two lethal irradiation models, (B10.D2→BALB/c[22] and B6 parent→B6D2F[26]) using minor histocompatibility antigen-mismatched or MHC-haploidentical donors and recipients, develop scleroderma as the

main cGVHD manifestation, which is dependent on tissue F4/80+ macrophage infiltration.

Pirfenidone (5-methyl-1-phenyl-2- (1H)-pyridone) is a small molecule known for its anti-fibrosis properties. In bleomycin-induced lung injury and lung allotranspant models, pirfenidone decreased hydroxyproline, fibrosis, procollagen I and II, PDGF isoforms, TGFb, fibroblast growth factor, and IL-13[122–130]. Moreover, pirfenidone increases scavenger of reactive oxygen species[131] and decreases inflammation pathways that initiate fibrosis responses, such as nitrites, IL-6[132] and tumor necrosis factor-α[133]. Recently, pirfenidone has been FDA approved as treatment for idiopathic pulmonary fibrosis treatment, reducing disease progression and increasing lung function, exercise tolerance, and progression-free survival[134]. Pirfenidone showed efficacy in treating localized scleroderma in a phase II study[135].

In this study, we explored the efficacy of pirfenidone in multiple murine cGVHD models and found that pirfenidone reversed lung disease in the BO model. cGVHD patients with BO have a high morbidity and mortality and therapeutic options for advanced BO are limited[136]. We show that pirfenidone treatment of mice with active cGVHD was associated with a reduction of macrophage infiltration, TGF-β production, and the GC reaction. Importantly, pirfenidone administration had long-lasting effects and could reverse later stage lung disease. In the sclerodermatous cGVHD models, pirfenidone diminished macrophage infiltration in both models, although the clinical benefit was

variable with significant attenuation of clinical and pathological changes evident only in the B10.D2→BALB/c model.

Materials and methods

Mice: For the BO model, C57Bl/6 (B6; H2b) mice were purchased from the National Cancer Institute. B10.BR (H2k) mice were purchased from the Jackson Laboratory. For the BALB/c (H2d)→B10.D2 (H2d) model, mice were propagated in the animal facility at the Johns Hopkins University Cancer Research Building I. For the B6 parent→B6D2F1(H2b/d) model, mice were purchased from ARC (Perth, WA, Australia) and used between 8-13 weeks of age. Mice were housed in a specific-pathogen–free facility and used with the approval of each institution's animal care committee.

Bone marrow transplantation: For the BO model, B10.BR mice were conditioned with Cytoxan (Sigma, 120mg/kg/day, i.p., day-3&-2) and TBI (8.3Gy, day-1), followed by infusion of 10×106 B6 T cell depleted bone marrow (TCD-BM) only as healthy control, or plus 75,000 purified splenic T cells to induce cGVHD (day0) [29,66]. For the B10.D2 to BALB/c scleroderma model, BALB/c mice were conditioned with TBI (7.75Gy, day0), followed by infusion of 10×106 B10.D2 TCD-BM only or plus 1.8×106 CD4 and 0.9×106 CD8 T cells (day0) [22]. For the B6 to B6D2F1 scleroderma model, B6D2F1 mice were conditioned with TBI (11Gy split into 2 doses, day-1) followed by infusion of 5×106 B6 TCD-BM only or plus 1×106 purified T cells (day0) [26]. Mice were monitored daily, and examined at least twice a week for clinical signs of cGVHD. Assessment of

cutaneous GVHD in the B10.D2 to BALB/c scleroderma model was done using established scoring system as previously described[137].

Pirfenidone treatment: Pirfenidone was manufactured to Good Manufacturing Practice grade at SAFC Pharma (St. Louis, MO) under contract with the National Institutes of Allergy and Infectious Disease. The crystalline drug compound was certified to be pure (≥97% area by HPLC) at the University of Minnesota using a process supplied by SAFC Natick. The drug has been used successfully in non-human primate models of fibrosis[138]. In this study, pirfenidone crystals were ground down into fine powder using mortar and pestle and then suspended in 0.4% methylcellulose. Mice were given pirfenidone (400mg/kg) by oral gavage from day28-56 or 56-84 (BO model), day21-55 (B10.D2 to BALB/c model) or day14-28 or 14-41 (B6 to B6D2F1 model). Mice in the vehicle control group were treated with the same volume of 0.4% methylcellulose.

Pulmonary function tests: Pulmonary function tests were performed as described previously[28]. Briefly, Nembutal anesthetized mice were intubated and ventilated using the Flexivent system (Scireq). Pulmonary resistance, elastance and compliance were recorded and analyzed using the Flexivent software version 5.1.

Hydroxyproline assay: Mice were sacrificed by cervical dislocation. Lungs were removed and homogenized in 200µl de-ionized water. 100 µl aliquot of the homogenate was hydrolyzed in 100 µl concentrated HCL (Sigma 320331) for 3 h in 120 °C. After

centrifugation, 5 to 10 µl of supernatant was carefully removed to a 96-well plate and incubated in 56 °C oven until dry. The amount of hydroxyproline in the lung homogenate aliquots was measured by Hydroxyproline Assay Kit (Sigma MAK008). The result was adjusted to reflect hydroxyproline content in the whole sample.

Histopathology and immunostaining: Lung and spleen were embedded in Optimal Cutting Temperature (OCT) compound, snap frozen in liquid nitrogen, and stored in -80°C. Lungs were inflated by 75% OCT prior to harvest. For trichrome staining 8 µm cryosections were fixed for overnight in Bouin's solution and stained with the Masson's trichrome staining kit (Sigma HT15). Collagen deposition was quantified as a ratio of blue area to total area using ImageJ.

For immunostaining, acetone fixed 8µm cryosections were stained with indicated markers. For GC detection, frozen sections of spleens were stained with rhodamine-peanut agglutinin (PNA) and DAPI (Vector Laboratories). For macrophage and TGF-β staining, frozen section of lung or skin were stained with anti CD68-ef660 (FA-11, eBioscience 50-0681) or rabbit anti mouse F4/80/TGF-β (Abcam ab66043/ab100790) followed by anti-rabbit HRP-DAB staining Kit (R&D CTS005). Confocal images were acquired on an Olympus FluoView500 Confocal Laser Scanning Microscope at 200X, analyzed using FluoView3.2 software (Olympus) and quantified by ImageJ.

Macrophage migration assay: J774 cells were cultured with vehicle, 0.25 or 0.5mg/ml pirfenidone for 24h. IL-17A (100ng/ml; eBioscience) or MCP-1/CCL2 (100ng/ml; GibcoTM) was added to the lower chamber as chemoattractant and J774 cells were plated in the upper chamber of 96 transwell plates (Corning®3374). Cells were allowed to migrate through the insert membrane for 4 h at 37°C under a 5% CO2 atmosphere. Calcein AM solution (Molecular Probes) was added to each well of receiver plate. Plates were incubated at 37°C in a 5% CO2 incubator for 60 minutes. The plate was read by SpectraMax i3X from Molecular Devices at 485/530[139].

Intravascular staining and lung single cell suspension preparation: Mice were injected with 4 micrograms of CD45-FITC antibody (CD45 iv) (eBioscience) through tail vein and rested for 5 minutes before sacrificed by cervical dislocation. Lungs were removed, dissociated by gentleMACS dissociator (Miltenyi Biotec) and digested in collagenase D (2mg/ml) for 30 minutes in 37°C incubator. The digested lungs were filtered through 40 um cell straining to create the single cell suspension.

Flow Cytometry: For Tfollicular helper (Tfh) and GC B cells, single cell suspension of spleens was obtained and stained with fixable viability dye, fluorchrome-labeled anti-CD4 (RM4-5, BD), anti-CXCR5 (SPRCL5, eBioscience), anti-PD-1 (J43, eBioscience), anti-CD19 (eBio1D3, eBioscience), anti-GL7 (GL-7, eBioscience) and anti-Fas (J02, BD). GC B cells were defined as Fas and GL7 double positive CD19 B cells. Tfh cells were defined as PD1 and CXCR5 high CD4 T cells. Cells were analyzed on BD

LSRFortessa. For flow analysis of lung macrophages, single cell suspension of lung was stained with anti-CD45-PE (CD45 ex vivo, 30-F11, eBioscience), anti-CD11c (3.9, eBioscience), anti-F4/80 (BM8, eBioscience) and anti-latency associated peptide (LAP, TW7-16B4, eBioscience).

Statistical analysis: GraphPad Prism 6 was used to conduct the statistical analysis. Groupwise comparisons were made by unpaired student T-test. Error bars indicated means +/- standard error of the mean (SEM). Significance: *P<0.05; **P<0.01; ***P< 0.001; ****P<0.0001.

Results:

Therapeutic administration of pirfenidone reverses fibrosis in a cGVHD BO model

To examine the efficacy of pirfenidone to reverse lung fibrosis caused by cGVHD, mice with BO that have systemic fibrosis with in vivo measurable fibrotic lung disease were treated with pirfenidone from day28-56 post-transplantation. In this model, pulmonary function loss and fibrotic change in the lung can be detected as early as day28, and progresses to day56[29]. The loss of lung function is detected using the FlexiVent (SCIREQ) system for forced oscillations measurements including resistance (increase of airway pressure per volume increase when the lung expands), elastance (reduction of airway pressure per volume reduction when the lung recoils) and compliance (increase of lung volume per pressure increase when the lung expands)[140]. On day56, cGVHD mice that received BM and T cells displayed fibrotic lung disease with higher resistance and

elastance, and lower compliance compared with the BM only mice. Pirfenidone treatment from day28-56 significantly reduced lung fibrosis ($P<0.01$) to comparable lung function with BM only mice (Figure 1A).

To document pirfenidone's effect on lung fibrosis, we measured hydroxyproline levels in the lung, which correlates with the amount of collagen - a major component of fibrotic tissue. The hydroxyproline level in cGVHD group lungs is ~2-fold higher than the non-cGVHD group, and pirfenidone treatment significantly reduced lung hydroxyproline content ($p< 0.01$) (Figure 1B), consistent with pulmonary function tests. In addition, Masson's trichrome staining that identifies collagen by blue staining in tissue section was performed. Mice in cGVHD group showed increased collagen deposition in the peribronchial and perivascular areas of lung and liver compared with BM only group; pirfenidone treatment significantly reduced collagen deposition in lung ($p<0.01$) and liver ($p< 0.05$) (Figure 1C, quantified in Figure 1 D and E). Taken together, these results showed that pirfenidone reversed lung fibrosis caused by cGVHD.

Pirfenidone reduces F4/80+ macrophage accumulation and TGF-β deposition in lung

Pirfenidone inhibits TGF-β signaling pathway[128,129,132,141] that contribute to tissue fibrosis[81]. TGF-β is preferentially produced from mononuclear cells following stem cell transplantation[82], including macrophages, that are potent TGF-β producers and required to induce cutaneous cGVHD model[26]. TGF-β recruits circulating fibrocytes and

inflammatory cells to the sites of tissue damage and induces the expression of fibrogenic cytokines (e.g. PDGF and IL-13) as well as transcriptionally activates the collagen gene. In B10.D2→BALB/c scleroderma model, TGF-β neutralization from day14 after allo-HSCT attenuated histologic abnormalities[82]. Depleting tissue macrophages by antibody reversed pulmonary fibrosis in the BO model[26].

To evaluate whether pirfenidone reduces macrophage infiltration and TGF-β production in the lung of cGVHD mice, serially sectioned slides of lung were stained with Masson's trichrome stain, anti-F4/80 antibody and anti-TGF-β antibody (Figure 2A). Macrophage and TGF-β staining were significantly increased in the cGVHD lungs (Figure 2B&C). The peribronchial and perivascular areas stained strongest and these are also the areas where extensive collagen deposition occurred, suggesting macrophages and TGF-β are mediators in cGVHD pathogenesis. Notably, pirfenidone treatment significantly reduces both macrophage and TGF-β in the lung.

To understand whether pirfenidone inhibits TGF-β production from macrophage, cGVHD mice were treated with pirfenidone from day28-35 and lung cells were analyzed by flow on day36. Due to the failure of lung perfusion to completely remove blood cells from lung vasculature[142], thus causing difficulties in discriminating tissue and blood-borne macrophages in the lung, we used intravascular CD45 antibody staining (CD45 iv) to identify blood-borne macrophages before mice were sacrificed[143]. Tissue macrophages are defined as F4/80+CD11c-CD45iv- cells and alveolar macrophages are defined as

F4/80+CD11c+ cells[144] (Supplementary Figure 1). LAP, a protein that is contained in TGF-β precursor at the N-terminus, was quantified for assessment of TGF-β surface expression[145]. LAP expression in both alveolar and tissue macrophages was increased significantly in the cGVHD mice, consistent with immunohistochemistry staining as above, and pirfenidone reduced LAP expression on both alveolar and tissue macrophages (Figure 2D-E). These results suggest that the reduced TGF-β production in lung by pirfenidone was due to a combined effect of reduced macrophage number and reduced TGF-β producing capacity of macrophages.

Activated macrophages are generally categorized into classically (M1) and alternatively (M2) activated phenotypes. M2 macrophages are crucial for wound healing, fibrosis and anti-inflammatory effects, while M1 macrophages are more important for pro-inflammatory effects. To determine the phenotype and origin of the infiltrating macrophages in the lung, we used CD45.1 B6 donors and stained the lungs of cGVHD mice with donor marker (CD45.1) and the M2 macrophage marker CD206, together with the macrophage marker CD68. Immunofluorescence staining showed that the majority of CD68+ cells are also CD45.1+ and CD206+ (Figure 2F), suggesting that infiltrating macrophages in cGVHD are donor BM-derived and are M2 phenotype. M2 macrophage infiltration has also been observed in several scleroderma cGVHD models and is required for pathogenesis[26].

Since pirfenidone reduces macrophage infiltration in nephrectomized rats[146], inhibits monocyte chemoattractant protein-1 (MCP-1/CCL2) in a bleomycin induced lung fibrosis model[132], and reduces macrophage infiltration into the lungs of cGVHD mice, we sought to further evaluate pirfenidone's effect on macrophage migration. For this purpose, a transwell assay was used. IL-17A and MCP-1 were chosen as chemoattractants[147] based on their implications in cGVHD pathogenesis in this[37] and other transplant settings[28,38,39,148–151]. Pirfenidone significantly inhibited both IL-17A and MCP-1 induced J774 macrophages migration in vitro (Figure 2G). Taken together, these results suggest that cGVHD lung disease is mediated by donor M2 macrophage infiltration and excessive TGF-β production, and that pirfenidone not only inhibits IL-17A facilitated macrophage infiltration, but also macrophage TGF-β production.

Pirfendone reduces the GC reaction in cGVHD mice

cGVHD pathogenesis in the BO model requires auto/allo antibodies production driven by elevated GC reaction[29,66]. Previously, we showed that cGVHD mice develop a spontaneous GC reaction reflected by increased size and frequency of splenic GCs and increased frequency of GC B cells and Tfh cells in cGVHD mice compared with BM only mice; further disrupting the GC reaction can ameliorate cGVHD in this model[66]. To examine whether pirfenidone interferes with this pathological process, we evaluated the effect of pirfenidone on the GC reaction. While GCs were significantly upregulated in cGVHD mice as indicated by GC B cell (Figure 3A&B) and Tfh cell (Figure 3C&D) frequencies, as well as by GC size (Figure 3E &F) and number (Figure 3G), pirfenidone

treatment significantly impaired these immunological effects. These results suggest that pirfenidone inhibits a known driving force of cGVHD pathogenesis.

The magnitude of GC reaction can be affected by both the function and quantity of required Tfh and GC B cells, and the availability of antigen[152]. Pirfenidone has been reported to suppress alloresponses in heart allograft recipients by suppressing T cell function[153]. To assess whether pirfenidone could directly affect the GC reaction in a non-cGVHD setting, we used a sheep red blood cell (SRBC) immunization model. Mice were immunized with SRBC to induce GC reactions on day0. In the pirfenidone treatment group, mice were treated with pirfenidone from day-1 to day6. On day7, spleens and serum were harvested for GC reaction evaluation and SRBC antibody detection. Interestingly, pirfenidone did not affect the magnitude of the GC reaction induced by SRBC, as indicated by comparable frequencies of GC B cells and Tfhs in pirfenidone treated and vehicle-treated groups (Supplementary figure 2A&B). There was no difference in the SRBC-specific antibody concentration between pirfenidone treated and vehicle treated groups (Supplementary figure 2C). These results suggest that pirfenidone interferes with cGVHD-specific antigen responses or the amplification of such responses that lead to the GC reaction rather than by globally suppressing GC formation in response to a potent GC inducing stimulus such as SRBCs.

Pirfenidone treatment has a long-lasting effect and is capable of reducing later stage disease

To determine whether pirfenidone inhibition of pulmonary fibrosis was transient, transplanted mice were treated with pirfenidone day28-56 after transplantation and were left untreated for 28 days before pulmonary function tests were performed. Day84 pulmonary function tests of mice treated with pirfenidone for 28 days and rested for another 28 days were still significantly better than for mice that never received treatment, although not reaching the levels of BM only mice (Figure 4A). Thus, pirfenidone has a long-lasting effect on cGVHD fibrosis.

To evaluate the efficacy of pirfenidone in a late stage of cGVHD, transplanted mice were treated from day56-84 after transplantation. Day84 pulmonary function tests indicated that pirfenidone reduced lung disease even at this later stage of the disease process (Figure 4A). Hydroxyproline assay (Figure 4B) and trichrome staining (Figure 4C-E) correlated with pulmonary function test results. Taken together, these results highlight the potential of pirfenidone to be an option for patients with established disease who cannot tolerate continuous treatment.

Pirfenidone treatment has variable efficacy in the scleroderma models

To examine whether pirfenidone can also attenuate skin fibrosis, we used 2 different skin cGVHD models. In the minor histocompatibility antigen-mismatched B10.D2 to BALB/c model, dermal fibrosis is dependent on both Th1 and Th17 CD4+ T cells[22] and preceded by infiltration of donor-derived CD11b+ cells consisting of monocytes and activated macrophages[154]. Clinical skin disease in this model develops ~day20 after

transplantation[137], thus pirfenidone treatment was started on day21 when clinical disease is already established in the majority of animals. Pirfenidone reduced skin lesion, as showed by reduced clinical and histological scores (Figure 5A&B). While the profoundness of pirifenidone's effects on the skin scores varied between the experiments, the drug effect on the reduction of collagen deposition and macrophage infiltration in cGVHD mice was consistently observed (Figure 5C&D). In the B6 to B6D2F1 haploidentical transplant model, F4/80 macrophage infiltration in the dermis is noted by day21 post-transplantation, and becomes localized in the subcutaneous fat layers. Infiltrated macrophages are donor BM-derived M2 macrophages and dependent on CSF-1 signaling. Pirfenidone treatment from day14-28 marginally but significantly decreased day28 macrophage infiltration but this was insufficient to translate to reductions in cutaneous pathology (Figure 5E).

Discussion

cGVHD patients have manifestations that are similar to fibrotic diseases such as systemic sclerosis and idiopathic pulmonary fibrosis[155]. Thus, anti-fibrosis treatments may offer a novel therapeutic approach for cGVHD patients. Although preclinical studies have shown that neutralization of TGF-β reduces skin fibrosis and gastrointestinal GVHD scores in the B10.D2→BALB/c cGVHD model[23,25,82], there is no anti-fibrosis drug available for cGVHD patients. Here, we demonstrated the efficacy of pirfenidone, an FDA approved drug for idiopathic pulmonary fibrosis, in reversing fibrosis in the multi-organ system, BO cGVHD model previously demonstrated to mimic several aspects of human cGVHD,

with the exception of sclerodermatous cGVHD[29]. Pulmonary function and pathological changes in the cGVHD lung were normalized by pirfenidone when treatment was begun at one month post-transplant, while improving but not completing reversing disease when delayed an additional month to day56 post-transplant. These results extend other studies showing that pirfenidone can reduced lung fibrosis in bleomycin- and lung allograft rodents models[129,130,132,156]. The protective effect of pirfenidone is associated with a decrease of infiltrating macrophages surrounding the bronchioles and a decrease of TGF-β production by these macrophages. Since BO is also a major problem in lung transplantation, the current finding in BO cGVHD model may also shed light on the management of lung transplantation complications.

Pirfenidone is a small molecule that is rapidly absorbed and metabolized into 5-carboxy-pirfenidone, whose anti-fibrotic effect is weaker than that of pirfenidone[157]. Pirfenidone's pharmacokinetics and metabolism profile have be characterized by Buckpitt et al[158], showing that after administration, the peak level of pirfenidone in tissues correlates with the degree of tissue penetration. Whereas pirfenidone alleviated skin fibrosis in 2 clinical trials for localized scleroderma and burn injury[135,159], in both scleroderma models tested here, pirfenidone had a variable and modest effect under the conditions tested, although a significant reduction in macrophage infiltration was observed in both models. The relative modest or absence of effect of pirfenidone on skin manifestations may be attributable to the fact that skin is not perfused as well as other organs where pirfenidone has a more evident effect such as lung and liver. In addition, rapid onset of skin scarring

may further limit the access of pirfenidone to its target sites. Since scleroderma in the B6→B6D2F1 haploidentical is known to be macrophage dependent[26], the lack of clinical and pathological improvement was unexpected. We hypothesize that the failure of pirfenidone to completely eliminate macrophage infiltration into the skin, perhaps due to tissue penetration may account for the inability of pirfenidone treatment in these systemic scleroderma models to reverse established disease. Thus, topical treatment of pirfenidone in scleroderma cGVHD models warrants testing in the future.

The cGVHD BO model depends on antigen-activated GC reactions that result in antibody deposition in multiple organs including lung and liver that trigger pro-fibrotic responses. This feature of the BO model mimic human cGVHD, as autoreactive antibodies have been identified in cGVHD patients[160]. In addition, antibodies against Y-chromosome encoded antigens have been identified in male patients transplanted with BM from female donors[44]. Although as discussed above, pirfenidone is well known for its anti-fibrosis ability, pirfenidone also has been reported to suppress allo-responses[161]. By using a cGVHD independent SRBC immunization model, we showed that pirfenidone does not directly regulate GC reactions as pirfenidone treated mice still developed strong GC responses against SRBC immunization. Rather than a direct effect of pirfenidone on the GC reaction, pirfenidone may be influencing the GC response via macrophages that are known to be required for cGVHD in the BO cGVHD model[26]. These data pointed to the capacity of pirfenidone to modify the particular antigen-driven response for cGVHD generation and maintenance. Wilkes and colleagues have shown that IL-17-dependent

immune responses against collagen V contribute to BO in preclinical and clinical lung transplant settings[162–164]. In rheumatoid arthritis, immune responses against collagen also may contribute to disease. As collagen content is significantly increased in cGVHD mice and reduced by pirfenidone treatment, we hypothesize that pirfenidone may be ameliorating disease by reducing IL-17A facilitated macrophage infiltration, macrophage TGF-β production and hence collagen production[147], especially based on its implication in cGVHD pathogenesis in this[37] and other cGVHD settings[38,39,149–151]. Consistent with this hypothesis, we directly demonstrate that pirenidone impedes macrophage migration to IL-17A in vitro and lung macrophage infiltration in a cGVHD system that is dependent upon IL-17A for disease generation[37]. Pirfenidone also impaired macrophage migration to MCP-1/CCL2. Although in sclerodermatous cGVHD, some studies have shown MCP-1 to be upregulated[165] with biological responses to pravastatin treatment associated with MCP-1 downregulation[166], whereas in another model [B6 parent→B6D2F[26]], MCP-1 neither affected the development or inflammatory response. Interestingly, the latter model did not have a robust clinical effect in response to pirfenidone treatment. In contrast, high MCP-1 levels have been associated with the pathogenesis of bronchiolitis obliterans[167] and in the BO cGVHD model here, pirfenidone was highly effective in treating disease, which was associated with reduced macrophage infiltration in the lung. B cells in cGVHD patients are in a more active state given the increased B cell-activating factor/B cell ratio after transplantation[87]. In this scenario, excessive collagen can be recognized by hyper-responsive B cells resulting in the production of auto-antigen that then triggers the GC response in cGVHD recipients. Thus, the reversal of GVHD observed with

pirfenidone treatment also may be attributed to the reduction of collagen as an autoantigen. Understanding the mechanism of action for this effect requires further experimentation.

In conclusion, we identify here the utility of pirfenidone in treating BO cGVHD and in reducing macrophage infiltration in cGVHD target organs including the lung and the skin. Our studies provide a rationale for the of topical pirfenidone for sclerodermatous cGVHD and consideration of future clinical trials for pirfenidone as cGVHD therapy in patients, particularly those that have BO, a devastating complication of allo-HSCT[136].

Acknowledgements:

The authors thank Dr. Steven W. Lane for generating the GVL model.

This work was supported in part by National Institutes of Health National Cancer Institute grants P01 CA142106-06A1, R01CA122779 and 5P01-CA047741-20; National Heart, Lung, and Blood Institute grants R01 HL126530 and K08HL107756; National Institute of Allergy and Infectious Diseases grants P01 AI 056299, R01 AI 091627 and T32 AI 007313; and Leukemia and Lymphoma Society translational research grants 6458-15 and 6462-15.

Authorship

Contribution: J.D. designed experiments, performed experiments, and wrote the paper; K.P., R.F. A.V., T.M.R., K.E.L., K.A.A, J.M. and M.L. designed and performed experiments; A.P.-M. performed histological analyses, discussed experimental design,

and edited the paper; G.R.H., J.S.S, I.M., D.B.M., J.K., C.S.C., J.H.A. and J.R. designed experiments and edited the paper; T.W.S provided reagents, discussed experiments, and edited the paper; and S.R., K.P.A.M., L.L and B.R.B. designed experiments and edited the paper.

Conflict-of-interest disclosure: The authors declare no competing financial interests.

Figure Legends

Figure 1. Therapeutic administration of pirfenidone reverses fibrosis in cGVHD BO model

B10.BR mice were conditioned with cytoxan (120mg/kg/day, i.p., day-3 & -2) and total body irradiation (8.3 Gy, day-1), followed by infusion of 10^7 B6 T cell depleted bone marrow only as healthy control, or plus 75,000 purified splenic T cells to induce cGVHD (day0). In the treatment group, cGVHD mice received pirfenidone (400mg/kg) from day28 to day56. (A) Pulmonary function tests on day56 post-transplantation showed that pirfenidone restored lung function of cGVHD mice. Data are representative of 3 experiments with similar results. (B) Hydroxyproline assay of the right lungs harvested on day56 indicated that pirfenidone significantly reduced hydroxyproline content. 5-6 mice from each group were analyzed. Data are representative of 2 experiments with similar results. (C) Representative images of Masson's trichrome staining images of lung (upper) and liver (lower). Collagen (blue stain) was quantified in (D) and (E). (F&G) Representative lung Ig deposition images and quantification. Data are representative of 2 experiments with similar results. $*p \leq 0.05$, $**p < 0.01$; $***p < 0.001$; data are shown as the mean plus or minus standard error of the mean.

Figure 2. Pirfendone reduces F4/80$^+$ macrophage accumulation and TGF-β deposition in lung

(A-C) Serial sections of lungs harvested on day56 post-transplantation were stained with trichrome staining (A, top panel), anti-F4/80 antibody (A, middle panel) and anti-TGF-β

antibody (A. bottom panel). F4/80 positive cell number and TGF-β staining area were quantified in (B) and (C). Pirfenidone reduced macrophages infiltration and TGF-β production in lung. (D&E) Mice were transplanted as described in Figure 1. cGVHD mice were treated by pirfenidone for a week from day28-35. On day35, LAP expression in alveolar macrophages (D) and tissue macrophages (E) were analyzed by flow cytometry. Pirfenidone significantly reduced LAP expression in both alveolar and tissue macrophages. (F) Donor B6 mice are CD45.1 and B10.BR CD45.2 recipient mice were used. Lung sections were fixed and stained with anti-CD45.1 (donor marker, red), CD68 (grey) and CD206 (green). Arrows pointed at cells that are $CD45.1^{+}CD68^{+}CD206^{+}$. This result suggests that infiltrating macrophages in the lung are donor derived M2 macrophages. (G) Macrophage migration was assessed in a transwell assay. IL-17A or MCP-1was used as chemoattractants to induce migration. Pirfenidone (0.25 or 0.5mg/ml) or vehicle was added to cell culture medium and migration medium. Pirfenidone inhibited IL-17A and MCP-1 induced J774 migration. 5-8 mice were analyzed for each group in each assay. Results are representative of at least 2 experiments with similar results. Migration assay result is representative of 3 experiments with similar results. $*p \leq 0.05$, $**p < 0.01$; $***p < 0.001$; data are shown as the mean plus or minus standard error of the mean.

Figure 3. Pirfendone reduces the GC reaction in cGVHD mice

Spleens were harvested on day56 post-transplantation. Splenocytes were stained with fluorochrome labeled antibodies against CD4, CD19, FAS, GL4, CXCR5 and PD1. Fixed

spleen sections were stained with GC B cell marker PNA and DAPI. (A-D) Representative flow cytometry plots of GC B cells ($FAS^{+}GL7^{+}$) (A) and Tfh cells ($PD1^{hi}CXCR5^{+}$) (C) in splenocytes. Cells were gated on live CD19 cells and CD4 cells, respectively. Quantification of GC B cell and Tfh cell frequency were showed in (B) and (D). Results were pooled from 2 independent experiments with 5-8 mice per group. (E) Representative GC immunofluorescence staining images of the spleens. (F) Size of GCs in the spleen. 5-6 GCs from each mouse were photographed and size was measured. 5-6 mice from each group were analyzed. Data are representative of 2 independent experiments with similar results. (G) Frequency of GC in the spleen. The number of GCs in each spleen was divided by the size of the spleen section. 5-6 mice from each group were analyzed. Data are representative of 2 independent experiments with similar results. *$p \leq 0.05$, **$p < 0.01$; ***$p < 0.001$; data are shown as the mean plus or minus standard error of the mean.

Figure 4. Pirfenidone treatment results in long-lasting effects and is able to reduce later stage disease

Mice were transplanted as in Figure 1. Mice were untreated or treated, as indicated, with pirfenidone from day28-56 or day56-84. All the mice are evaluated on day84. (A) Pulmonary function tests on day84 showed that pirfenidone effects were significant even 4 weeks after treatment cessation. Additionally, pirfenidone treatment was effective even when treatment started at late-stage (day56) of the disease. (B) Hydroxyproline assay correlated with pulmonary function test result. (C) Masson's Trichrome staining of lung

and liver. (D&E) Quantification of trichrome staining area in the lung and liver. 5-8 mice were analyzed for each assay. *$p \leq 0.05$, **$p < 0.01$; ***$p < 0.001$; data are shown as the mean plus or minus standard error of the mean.

Figure 5. Pirfenidone treatment shows variable efficacy in the scleroderma models (A-D) BALB/c mice were conditioned with TBI (7Gy, day0), followed by infusion of 10^7 B10.D2 BM only or plus 1.8 x10^6 CD4 and 0.9 x10^6 CD8 T cells (day0). In the treatment group, mice were treated with pirfenidone from day21-55. (A) Skin clinical score based on the area of skin lesion. (B) HE staining of the skin (left) and pathology score (right). Pirfenidone reduced both clinical score and pathology score. (C) Trichrome staining of skin. Collagen was stained blue. Fibrosis was scored on a 1-5 scale based on the intensity of blue staining. Pirfenidone significantly reduced collagen deposition in skin. (D) Immunofluorescence staining of macrophage in skin samples. CD68 (red) identified macrophages. Pirfenidone significantly reduced macrophage infiltration in skin. (E) Flow cytometry analysis cytokine production and Treg percentage of splenocytes from transplanted mice. (F) B6D2F1 mice were conditioned with TBI (11 Gy split into 2 doses, day-1) followed by infusion of 5×10^6 B6 BM only or plus 1×10^6 purified T cells (day0). Where indicated, mice were treated with pirfenidone from day14-28 or day14-41. HE staining on day28 (top) & 42 (bottom) and day28 F4/80 staining (middle) indicating that pirfenidone alleviated macrophage infiltration but failed to significantly improve pathological changes. In each experiment, 5-10 mice from each group were tested. *$p \leq$

0.05, **p < 0.01; ***p < 0.001; data are shown as the mean plus or minus standard error of the mean.

Supplementary figure 1. Intravascular staining and gating strategy of lung flow cytometry analysis

(A) Flowchart of intravascular staining: Mice were injected with 4 micrograms of CD45-FITC antibody (CD45 iv) through tail vein and rested for 5 minutes before sacrificed by cervical dislocation. Blood and lymph nodes were collected. Lungs were removed, dissociated by gentleMACS dissociator (Miltenyi Biotec) and digested in collagenase D (2mg/ml) for 30 minutes in 37°C incubator. The digested lungs were filtered through 40 um cell straining to create the single cell suspension. Lung cells were stained with CD45-PE (CD45ex vivo) together with other markers of interested. Blood lymphocytes cells are $CD45iv^+$ $CD45ex\ vivo^+$, while lymphocytes in lymph nodes are $CD45iv^-$ $CD45ex\ vivo^+$. (B) Gating strategy used to identify tissue macrophages and alveolar macrophages in the lung. Tissue macrophages are identified as $CD45ex\ vivo^+F4/80^+CD11c^-CD45iv^{low}$ cells. Alveolar macrophages are identified as $CD45ex\ vivo^+F4/80^+CD11c^+$ cells.

Supplementary figure 2. Macrophage deficient and sufficient donor grafts have comparable GVL effects.

B6D2F1 recipients were conditioned with TBI (11 Gy split into 2 doses, day-1) followed by infusion of 5×10^6 B6 BM from either B6 WT FLC or $CSF1R^{-/-}$FLC only or plus 1×10^6 purified T cells (day0). 0.1×10^6 MLL-AF9-GFP leukemia cells were infused on day

0. (A) Survival curve suggests that WT and CSF1R$^{-/-}$ donor bone marrow had similar GVL responses. (B) Blood leukemia cell counts determined by GFP staining suggest that CSF1R$^{-/-}$ BM recipients have similar GVL effect on day 7 and day 30 to WT BM recipients.

Supplementary figure 3. Pirfenidone treatment does not impair the GC reaction induced by SRBC immunization

Naïve B6 mice were immunized with SRBC or PBS. In the treatment group, mice were with Pirfenidone from day-1 to day7 after immunization. Flow analysis of GC B cell (A) and Tfh cell frequencies showed that pirfenidone didn't suppress germinal center reaction induced by SRBC. (C) Serum concentration of anti-SRBC antibody analyzed by ELISA correlated with flow results. In each experiment, 5-10 mice were tested. *$p \leq 0.05$, **$p < 0.01$; ***$p < 0.001$; data are shown as the mean plus or minus standard error of the mean.

Supplementary figure 4. Pirfenidone suppresses Tcon proliferation but does not affect Treg suppressive function.

Tregs were isolated from naïve B6 mice, conventional CD4 T cells (Tcon) and antigen presenting cells (APCs) were isolated from the spleen of C57BL/6-Ly5.1 mice expressing CD45.1. Tcons were labeled with CFSE and stimulated in 0.25 microgram/ml anti-CD3. (A) Treg and Tcons were mixed at indicated ratio. APC were added to the system. Cells were cultured for 3 days with Pirfenidone or vehicle. (B) Treg were pre-treated with pirfenidone or vehicle for 1h and washed to remove residual pirfenidone. Tcon were

mixed with Treg at 3:1 ratio. CFSE dilution was analyzed by flow cytometry. Pirfenidone suppresses CD4 proliferation but does not inhibit Treg suppressive function.

Figures

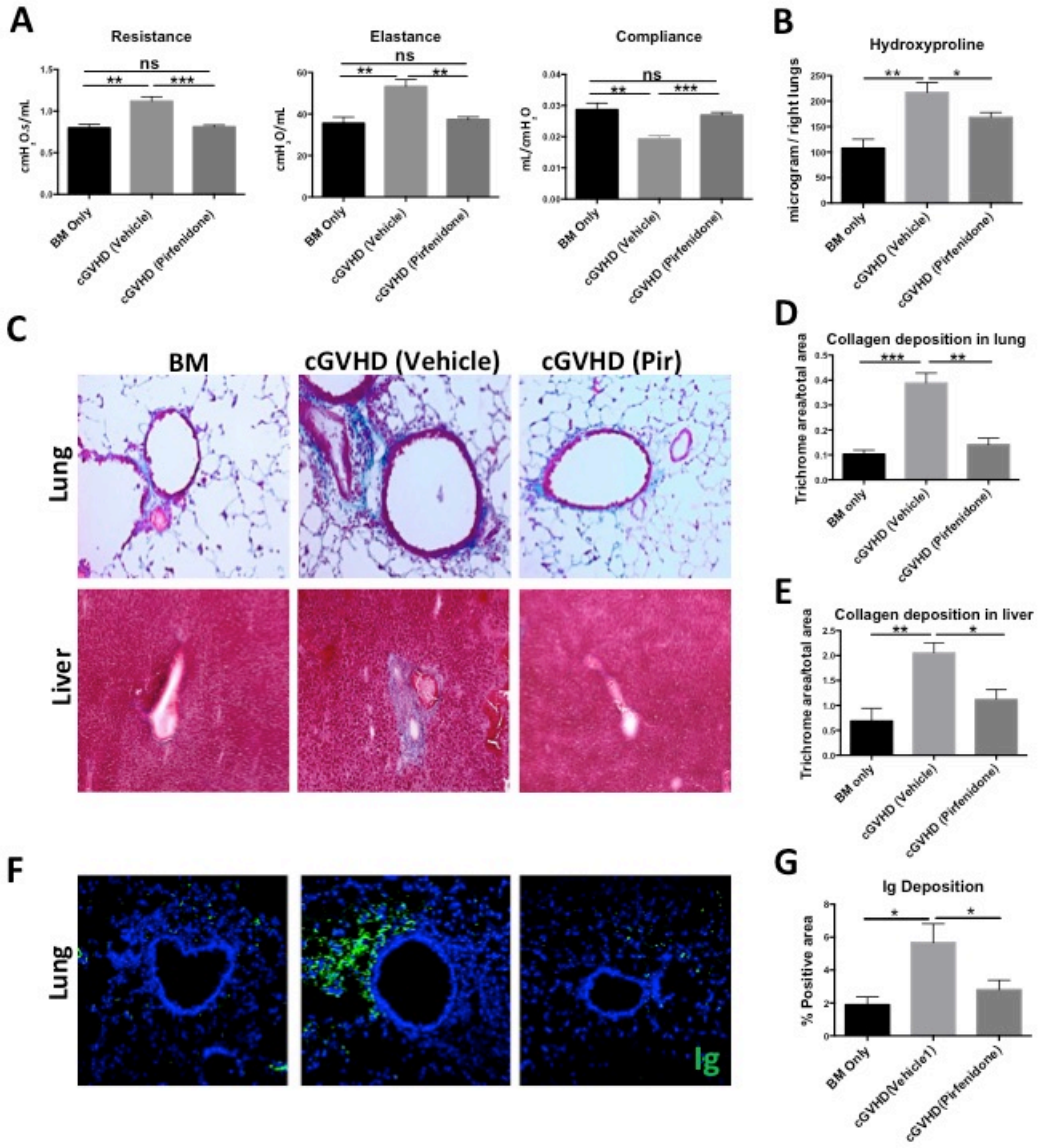

Figure 1

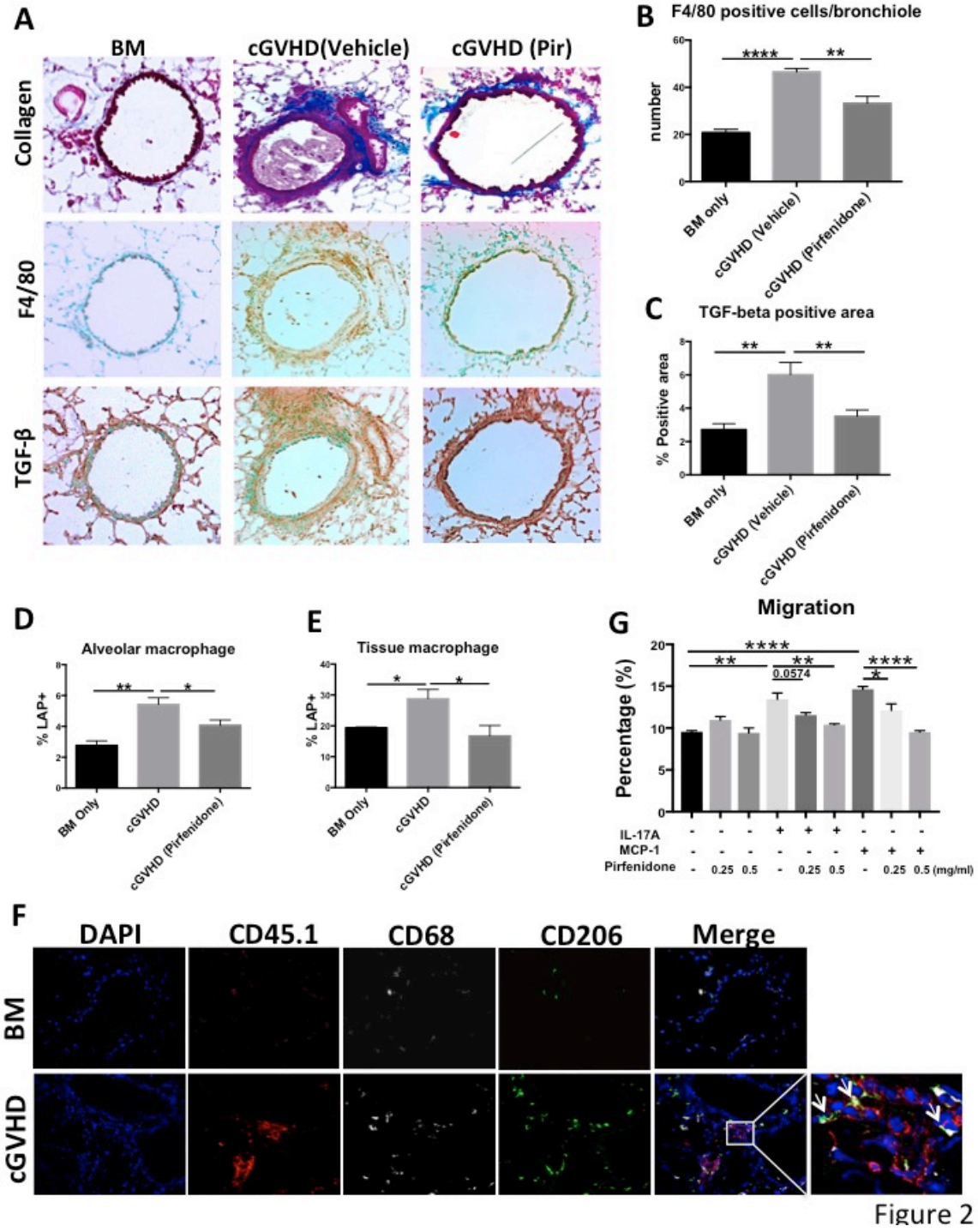
A
BM
cGVHD(Vehicle)
cGVHD (Pir)
Collagen
F4/80
TGF-β
B
F4/80 positive cells/bronchiole
number
BM only
cGVHD (Vehicle)
cGVHD (Pirfenidone)
C
TGF-beta positive area
% Positive area
D
Alveolar macrophage
% LAP+
E
Tissue macrophage
G
Migration
Percentage (%)
IL-17A
MCP-1
Pirfenidone
F
DAPI
CD45.1
CD68
CD206
Merge

Figure 2

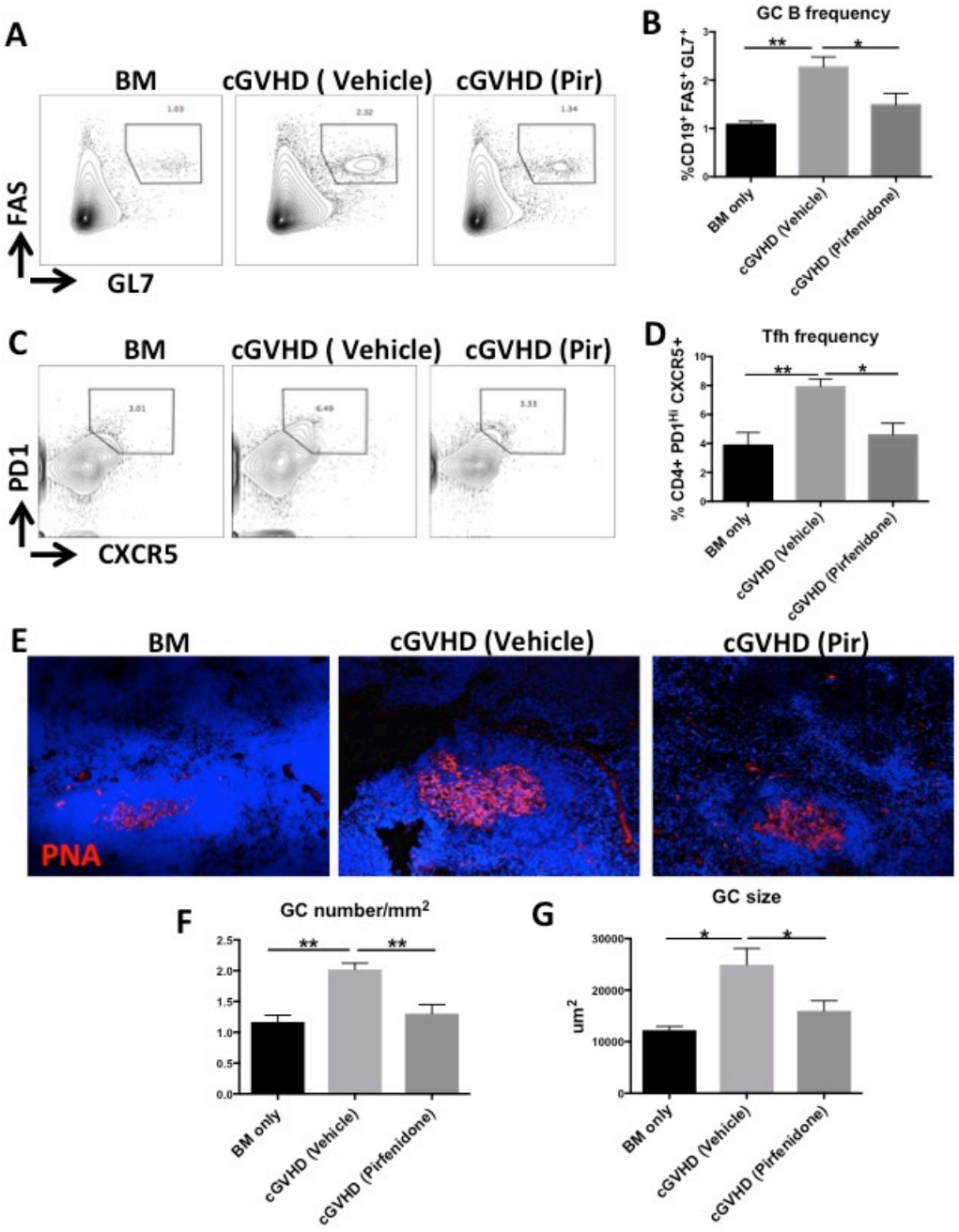
A
BM
cGVHD (Vehicle)
cGVHD (Pir)
FAS
GL7
B
GC B frequency
%CD19+ FAS+ GL7+
BM only
cGVHD (Vehicle)
cGVHD (Pirfenidone)
C
BM
cGVHD (Vehicle)
cGVHD (Pir)
PD1
CXCR5
D
Tfh frequency
% CD4+ PD1Hi CXCR5+
BM only
cGVHD (Vehicle)
cGVHD (Pirfenidone)
E
BM
cGVHD (Vehicle)
cGVHD (Pir)
PNA
F
GC number/mm2
BM only
cGVHD (Vehicle)
cGVHD (Pirfenidone)
G
GC size
um2
BM only
cGVHD (Vehicle)
cGVHD (Pirfenidone)

Figure 3

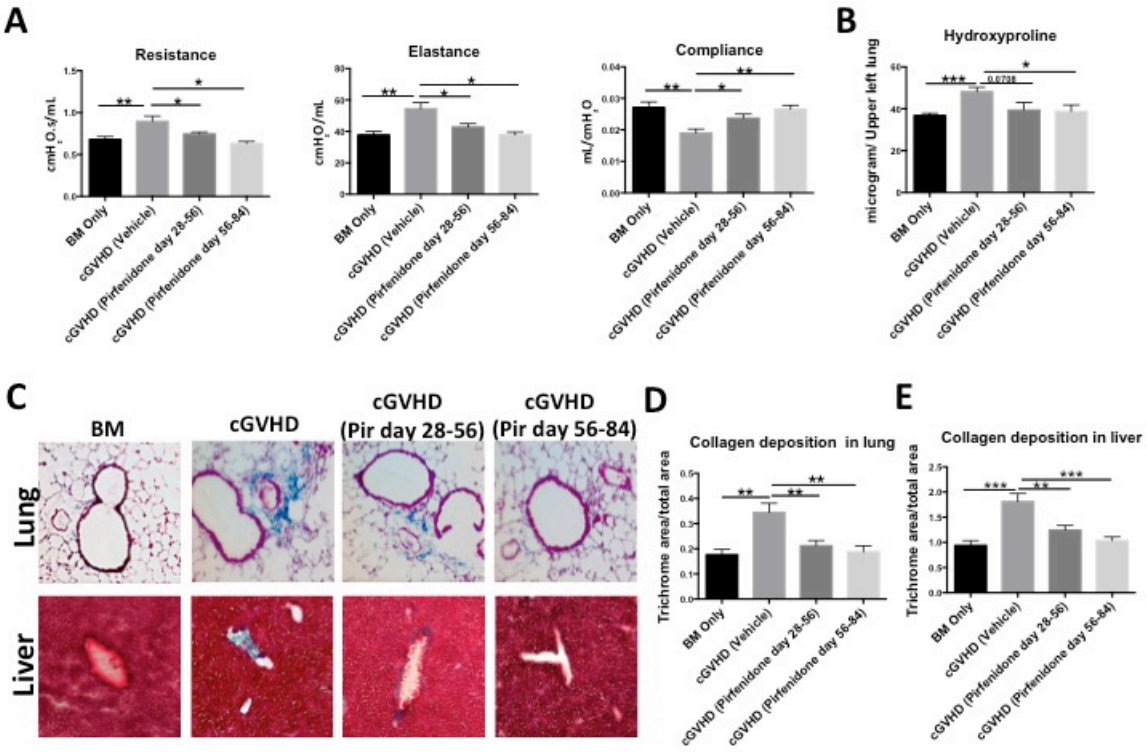
A
Resistance
Elastance
Compliance
B
Hydroxyproline
BM Only
cGVHD (Vehicle)
cGVHD (Pirfenidone day 28-56)
cGVHD (Pirfenidone day 56-84)
C
BM
cGVHD
cGVHD (Pir day 28-56)
cGVHD (Pir day 56-84)
Lung
Liver
D
Collagen deposition in lung
Trichrome area/total area
E
Collagen deposition in liver

Figure 4

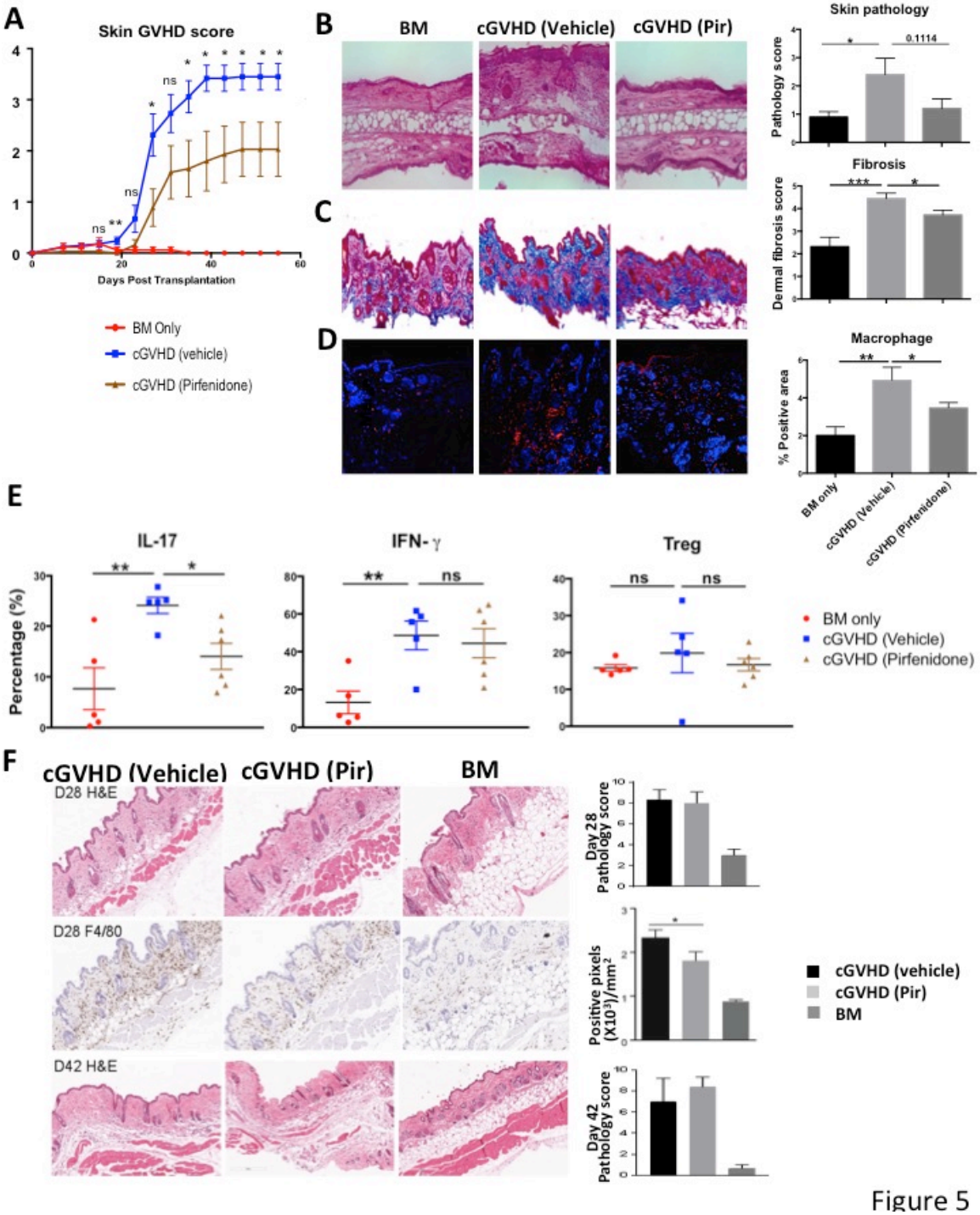
A
Skin GVHD score
Days Post Transplantation
BM Only
cGVHD (vehicle)
cGVHD (Pirfenidone)
B
BM
cGVHD (Vehicle)
cGVHD (Pir)
C
D
Skin pathology
Pathology score
Fibrosis
Dermal fibrosis score
Macrophage
% Positive area
BM only
cGVHD (Vehicle)
cGVHD (Pirfenidone)
E
IL-17
IFN-γ
Treg
Percentage (%)
BM only
cGVHD (Vehicle)
cGVHD (Pirfenidone)
F
cGVHD (Vehicle)
cGVHD (Pir)
BM
D28 H&E
D28 F4/80
D42 H&E
Day 28 Pathology score
Positive pixels (X10³)/mm²
Day 42 Pathology score
cGVHD (vehicle)
cGVHD (Pir)
BM

Figure 5

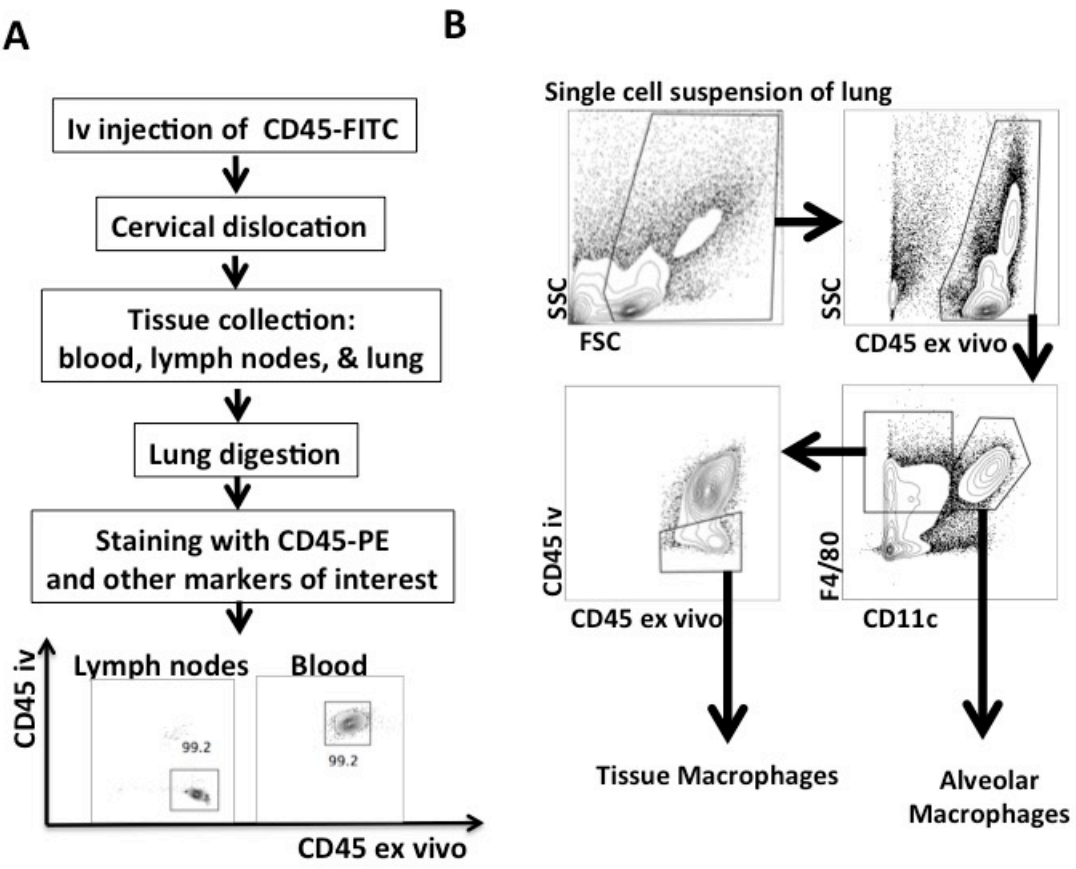

Supplementary Figure 1

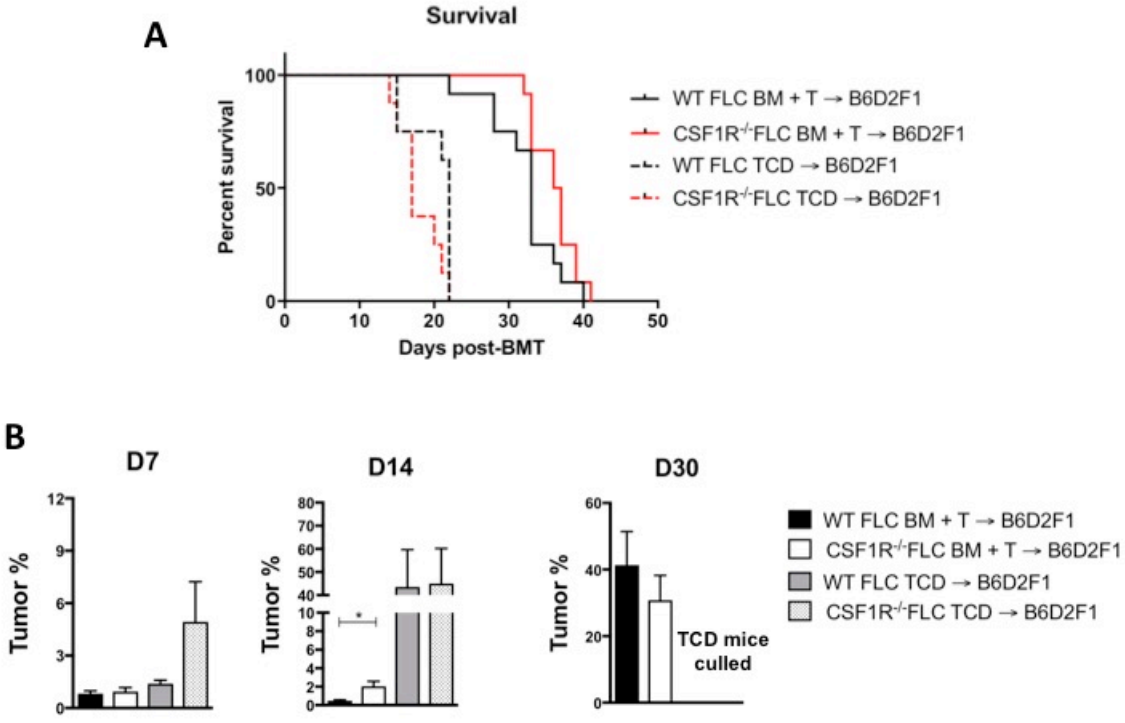

Supplementary Figure 2

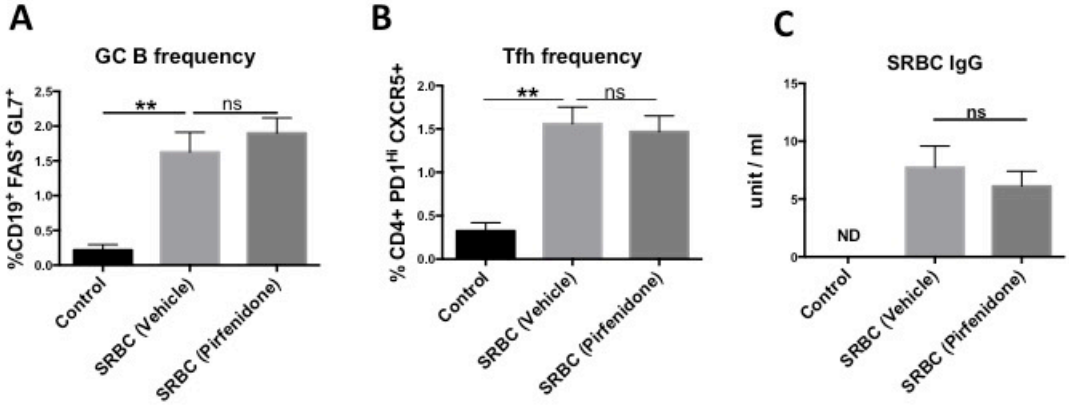

Supplementary Figure 3

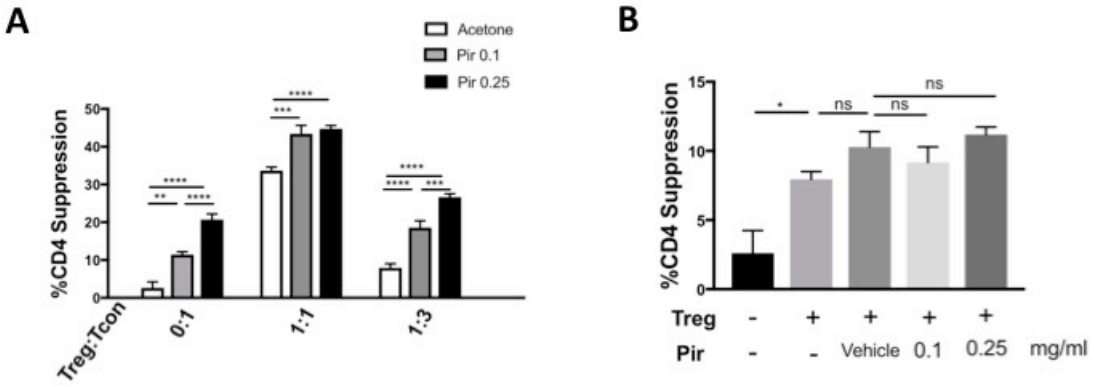

Supplementary Figure 4

Chapter 5 Murine chronic graft-versus-host disease proteome profiling discovers CCL15 as a novel druggable biomarker in patients

Submitted to the American Society for Hematologist for publication in the journal Blood.

Jing Du, Ryan Flynn, Honggang Ren, Yuko Ogata, Qing Zhang, Philip R. Gafken, Barry E. Storer, Nathan H. Roy, Janis K. Burkhardt, Wendy Mathews, Jakub Tolar, Stephanie J. Lee, Bruce R. Blazar, and Sophie Paczesny

Abstract

Improved diagnostic and treatment methods are needed for chronic graft-versus-host disease (cGVHD), the leading cause of non-relapse mortality (NRM) in long-term survivors of allogenic hematopoietic cell transplantation (allo-HCT). Validated biomarkers that facilitate disease diagnosis, classification and prognosis generally are lacking in cGVHD. Here, we conducted whole serum proteomics analysis of a well-established murine multi-organ system cGVHD model. We discovered 4 up-regulated proteins during cGVHD that are targetable by genetic ablation or blocking antibodies, including the RAS and JUN kinase activator, CRKL, and CXCL7, CCL8 and CCL9 chemokines. Donor T cells lacking CRK/CRKL prevented the generation of cGVHD, germinal center reactions and macrophage infiltration seen with wild-type T cells. Whereas antibody blockade of CCL8 or CXCL7 was ineffective in treating cGVHD, CCL9 blockade reversed cGVHD clinical manifestations, histopathological changes and immunopathological hallmarks. Mechanistically, elevated CCL9 expression was present predominantly in spleen vascular smooth muscle cells and uniquely seen in cGVHD mice. Importantly, plasma concentrations of CCL15, the human homologue of mouse CCL9, were elevated when analyzed in a previously published, well-defined cohort of 211 cGVHD patients compared to controls. High CCL15 levels were associated with high NRM. Our findings demonstrate for the first time the utility of preclinical proteomics screening to identify potential new targets for cGVHD and specifically CCL15 as a marker for cGVHD diagnosis. Successful anti-CCL9 treatment of established murine cGVHD coupled with cGVHD patient CCL15 elevation in a retrospective analysis

warrants prospective biomarker validation studies and, if confirmed, consideration for CCL15 blockade testing in human cGVHD therapeutic trials.

Introduction

Chronic GVHD occurs in approximately 30-50% of allo-HCT patients and is the leading cause of late morbidity, mortality and non-relapse mortality (NRM)[168–172]. Despite advances in the understanding of the pathobiology of cGVHD[31,173], clinical management of cGVHD remains challenging. Standard treatment for cGVHD relies on non-selective systemic immune suppression, which may render the patients susceptible to infection and relapse of primary malignancy. The diagnosis of cGVHD depends largely on clinical examinations following the National Institute of Health (NIH) diagnosis criteria [174,175]. Early diagnosis of cGVHD is crucial for disease management but is complicated by factors such as variations of time and site of disease onset, lack of fully distinctive manifestations in the early stage, overlapping symptoms with acute GVHD and lack of qualified biomarkers[176,177].

There has been increasing interest in identifying cGVHD biomarkers, driven by the applications in diagnosis, prognosis, disease stratification and guiding treatment strategies[176,178]. Different types of biomarkers have been identified. For example, B cell activating factor (BAFF) plasma levels prior to or at cGVHD diagnosis were associated with subsequent cGVHD and NRM, respectively[56,179]. Regulatory T cells (Treg) have been inversely correlated with cGVHD severity[180] and incidence[181] and may be used for

cGVHD early diagnosis[182] and prediction[183]. The majority of published biomarkers are generated from hypothesis-driven studies where a putative causative factor was specifically quantified. This method is limited by current knowledge regarding cGVHD pathogenesis. In contrast, proteomics analysis is an non-biased strategy to study the broad spectrum of differentially expressed proteins from disease and control individuals, which has proven useful in identifying new biomarkers[150,177,184]. Using this strategy, researchers has discovered that plasma matrix metalloproteinase-3 (MMP-3) is associated with lung cGVHD[185], manifested as a bronchiolitis obliterans (BO) syndrome, the most lethal form of cGVHD. In other studies, a pattern of 14 differently secreted peptides in urine allowed for early and accurate prediction of cGVHD[186].

Although allo-HCT patients have been the major target of cGVHD biomarker studies, significant heterogeneity due to distinct biological and/or clinical profiles can impede the discovery of new biomarkers[176]. On the other hand, mouse models using inbred strains housed in a specific-pathogen free facility and studied contemporaneously present an opportunity to study a more homogeneous biology without as many confounding clinical and temporal variations[121].

In this study, we conducted full spectrum proteomic analysis of serum samples from a well-established murine multi-organ system cGVHD model that incorporates clinically relevant regimens and develops auto/allo immune responses and systemic fibrosis including of BO. Using high throughput, discovery-based Mass Spectrometry (MS)

technique, we identified 4 potential biomarkers of cGVHD, of which CCL15 proved druggable and was verified in highly characterized and previously reported patient cohorts.

Materials and methods

Mice

C57Bl/6 (B6; H2b) mice were purchased from the National Cancer Institute and used at 8-12 weeks old. B10.BR (H2k) mice were purchased from the Jackson Laboratory and used at 10-14 weeks old. Mice homozygous for both floxed Crk and Crkl genes were crossed with Cd4-Cre transgenic mice on the C57BL/6 background (Taconic) to generate Crk/Crkl$^{-/-}$ T cells[187,188]. Animal protocols were approved by Institutional Animal Care and Use Committee at the University of Minnesota.

Induction of cGVHD

B10.BR mice were conditioned with intraperitoneal Cytoxan (Sigma, 120mg/kg/day, i.p., day-3&-2) and total body irradiation (8.3 Gray, day-1), followed by infusion of 10^7 B6 T cell depleted bone marrow (TCD-BM) only as non-cGVHD control, or plus 70,000 purified splenic T cells to induce cGVHD (day 0), purified as described[29,66].

Pulmonary Function Tests

cGVHD was assessed by pulmonary function tests on day 56 ± 4 days as previously described[29,66]. Nembutal anesthetized mice were intubated and ventilated using the Flexivent system (Scieq). Airway resistance, elastance and compliance were recorded and analyzed using the Flexivent software version 5.1.

Serum collection for murine proteomics

Mice were first anesthetized using a ketamine/xylazine mix. An intracardiac puncture was performed using a 27G needle and 1 mL syringe from the right ventricle. Blood was directly transferred into a dry Eppendorf tube on ice for 30 min then spun at 2000g for 10-15 min. Serum was collected and frozen at -80°C until day of use (only one freeze-thaw cycle was permitted).

Proteomics

Sample preparation and protein fractionation

Each pool contained 100 µl of serum. The two pooled serum samples were then individually immunodepleted of the 3 common hyper-abundant proteins (albumin, IgG, and transferrin) with a Multi Affinity Removal Column (MARS) 4.6 x 50 mm (Agilent) according to manufacturer's protocol. After measuring protein concentrations of depleted serum with a Micro BCA protein assay reagent kit (ThemroFisher Scientific), the volume of 100 µg aliquots were reduced to approximately 1/10 using Vivaspin® 500 (Vivaproducts) and precipitated using acetone at -20°C overnight. After centrifugation for 25 minutes at 15,000×g, acetone was decanted, and the air-dried protein pellets were dissolved in 100 µL of 8 M urea. Each sample was reduced by adding 50 µL of 10 mM dithiothreitol (DTT) in 100mM ammonium bicarbonate and incubated for 45 min at 56°C. The cysteine residues were alkylated by adding 30 µL of 50 mM iodoacetamide in 100mM ammonium bicarbonate to each vial and incubating for 30 minutes in darkness. Additional 30 µL of 10 mM DTT in 100mM ammonium biarbonate was added to neutralize iodoacetamide, and all solutions were diluted with 50 mM ammonium

bicarbonate to 1M urea concentration. All samples were trypsinized by adding 2 µg of trypsin (Promega) in 20 µL of 50 mM ammonium bicarbonate to each and incubating them overnight at 37°C. Each sample was diluted further with 0.1% TFA to 800 µL and cleaned using Oasis HLB 10mg cartridge (Waters). The cartridges were conditioned with 1 mL acetonitrile, 2 × 1 mL 65% acetonitrile 0.1% TFA in water, and 2 × 1 mL 0.1% TFA. After sample loading and washing 2 × 1 mL 0.1% TFA, peptides were eluted using 1 mL of 65% acetonitrile and 0.1% TFA in water and dried in a speed vac. Each sample was then labeled with a unique tag allowing for differential quantification. The dried peptides were dissolved in 100 µL of 200mM HEPES, pH8.5. 41 µL of acetonitrile was added to 0.8 mg each of TMT reagent, 126 and 127 (Thermo Scientific). The samples were labeled in the following order: 1) control (bone marrow (BM) only) with label 126, and 2) cGVHD (BM and T cells) with label 127. 40 µL out of 41 µL TMT solution was then added to each sample vial, and the vials were incubated at room temperature for 1 hour. The labeling reaction was quenched by adding 8 µL hydroxlamine in water. All vials were dried in a speed vac separately, re-dissolved in 0.1% TFA, combined, and cleaned with Oasis HLB 10mg cartridge (Waters) as before. The dried TMT labeled peptide sample was stored at -20°C until fractionation by strong cation-exchange (SCX) chromatography.

The sample was dissolved in buffer A (7mM potassium phosphate, 30% acetonitrile, pH 2.65) before fractionation with a SCX column (polySULFOETHYL A, 5 µm, 2.1 × 100 mm, PolyLC). Fractions were collected at 1 minute intervals at a flow rate of 200 µL/min

from 1% solvent B (7 mM potassium phosphate, 500 mM KCl, 30% acetonitrile, pH 2.65) to 60% over 40 min (1% B for 7 minutes, 6–15% B for 23 min, 15–34% B for 15 min, and 34–60% B for 10 min) as well as during column washing with 98% solvent B for 10 min. The chromatographic elution was monitored using a UV detector at λ=220 nm. These fractions were consolidated into 12 fractions using the UV trace to distribute the peptide quantities similarly. After drying them in a speed vac, peptides were desalted with Oasis HLB 10mg cartridge (Waters) as before and dried in a speed vac.

LC-MS/MS analysis

LC-MS/MS analysis was performed with an Easy-nLC 1000 (Thermo Scientific) coupled to an Orbitrap Fusion mass spectrometer (Thermo Scientific). The LC system configured in a vented format[189] consisted of a fused-silica nanospray needle (PicoTip™ emitter, 75 µm ID, New Objective) packed in-house with 25 cm of Magic C18 AQ 100Å reverse-phase media (Michrom Bioresources Inc.), and a trap (IntegraFrit™ Capillary, 100 µm ID, New Objective) containing 2 cm Magic C18 AQ 200Å. The peptide sample was diluted in 30 µL of 2% acetonitrile and 0.1% formic acid in water, and injection volumes ranging between 1-4 uL were loaded onto the column in triplicate and separated using a two-mobile-phase system consisting of 0.1% formic acid in water (A) and 0.1% formic acid in acetonitrile (B). A 90-min gradient from 7% to 30% B at a flow rate of 400 nL/min was used for chromatographic separation. The mass spectrometer was operated in a data-dependent MS/MS mode over the m/z range of 400–1500. The precursor scan mass resolution was set to 120,000. The cycle time was set to 3 seconds, and the most

abundant ions from the precursor scan were isolated for MS/MS analysis using a quadrupole with 1.6 (*m/z*) mass window, dissociated with 37% normalized HCD collision energy and analyzed with an orbitrap with the resolution set to 60,000. Selected ions were dynamically excluded for 30 seconds.

Peptide and protein identification from mass spectra of digested fragments

Proteome Discoverer™ version 2.1 was used for data analysis. The acquired LC-MS/MS data were data were searched against the Swiss-Prot mouse proteome database (August 4, 2015) using SEQUEST[190] with the following parameters: trypsin was set as the digestion protease, with 2 maximum missed cleavages; precursor and fragment error tolerance were 10 part per million (ppm) and 0.6 Dalton, respectively; Tandem Mass Tag™ (TMT) modification of N-termini was a fixed modification; and TMT modification of lysine residues, carbamidomethyl on cysteine residues, and oxidation of methionine residues as variable modifications. Identified peptides were filtered according to a 1% peptide-level false discovery rate (FDR) using Percolator[191]. Proteins with at least one identified peptide were reported. Ratios were normalized to the median of all PSMs (Peptide Spectrum Match).

The mass spectrometry proteomics data have been deposited in the ProteomeXchange Consortium[192] via the PRIDE partner repository with the dataset identifier PXD00627.

Candidate biomarker selection

This study was designed to discover and validate biomarkers by profiling the proteome of murine cGVHD sera then validating the cause-and-effect relationship for those preferentially elevated in cGVHD mice by using donor cells from relevant knockout mice or infusing neutralizing antibody to reverse established cGVHD. Four candidates (CCL8, CXCL7, CCL9, CRKL) were chosen for further in vivo analysis. Based on the murine in vivo data, three proteins (CCL15, the human equivalent of CCL9; CXCL7; CRKL) were selected to be measured in the plasma of a cohort of 211 allo-HCT recipients previously reported.[193].

Chemokine neutralizing antibody treatment

Monoclonal rat anti mouse CCL9 (MAB463), CCL8 (MAB1091) and CXCL7 (MAB790) were purchased from R&D Systems. To determine whether chemokine blockade could reverse cGVHD, cGVHD mice were intraperitoneally injected with 50-200 μg of each antibody, as indicated, from day 28-56, 3 doses/week. To evaluate the effect of anti-CCL9 on the GC reaction induced by sheep red blood cells (SRBCs), mice were immunized using SRBCs as described previously[194]. A cohort of mice was treated with anti-CCL9 antibody on days -1, 1, and 3 after immunization. On day 6 post-immunization, GC reactions were evaluated as above.

Immunohistochemical, immunofluorescence and flow cytometry analysis

Mouse lungs were inflated by 75% OCT and embedded in Optimal Cutting Temperature (OCT) compound, snap frozen in liquid nitrogen, and stored in -80°C. For trichrome staining, 8 μm cryosections were fixed for 15 min in Bouin's solution at 56°C and stained with the Masson's trichrome staining kit (Sigma HT15). For immunofluorescence staining, acetone fixed 8μm cryosections were stained with antibodies against mouse immunoglobulin (Ig) (BD 554001), αSMA (ThermoFisher 53-9760-82), CCL9 (Abcam ab9913) and CD45 (ThermoFisher 11-0451-82). Splenic GCs were identified using PNA (Vector Laboratories). Confocal images were acquired on an Olympus FluoView500 Confocal Laser Scanning Microscope at 200X, analyzed using FluoView3.2 software (Olympus). The collagen deposition area, CD68 and Ig staining were quantified using the "color segmentation" plugin of Fiji software. The intensity of CCL9 staining was quantified using the "Measure" function of Fiji software.

Flow cytometry analysis of GCs, T follicular helper and T follicular regulatory cells

To analyze GC reaction, single cell suspension of spleens was obtained and stained with fixable viability dye, fluorchrome-labeled anti-CD4 (RM4-5, BD), anti-CXCR5 (SPRCL5, eBioscience), anti-PD-1 (J43, eBioscience), anti-CD19 (eBio1D3, eBioscience), anti-GL7 (GL-7, eBioscience) and anti-Fas (J02, BD). Cells were analyzed on BD LSRFortessa. GC B cells were defined as Fas and GL7 double positive $CD19^+$ B cells. Follicular helper T (Tfh) cells were defined as PD1 and CXCR5hi $CD4^+$ $Foxp3^-$ T cells. Follicular regulatory T (Tfr) cells were defined as PD1 and CXCR5hi $CD4^+$ $Foxp3^+$ T cells.

Patients characteristics

This study was approved by the Institutional Review Board of the Fred Hutchinson Cancer Research Center (FHCRC), and informed consent was obtained from all patients or their legal guardians. The cohort of patients has previously been described[195]. Patient and GVHD characteristics for the two groups are presented in Table 1. Briefly, the cohort was composed of 211 patients treated at FHCRC from 2008 to 2011. Samples were obtained at the time of enrollment on an IRB-approved long-term follow-up study. Patients entered this study from 3 months to 66 months post-transplant. The cohort was divided into 2 groups: controls without cGVHD (n = 33), patients diagnosed with cGVHD (n = 178).

Enzyme-linked immunosorbent assay (ELISA) of human plasma

Candidate proteins validation was performed with a sequential ELISA protocol[196–198]. Commercial antibody pairs were available for 2 proteins (CXCL17 and CCL15, R&D Systems, Minneapolis, MN), and the CRKL kit was customized by Raybiotech, Norcross, GA. Elisa was run according to manufacturer's recommendations. Samples were diluted as necessary (CRKL undiluted; CXCL7 1/500; and CCL15 1/25). Lower Limit of Quantification (LLOQ), and Upper Limit of Quantification were as followed: CRKL: 1.2, 50 ng/mL; CXCL7: 15, 1000 pg/mL; CCL15: 15, 1000 pg/mL. Samples and standards were analyzed in duplicate as described previously[196–198].

Statistics

For murine experiments:

We assumed that the observations came from a normally distributed population as the recipient mice are from the same genetic background and the BM and T cells they receive are from the same donor. Differences between two groups were compared using two-tailed unpaired t test using GraphPad Prism software, version 7.02. Error bars in graphs represent mean ± standard error of the mean (SEM). Values of p less than .05 were considered significant.

For patients:

Clinical differences in the groups with and without cGVHD were compared with Student's t tests for continuous variables and Fisher's exact tests for categorical variables. Differences of CCL15 raw levels (without log transformation) between patients with and without cGVHD were compared using Mann-Whitney test using GraphPad Prism software, version 7.02. Error bars in graphs represent mean ± standard error of the mean (SEM). Logistic regression was used to evaluate the associations between cGVHD and biomarker after log transformation. Differences in cGVHD severity between groups were evaluated using the Wilcoxon two-sample tests. The analysis of NRM divided CCL15 levels at the median value among cGVHD cases and compared cases above and below the median. NRM was estimated using cumulative incidence methods, treating relapse as a competing risk, and compared between groups using Cox regression. All analyses were adjusted for significant clinical variables considering age, sex, stem cell source, conditioning (myeloablative vs. others), donor (matched sibling vs. others), and time

from HCT to sample collection. All statistical analysis was performed using SAS (Cary, NC).

Results

Murine cGVHD proteome profiling discovers novel druggable candidate biomarkers.

Using a well-established experimental models of cGVHD[29], we performed a proteomics-based approach using the Tandem Mass Tag™ (TMT) labeling with improvement in the workflow used for our recent manuscripts[185,193] that includes new depletion column, high pH reverse phase separation, and new instrument (shotgun mass spectrometry analysis on the Thermoscientific OrbiTrap fusion mass spectrometer on a 2-hour gradient). We compared 2 pools of serum in the same proteomic experiment. Pool 1 contained serum from 3 mice without cGVHD and pool 2 contained serum from 3 mice with cGVHD, all collected on day 56 post-HCT. Each pool contained 100 µl of serum and was labeled with a different TMT tag allowing for differential quantification (see details in methods). There were three replicates for each pool and analysis was performed as previously[185,193]. 885 proteins were identified. Fifty-six proteins were quantified in at least one replicate that had a ratio cGVHD/no cGVHD > 1.2 fold increase. Among these 56 proteins, four lead candidates (CRKL, CCL8, CXCL7 and CCL9) were selected based those most likely to have biological relevance for cGVHD and the availability of murine neutralizing antibody or knock-out animals, permitting in vivo cause-and-effect testing.

CRK/CRKL$^{-/-}$ T cells do not cause cGVHD mediated BO

CRKL together with CRKI and CRKII belongs to the CRK adaptor proteins family that converge and regulate a wide variety of tyrosine kinase pathways based on their protein binding domains Src Homology 2 (SH2) and SH3[199–201]. The role of CRK adaptor proteins in GVHD has been recently explored in an acute model[188]. CKR/CRKL$^{-/-}$ donor T cells do not induce acute GVHD but can generate a graft-versus- leukemia (GVL) effect, as CKR/CRKL$^{-/-}$ T cells loss the ability of integrin dependent adhesion and diapedesis to inflammatory sites; but their homing to lymphoid organs is generally intact[188].

To study the role of CRK proteins in cGVHD, we transplanted conditioned B10.BR mice with BM only or plus wildtype (wt) or CKR/CRKL$^{-/-}$ T cells[66]. Pulmonary dysfunction (indicated by increased pulmonary resistance and elastance and decreased compliance) is a hallmark feature of cGVHD in the BO model[140] and due to macrophage mediated collagen deposition and fibrosis in peribronchial areas[24], pathologically linked to Ig deposition associated with a GC response[66]. Mice received BM plus CKR/CRKL$^{-/-}$ T cells did not develop cGVHD pulmonary dysfunction as the wt T cells recipients did (Figure 1A). Collagen deposition (Figure 1B) and macrophage infiltration (Figure 1C) in peribronchial areas were significantly lower in mice that received CKR/CRKL$^{-/-}$ vs wt T cells. In addition, improved survival and significantly increased body weights were seen in mice receiving CKR/CRKL$^{-/-}$ T cells (Supplementary figure 1).

Previously, we showed that cGVHD mice develop a GC reaction and disrupting the GC reaction can ameliorate cGVHD in this model [66]. The GC reaction occurs as an result of increased Tfh/Tfr ratio and is the immunological hallmark of cGVHD[29,66]. To study the effect of donor T cell CRK/CRKL ablation on GC reaction, splenic GC B cells, Tfh and Tfr frequencies were analyzed by flow (Figures 1D-G). Recipients of CRK/CRKL$^{-/-}$ T cells have decreased Tfh frequencies (Figure 1D) and a lower Tfh/Tfr ratio (Figure 1F) than recipients of wt T cells. Although GC B cell frequencies did not differ at this time point (Figure 1G), Ig deposition in the lung was significantly lower in recipients of CRK/CRKL$^{-/-}$ vs wt T cells (Figure 1H). Taken together, these results suggest that CRK/CRKL signaling in donor T cells are required for GC reactions and the development of cGVHD, suggesting CRK/CRKL can be a therapeutic target.

CCL9 but neither CXCL7 nor CCL8 blockade in vivo reverses established cGVHD

To determine the potential role of CXCL7, CCL8 and CCL9 in cGVHD pathogenesis, in vivo antibody blockade studies were performed. To evaluate the therapeutic role of blocking each chemokine, cGVHD mice were given each antibody intraperitoneally starting from day 28, when lung dysfunction is readily evident, to the end of each experiment. Neutralizing antibody (100 μg/dose) to CCL8 did not affect cGVHD. Neutralizing antibody (100 μg/dose) to CCL7 showed a trend toward disease reduction. However increased CXCL7 antibody dose (200 μg) did not improve the effect but resulted in similar pulmonary function as non-treated mice (Figure S2). CCL9 blockade at a lower dose (50 μg) incompletely reduced the lung disease (data not shown), while an

increased dose at 100 μg significantly improved each pulmonary function parameters (Figure 2A). Survival and weight of anti-CCL9 treated mice were also slightly improved (Figure S3).

CCL9 and its human analogue CCL15 are well-recognized for its role in wound healing[202]. Therefore, we examined collagen deposition in the lung by trichrome staining. CCL9 blockade significantly reduced collagen deposition in lung compared to non-treated cGVHD mice (Figure 2B). CCL9 also plays important role in the chemotaxis of innate myeloid suppressor cells[203–205] and adaptive immune cells such as CD4 and CD8 T cells [206–208]. Thus we sought to determine whether CCL9 blockade has an effect on macrophage infiltration into the lungs of cGVHD mice, which has been proven to participate cGVHD pathogenesis[24,26]. CCL9 blockade significantly reduced macrophage infiltration compared to cGVHD controls (Figure 2C). CCL9 blockade also significantly reduced Ig deposition in the lung (Figure 2D), and splenic GC B cells and Tfh frequencies along with the Tfh/Tfr ratio (Figure 2E-H). .

Spleen vascular smooth muscle cells and lung increase CCL9 expression during cGVHD

To determine the cellular source that contributed to increased serum CCL9 concentrations in cGVHD, we examined the expression of CCL9 in the spleen, the site of the GC response. CCL9 expression is significantly higher in cGVHD mice than in BM only mice (Figure 3A). However, neither CD11b myeloid cells nor cells in the GCs were the main

source of CCL9 (Figure 3A). Instead, CCL9 was dominantly expressed in the vasculature (Figure 3A), but not in hematopoietic cells that express CD45 (Figure S4A). To further explore the cell types that produce CCL9 during cGVHD, we co-stained CCL9 with smooth muscle marker α smooth muscle actin (αSMA) (Figure 3B) and endothelial cell marker CD31 (Figure S4B). CCL9 was mainly produced by smooth muscle cells (SMCs) but not endothelial cells in cGVHD mice. CCL9 expression in splenic SMCs was only seen in cGVHD mice but not BM only mice (Figure 3B), suggesting CCL9 expression may be induced by allo-responsive donor T cells. Blockage CCL9 using monoclonal antibody did not alter the expression level or pattern of CCL9 expression on SMCs, suggesting anti-CCL9 antibody blocked the function, rather than expression of CCL9.

Having shown that CCL9 is increased in the spleens of cGVHD mice and CCL9 is expressed in higher amounts at sites of vasculature, we next sought to determine whether increased CCL9 expression in splenic GCs is uniquely induced in cGVHD, or this is a common mechanism during GC reactions. Naïve mice were immunized with SRBCs to induce GC reactions and treated with anti-CCL9 antibody (100 microgram) on days -1, +1, and +3. CCL9 staining suggests that in the vessel areas of the SRBCs immunized spleens, CCL9 expression was not increased as in cGVHD mice (Figure S5A). GC B cells and Tfh cell frequencies were unaltered by CCL9 blockade (Figure S5B), in accordance with lack of increased CCL9 expression in spleen SMCs. This result suggests that CCL9 expression in the vascular SMCs is uniquely induced during cGVHD and targeting this unlikely affect antibody responses.

A recent study suggested angiogenesis happens early after allo-HSCT, and play an important role in initiating acute GVHD[209]. Since SMCs are a major cellular component of the vascular wall, we explored whether cGVHD has higher SMCs volume. We quantified αSMA and found that cGVHD spleens have significantly higher αSMA staining areas than BM only mice, suggesting neoangiogenesis may be associated with cGVHD. Increased smooth muscle volume was not altered by CCL9 blockade (Figure S6), suggesting CCL9 acts downstream of increased SMCs during cGVHD pathogenesis. We further examine CCL9 expression in the lung, where fibrosis occurs as a result of GC reaction and macrophage activation. Different from the BM only splenic SMCs with barely detectible CCL9, BM only lungs express low level of CCL9, mainly by the lung bronchiolar wall (Figure 3C). This expression is increased during cGVHD, but not altered by CCL9 antibody blockade (Figure 3C). Together, these results suggest that during cGVHD CCL9 expression is specifically induced in splenic SMCs and increased in lung, and that the effect of blocking antibody on cGVHD is likely due to blockade of CCL9 chemotaxis function (Figure 3D).

CCL15, the human homologue of murine CCL9, is a predictive biomarker for cGVHD incidence and NRM in a well-defined patient cohort.

CCL9 blockade and CRK/CRKL deficiency of donor T cells significantly ameliorated mouse cGVHD. Therefore, we sought to determine the relevance of CCL9 and CRKL as biomarkers in human plasma by comparing patients with and without cGVHD. We also tested CXCL7 to confirm the strength of our workflow focusing on mechanistically

relevant and druggable markers. We measured the concentrations of these 3 proteins in samples from well-defined cohorts, consisting of 178 HCT patients with cGVHD and 33 HCT controls without cGVHD. We also measured the proteins in 15 healthy donors as baseline values. Patient and GVHD characteristics for the two groups are presented in **Table 1**. Patient sex and median age at the time of transplantation were similar between the two groups. There was a trend toward over-representation of unrelated donors in the cGVHD group. As expected, the use of peripheral blood stem cells (PBSCs) was a risk factor for cGVHD, whereas the use of full-intensity conditioning was not. The incidence of prior aGVHD was similar in both groups. According to the NIH global severity score, 7% of the patients had mild cGVHD, 58% had moderate cGVHD, and 35% had severe cGVHD. Plasma samples were collected at similar times from both cGVHD patients and controls: a median of 391 days (192–1852 days) post-HCT in the cGVHD group compared to 369 days (161–3641 days) post-HCT in the control group (p=0.84).

As hypothesized based on the murine cGVHD data, there was no significant difference in CXCL7 levels between patients with and without cGVHD (data not shown). Using a customized CRKL1 ELISA kit > 95% of the plasma values were below the detection level of 1.2ng/ml even when using undiluted plasma. Thus, we have no evidence of CRKL1 elevation in cGVHD patients.

In contrast, CCL15 concentrations were significantly increased in cGVHD patients as compared to patients following allo-HCT without cGVHD, p=0.0125 (**Figure 4A**). We next evaluated whether CCL15 was associated with cGVHD severity. Very few patients

had mild cGVHD, and thus, these patients were combined with those who presented with moderate cGVHD. CCL15 was log-transformed and logistic regression was used to evaluate its association with cGVHD. Analyses of CCL15 were adjusted for the following seven clinical variables: age, sex, donor (matched sibling vs. others), stem cell source (PBSC vs. others), conditioning intensity (myeloablative vs. others), prior aGVHD, and time from HCT to sample collection. Notably, only donor type (p=0.03) and PBSCs as the stem cell source (p=0.01) were significant in multivariate analysis. Using Wilcoxon two-sample tests, we compared CCL15 between groups with different cGVHD severity (none, mild/moderate, and severe). The differences of CCL15 between the two severity groups and controls are statistically significant (p=0.02 and p=0.03, respectively) but not between the severity groups (p=0.99), (**Figure 4B**). cGVHD patients with CCL15 values above the median were at higher risk of NRM than patients with low CCL15 levels [Hazard Ratio (HR)=2.89 (1.1-7.4), p=0.03, (**Figure 4C**). Altogether, these data suggest that CCL15 represents a clinically relevant biomarker as well as a druggable biomarker with in vivo activity.

Discussion

Using high throughput, discovery-based Mass Spectrometry (MS) technique, we conducted full spectrum proteomic analysis of serum samples from a well-established murine multi-organ system cGVHD model and identified 56 differentially expressed proteins, 4 of which were potential biomarkers of cGVHD. We identified two biomarkers, CRK/CRKL and CCL9, that were shown to be essential for inducing and maintaining

murine cGVHD. Of these, the human homologue of CCL9, CCL15, was found to be increased in cGVHD patient plasma and correlated with NRM rate, suggesting that CCL15 may serve as a potential biomarker for cGVHD early diagnosis and therapy. cGVHD patients have very limited treatment therapies. Targeting CCL9 in the mouse model reversed cGVHD clinical manifestations and restored immunological balance, which was disturbed during cGVHD. Of interest, blocking RANTES (CCL5), which is increased in the lung after allo-HSCT[210] and shares the same receptor CCR1 with CCL15, has been shown to alleviate acute GVHD[211], suggesting that CCL15 may be useful as a biomarker and potentially as a therapeutic target in patients with concurrent acute and chronic GVHD.

CCL15 is produced in a wide variety of tissue and cell types[212] in steady state and is increased in autoimmune diseases such as rheumatoid arthritis[213] and asthma[214]. Similar to CCL15, CCL9 is expressed constitutively in tissues and cells including both hematopoietic and non-hematopoietic origin. CCL-9 produced by structural cells such as follicle associated epithelium[207], airway smooth muscle[215] and lung endothelial cells[216] play roles in recruiting dendritic cells and monocytes and contribute to disease pathogenesis. In this study, we show uniquely increased CCL9 expression in cGVHD spleens in the αSMA positive vascular SMCs areas but not in CD11b myeloid cells or CD45 hematopoietic cells, highlighting a previously unappreciated role of vascular SMCs in cGVHD pathogenesis. Vascular SMCs can be converted into chemokine-expressing cells that trigger the recruitment of immune cells in response to inflammatory signals[217,218]. Increased spleen SMCs CCL9 expression during cGVHD is not due to pre-

transplantation conditioning or a consequence of germinal center reaction, as neither BM only recipients nor SRBC immunized mice display this pattern, highlighting CCL9 increase is a specific mechanism to meet the need of increased GC reactions during cGVHD and can be a target for cGVHD therapy. A recent study suggests neo angiogenesis occurs early after allo-HCT that proceeds inflammation and play a active role in the initiation of acute GVHD[209]. We identified that SMCs - the major cellular component of vascular wall were also increased in spleen during cGVHD. Thus increased CCL9 expression in cGVHD spleen was a combined effect of increased SMCs volume and increased CCL9 expression from SMCs. To identify potential cell populations recruited by CCL9 in spleen, we co-stained CD11b, CD4 and CD68 but did not find a positive correlation (data not shown). Thus the cells being recruited by CCL9 in spleen can be heterogenic.

Increased CCL9 was also noticed in cGVHD lungs and blocking CCL9 reduced macrophage infiltration, collagen deposition and improved pulmonary function. Previously we reported that macrophages infiltrate the cGVHD lung and contribute to cGVHD pathogenesis by producing TGF-β[24]. Thus reverse of cGVHD by CCL9 blockade is at least partially due to blocking macrophage chemotaxis by the CCR1/CCL9 axis. Thus we hypothesize the during cGVHD, splenic SMCs and lung bronchiolar wall are activated by allo-responsive donor T cells to recruit cells for GC reactions in spleen and macrophages in lung, thus blocking CCL9 function by CCL9 antibody reverse cGVHD (Figure 3D).

Although CXCL7 and CCL8 levels were increased in cGVHD sera, blocking neither of them showed benefit to cGHVD. Both CXCL7 and CCL8 can be produced in response to inflammatory stimuli and exert chemotactic functions towards neutrophils and Th2 cells, respectively[219,220]. We hypothesize the CXCL7 and CCL8 was produced as a result of tissue damages caused by pre-transplantation conditioning and donor T cell allo-responses. However, CXCL7 and CCL8 may not directly involve in cGVHD pathogenesis based upon neutralizing antibodies results. In addition, plasma CXCL7 was not increased in cGVHD patients, in accordance with lack of treatment effect by CXCL7 blockade on murine model. We did not test CCL8 in human plasma both due to its total lack of cGVHD inhibition and its elevation in several inflammatory and tumoral diseases lacking specificity as a possible cGVHD plasma marker. CRK/CRKL are intracellular adaptors proteins that can regulate immune responses[221]. Both our mice proteomics data and a previous report[201] suggest CRK/CRKL can be secreted into the extracellular milieu. However, the circulating levels of CRK/CRKL in patient plasma were below the detection limit when measured by Elisa and therefore definitive conclusions cannot be made on its potential role as a biomarker until more sensitive ELISAs become available.

In summary, we conducted for the first time full-spectrum proteomic analysis of a well-characterized murine model of cGVHD as a novel discovery engine for potential cGVHD biomarkers that could be translated into the clinic. This has led to the identification of 2 druggable candidate biomarkers, of which the human homologue of CCL9, CCL15, was verified in a previously published cGVHD cohort of 211 HCT patients. This study

highlighted the potential of CCL9/CCL15 as a biomarker for cGVHD early diagnosis and prediction of NRM, both unmet need yet crucial for cGVHD management, and as a treatment target. Further validation on larger independent cohort is warranted.

Acknowledgements:

The authors would like to thank the clinicians at all of the institutions who participated in accrual of samples; the Fred Hutchinson Cancer Research Center data managers, particularly Kate Chilson, for excellent management of the database and biobank.

Funding:

This work was supported by the National Cancer Institute (R01CA168814, to S.P.; R01CA118953 to S.J.L.; U54CA163438 to S.J.L.; P01CA142106 to B.R.B.), National Institute of Allergy and Infectious Diseases (P01 AI056299 to B.R.B.), the Leukemia & Lymphoma Society Scholar Award (1293-15, to S. P.) and Translational Research Grant (6452-15 to B.R.B.), and the Lilly Physician Scientist Initiative Award (to S.P.). The Chronic GVHD Consortium (U54 CA163438) is part of the National Center for Advancing Translational Science (NCATS) Rare Diseases Clinical Research Network (RDCRN). RDCRN is an initiative of the Office of Rare Disease Research (ORDR), NCATS, funded through a collaboration between NCATS and the National Cancer Institute. The FHCRC Proteomics Facility is partially funded by Cancer Center Support grant P30 CA015704 from the National Institutes of Health. The Fusion Orbitrap mass spectrometer was purchased with a grant from the M.J. Murdock Charitable Trust. The

content of this article is solely the responsibility of the authors and does not necessarily represent the official views of the NIH.

Author Contributions:

J.D. designed and performed research, analyzed data, and wrote the paper; R.F., H.R., N.H.R., J.K.B., W.M. and J.T. designed and performed research, analyzed data; Y.O., Q.Z., and P.G. designed, performed and analyzed proteomics data; B.E.S. was the study statistician, S.J.L. performed clinical data collection and quality assurance, interpreted the patients data; B.R.B and S.P. conceived the project, designed experiments, analyzed data, and wrote the paper.

Conflict of Interest:

S.P. is an inventor on a patent on "Methods of detection of graft-versus-host disease" (13/573766).

Table 1: Patient and cGVHD characteristics

Table 1: Patient and GVHD characteristics

	cGVHD Cohort (n=211)		
	cGVHD (n=178)	Controls (n=33)	p
Age, years			
Median	52	54	0.55
Range	19-79	22-72	
Sex, n (%)			
Female	77 (43)	18 (55)	0.23
Male	101 (57)	15 (45)	
Donor type and match, n (%)			
Matched sibling	66 (37)	18 (55)	0.06
Other*	112 (63)	15 (45)	
Stem cell source, n (%)			
PBSC	161 (90)	26 (79)	0.05
Other	17 (10)	7 (21)	
Conditioning regimen intensity, n (%)			
Myeloablative	105 (59)	19 (58)	0.88
Non Myeloablative	73 (41)	14 (42)	
Prior acute GVHD, n (%)			
yes	135 (76)	24 (73)	0.70
No	43 (34)	9 (37)	
Time post-HCT to cGVHD diagnosis, days			
Median	210	na	na
Range	38-1757	na	
Time post-HCT to sample acquisition, days			
Median	391	369	0.84
Range	192-1852	161-3641	
NIH global severity, n (%)			
Mild	13 (7)	na	na
Moderate	103 (58)	na	
Severe	62 (35)	na	

na: not applicable.*other: only 4 cord blood cells transplant among the cases and none among the controls
§ matched for time since transplant to sample collection, transplant center, prior acute GVHD, conditioning intensity, and graft source from the U54 multicenter cohort (Fred Hutchinson Cancer Research Center, Dana-Farber Cancer Institute, University of Minnesota, H. Lee Moffitt Cancer Center, Vanderbilt University Medical Center, Roswell Park Cancer Institute, Washington University St. Louis, Cleveland Clinic).
‡ 8 patients missing data for prior acute GVHD, 4 cases missing data for NIH severity.

Figures legends

Figure 1: CRK/CRKL$^{-/-}$ T cells do not cause cGVHD mediated BO

Conditioned B10.BR mice were transplanted with B6 donor BM only, or plus 70000 wt or CRK/CKRL$^{-/-}$ T cells. (A). Pulmonary tests including lung resistance, elastance and compliance suggest CRK/CKRL$^{-/-}$ donor T cells did not cause cGVHD. (B). Masson's Trichome staining in lung identified collagen in blue. Quantification of blue areas suggests recipients of CRK/CKRL$^{-/-}$ donor T had significantly lower collagen deposition the wt T cell recipients. (C). Immunofluorescence staining of macrophage marker CD68 suggests significantly lower macrophage infiltration in the CRK/CRKL$^{-/-}$ T recipients. (D-G). Flow cytometry analysis of cell frequencies in GC reactions including Tfh (D), Tfr (E), Tfh/Tfr ratio (F) and GC B cell (G). GC analysis suggest CRK/CKRL$^{-/-}$ donor T cells did not induce GC reactions. (H) Immunofluorescence staining of Ig deposition in the lung. Quantification suggests recipients of CRK/CKRL$^{-/-}$ donor T cells have lower Ig deposition. Images were taken by Olympus FV1000 upright confocal at 200x magnification. Data shown are representative of 2 independent experiments with 5-8 mice per group. Unpaired student T-test was used when comparing 2 groups. Significance: *P<0.05; **P<0.01; ***P< 0.001; ****P<0.0001.

Figure 2: CCL9 blockade reverses cGVHD clinical manifestations and immunological hallmark

Transplanted mice were treated with anti CCL9 (100mg) from day28 post bone marrow transplant. Experiments were terminated at day 42-56. (A). Pulmonary function tests

suggest CCL9 blockade reverse cGVHD lung disease. Collagen deposition (B), macrophage infiltration (C) and Ig deposition (D) were significantly reduced by CCL9 blockade. (E-H). Splenic GC reactions analysis. Frequency of GC B Cells (E), Tfh (F) and Tfh/Tfr ratio (H) were normalized by CCL9 blockade. Data shown are representative of 2-3 independent experiments with 5-8 mice per group. Unpaired student T-test was used when comparing 2 groups. Significance: *P<0.05; **P<0.01; ***P< 0.001; ****P<0.0001.

Figure 3: Spleen vascular smooth muscle cells and lung increase CCL9 expression during cGVHD

(A). Immunofluorescence staining (200 x magnification) of spleen sections of BM only and cGVHD mice. White arrow indicates CCL9 was dominantly expressed by spleen vasculature, but not CD11b cells or cells in the GC areas. Quantification of CCL9 staining areas suggests cGVHD mice have increased CCL9 expression in spleen. (B). Costaining of αSMA with CCL9 in the spleen. Images were taken at 400x magnification. αSMA positive cells of cGVHD mice had increased CCL9 expression that was not altered by CCL9 blockade. Images were quantified by Fiji software "color segmentation" plugin. (C). CCL9 expression in lung. Quantification was done by Fiji software "measure" function. Data shown are representative of 2-3 independent experiments with 5-8 mice per group. Unpaired student T-test was used when comparing 2 groups. Significance: *P<0.05; **P<0.01; ***P< 0.001; ****P<0.0001. (D) Possible mechanism by which CCL9 contributes to cGVHD pathogenesis.

Figure 4: Increased CCL15 levels are associated with high non-relapse mortality rate but not disease severity

(A) Plasma concentrations of CCL15 was measured by ELISA in a cohort of 178 cGVHD patients, 33 no cGVHD transplant recipients and 15 healthy donors. Differences of CCL15 levels between patients with and without cGVHD were compared with Wilcoxon two-sample tests. CCL15 concentration was significantly higher in cGVHD patients as compared to no cGVHD. (B) cGVHD patients were sub-categorized into 2 groups based on severity of disease. Data are illustrated as box and whisker plots, with the whiskers indicating the 90th and 10^{th} percentiles. P values compare controls (n=33) versus patients with mild to moderate cGVHD (n=116), and patients with mild to moderate cGVHD versus those with severe cGVHD (n=62), according to Wilcoxon two-sample tests. CCL15 levels were not different between severity groups. (C) Nonrelapse mortality (NRM) stratified by CCL15 concentrations. The cumulative incidence of NRM is plotted (total of 21 NRM deaths), divided according to the median value of CCL15 among patients with cGVHD. The NRM at 48 months was higher for the group above the median value [Hazard Ratio (HR) = 2.89 (1.1-7.4), P = 0.03].

Figure S1. CRK/CRKL-/- donor T cells result in improved survival and significantly higher body weight

Survival and weight were recorded after transplantation. CRK/CKRL$^{-/-}$ donor T recipients had 100% survival versus 75% in wt T recipients, which were not significantly different. At periodic time points, mean weights were significantly higher in CRK/CKRL$^{-/-}$ vs wt

donor T recipients. Data shown are representative of 2 independent experiments with 5-8 mice per group. Unpaired student T-test was used when comparing 2 groups. Significance: *P<0.05; **P<0.01; ***P< 0.001; ****P<0.0001.

Figure S2: Neutralizing CXCL7 or CCL8 did not affect cGVHD

Transplanted mice were treated with anti CXCL7 (100mg or 200mg/dose) or CCL8 (100mg/dose) from 28-56 days post bone marrow transplant. Pulmonary function test suggest neither anti-CXCL7 nor anti-CCL8 significantly altered cGVHD lung disease. Unpaired student T-test was used when comparing 2 groups. Significance: *P<0.05; **P<0.01; ***P< 0.001; ****P<0.0001.

Figure S3 Anti-CCL9 treatment slightly improve survival and weight of cGVHD mice.

Survival and weight were recorded after transplantation. Anti-CCL9 treatment group had 100% survival versus cGVHD group 80%. No significant differences were seen in weight curves.

Figure S4: Neither CD45 hematopoietic cells or CD31 endothelial cells are the main producers of CCL9 in cGVHD spleen

(A). Staining of CD45 and CCL9 in spleen suggest hematopoietic cells were not the main producers of CCL9 during cGVHD. Images were taken at 200 x magnification. (B) CCL9

and CD31 staining did not co-localize suggesting CD31 endothelial cells were not the source of CCL9. Images were taken at 200 x magnification.

Figure S5: CCL9 did not involve in SRBC induced GC response

Naïve B6 mice were immunized by 100 microliter of 10% SRBC. CCL9 (100mg) was given on days -1, +1, and +3 of immunization. Mice were sacrificed on day 6. (A) Immunofluorescence staining of spleen sections suggests CCL9 was not increased in SRBC immunized mice. Images were taken at 200 x magnification (B) Flow cytometry analysis of GC reactions suggests anti-CCL9 antibody had not effect on SRBC induced GC reactions. Unpaired student T-test was used when comparing 2 groups. Significance: *P<0.05; **P<0.01; ***P< 0.001; ****P<0.0001.

Figure S6: cGVHD mice have higher vascular SMCs volume that was not altered by anti-CCL9 antibody.

Immunofluorescence staining of αSMA in spleen at 100 x magnfication. cGVHD group had significantly higher aSMA positive areas than BM only group, which was not altered by anti-CCL9 treatment. Data shown are representative of 2 independent experiments with 5-8 mice per group. Unpaired student T-test was used when comparing 2 groups. Significance: *P<0.05; **P<0.01; ***P< 0.001; ****P<0.0001.

Figures

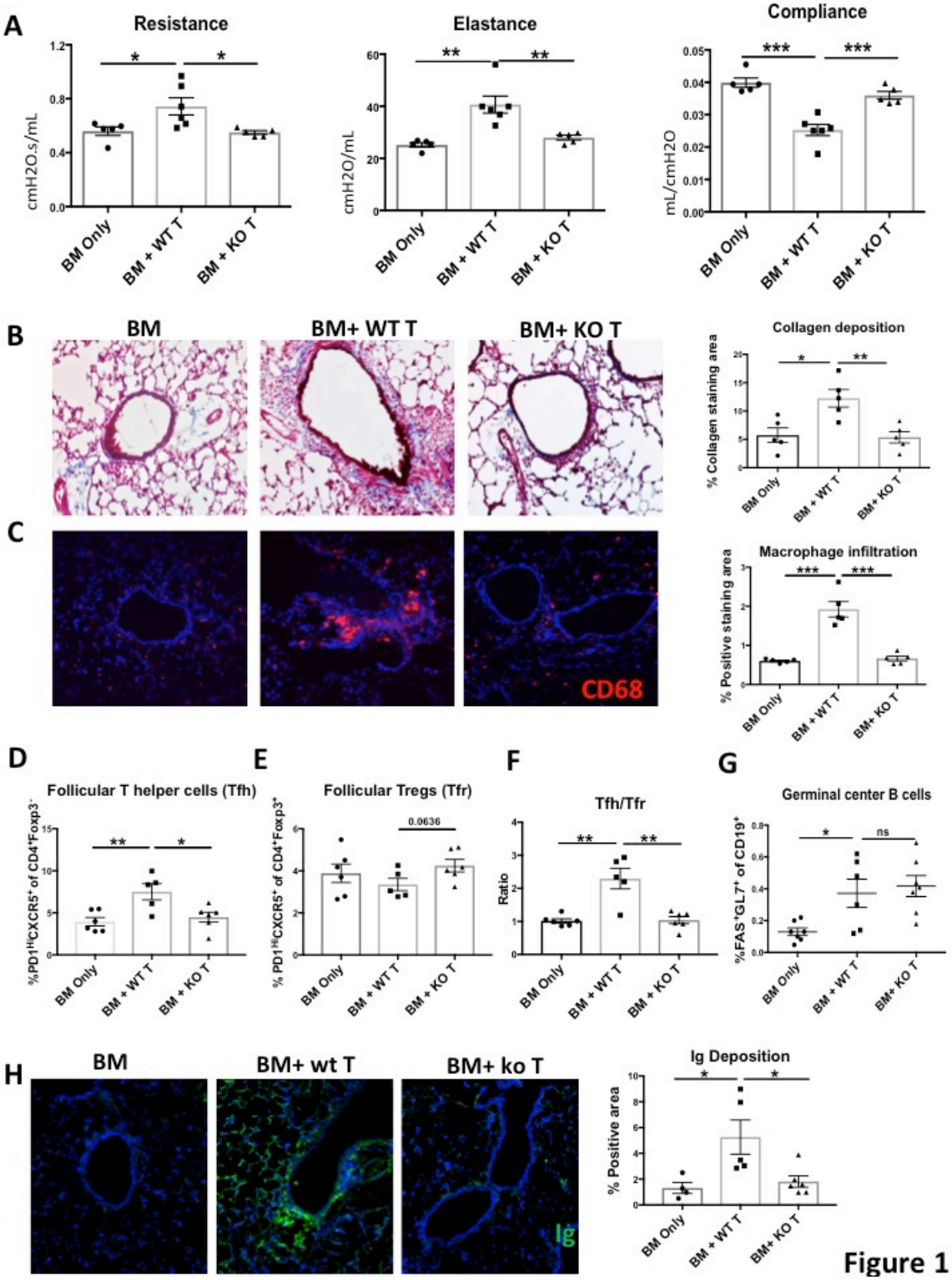

Figure 1

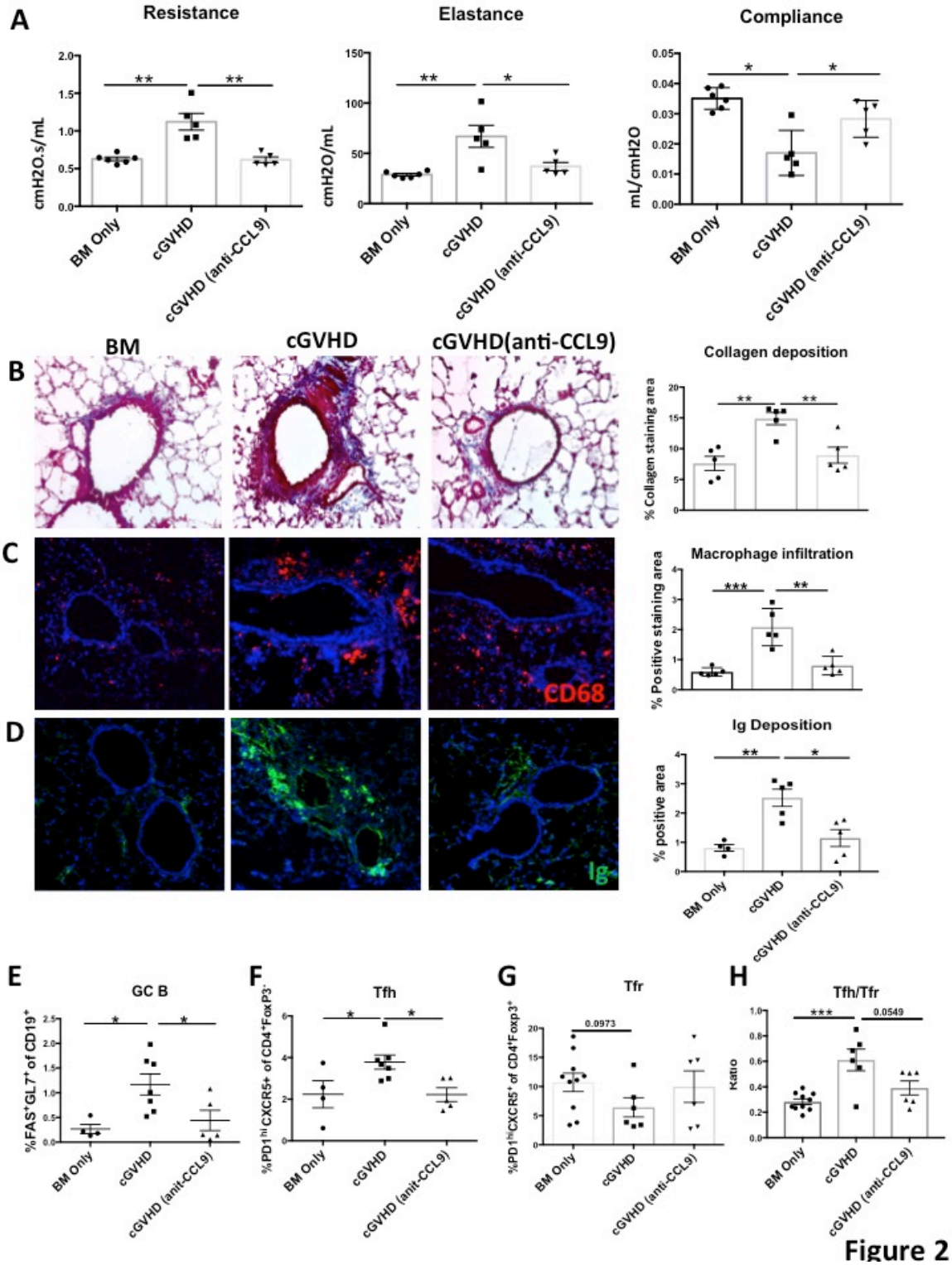
A
Resistance
Elastance
Compliance
cmH2O.s/mL
cmH2O/mL
mL/cmH2O
BM Only
cGVHD
cGVHD (anti-CCL9)
B
BM
cGVHD
cGVHD(anti-CCL9)
Collagen deposition
% Collagen staining area
C
CD68
Macrophage infiltration
% Positive staining area
D
Ig
Ig Deposition
% positive area
E
GC B
%FAS+GL7+ of CD19+
F
Tfh
%PD1hi CXCR5+ of CD4+FoxP3-
G
Tfr
0.0973
%PD1hiCXCR5+ of CD4+Foxp3+
H
Tfh/Tfr
0.0549
Ratio

Figure 2

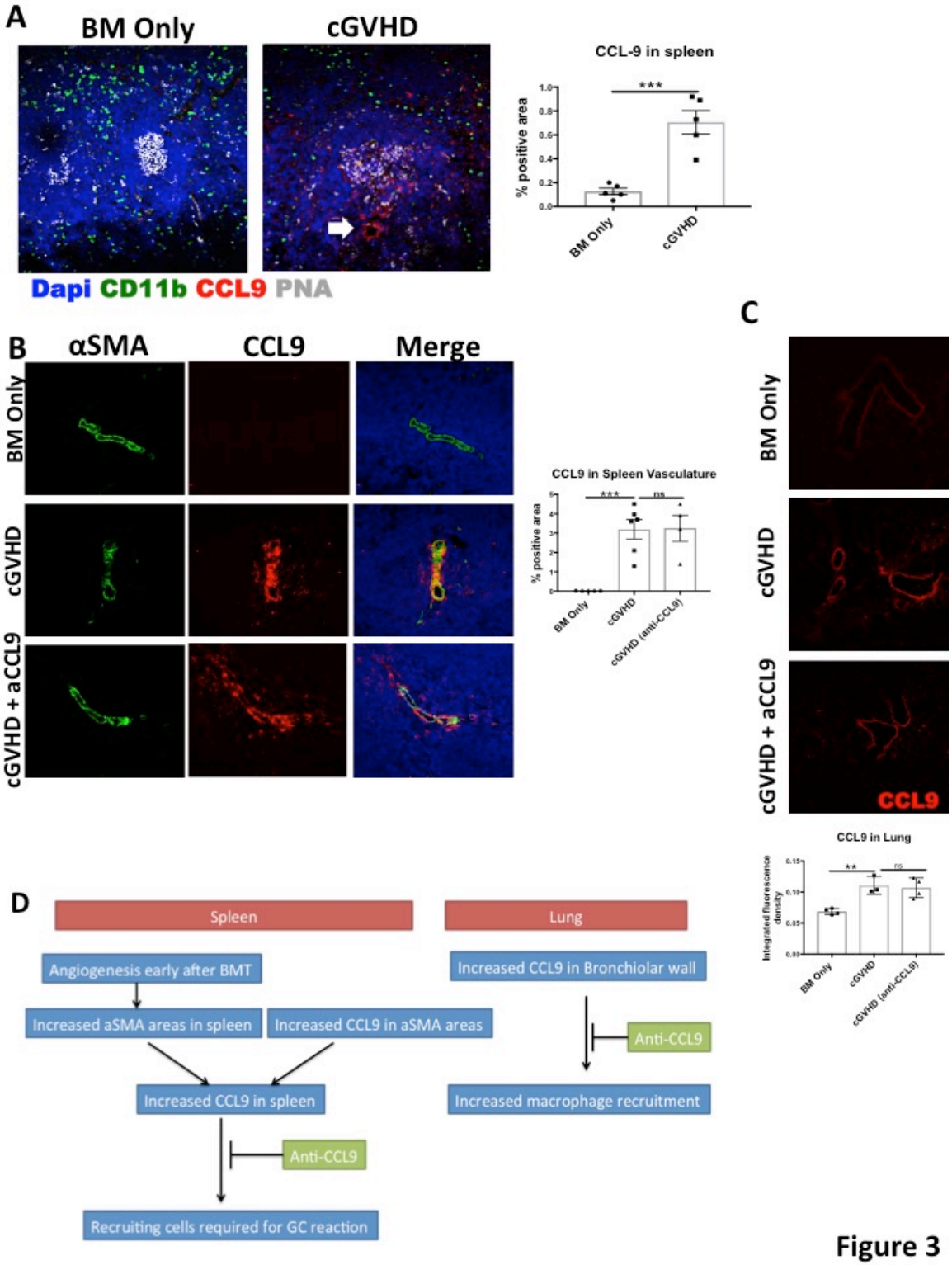
A
BM Only
cGVHD
CCL-9 in spleen
% positive area
***
BM Only
cGVHD
Dapi CD11b CCL9 PNA
B
αSMA
CCL9
Merge
BM Only
cGVHD
cGVHD + aCCL9
CCL9 in Spleen Vasculature
% positive area
***
ns
BM Only
cGVHD
cGVHD (anti-CCL9)
C
BM Only
cGVHD
cGVHD + aCCL9
CCL9
CCL9 in Lung
Integrated fluorescence density
**
ns
BM Only
cGVHD
cGVHD (anti-CCL9)
D
Spleen
Lung
Angiogenesis early after BMT
Increased CCL9 in Bronchiolar wall
Increased aSMA areas in spleen
Increased CCL9 in aSMA areas
Anti-CCL9
Increased CCL9 in spleen
Increased macrophage recruitment
Anti-CCL9
Recruiting cells required for GC reaction

Figure 3

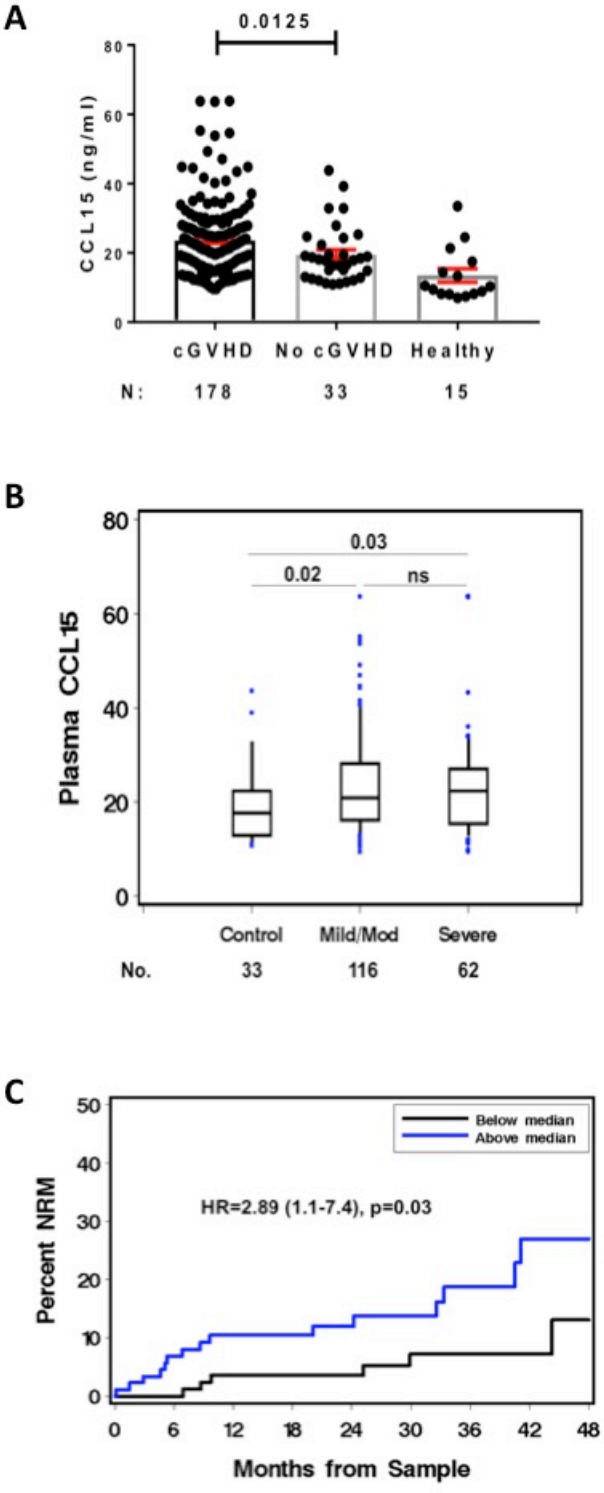
A
0.0125
CCL15 (ng/ml)
80
60
40
20
0
cGVHD
No cGVHD
Healthy
N:
178
33
15
B
0.03
0.02
ns
Plasma CCL15
80
60
40
20
0
Control
Mild/Mod
Severe
No.
33
116
62
C
Below median
Above median
HR=2.89 (1.1-7.4), p=0.03
Percent NRM
50
40
30
20
10
0
0
6
12
18
24
30
36
42
48
Months from Sample

Figure 4

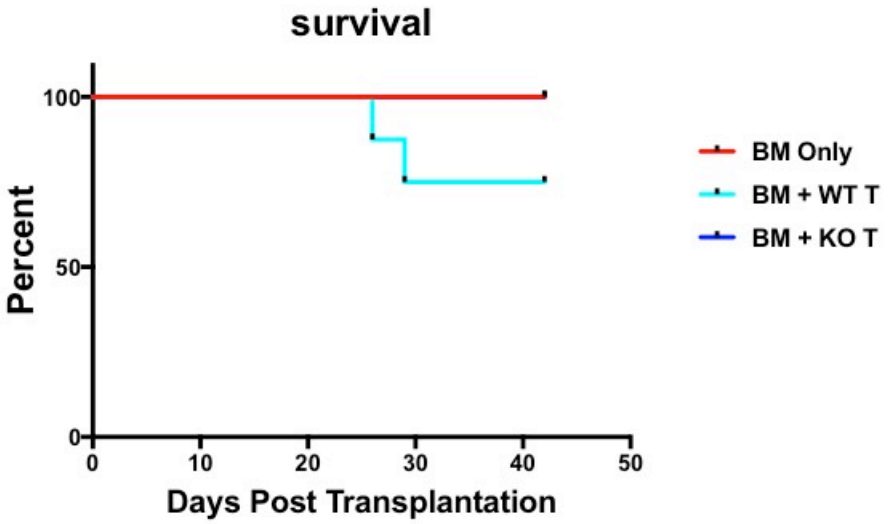

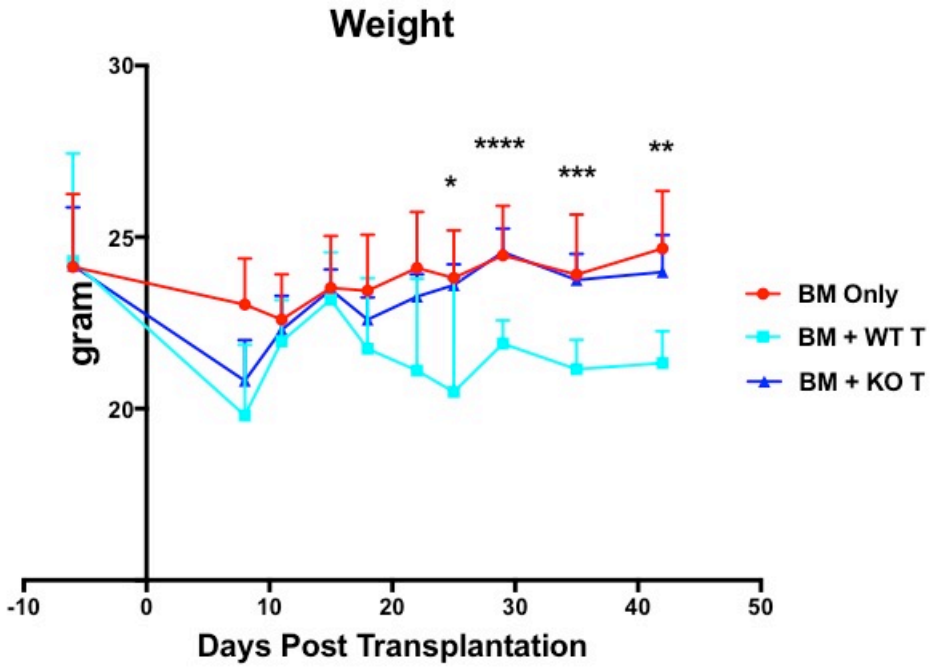

Supplementary Figure 1

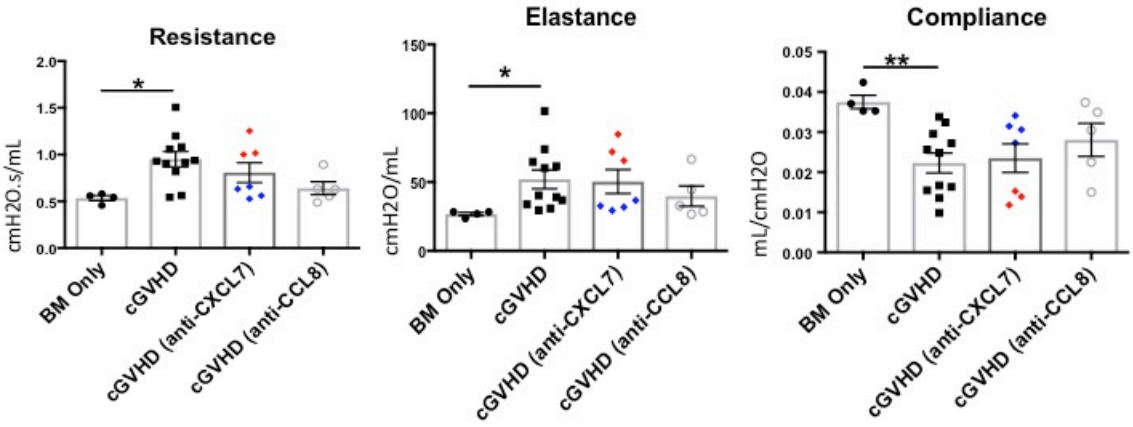

CXCL-7: ♦ 100 mcg
♦ 200 mcg

Supplementary Figure 2

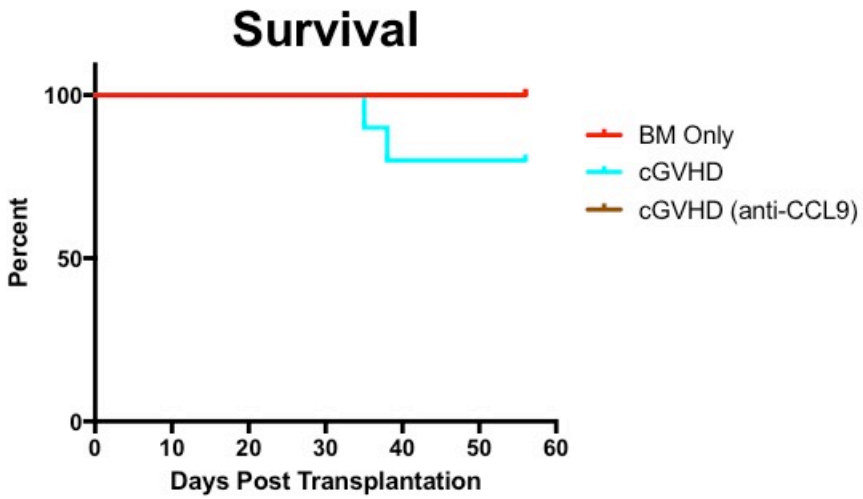

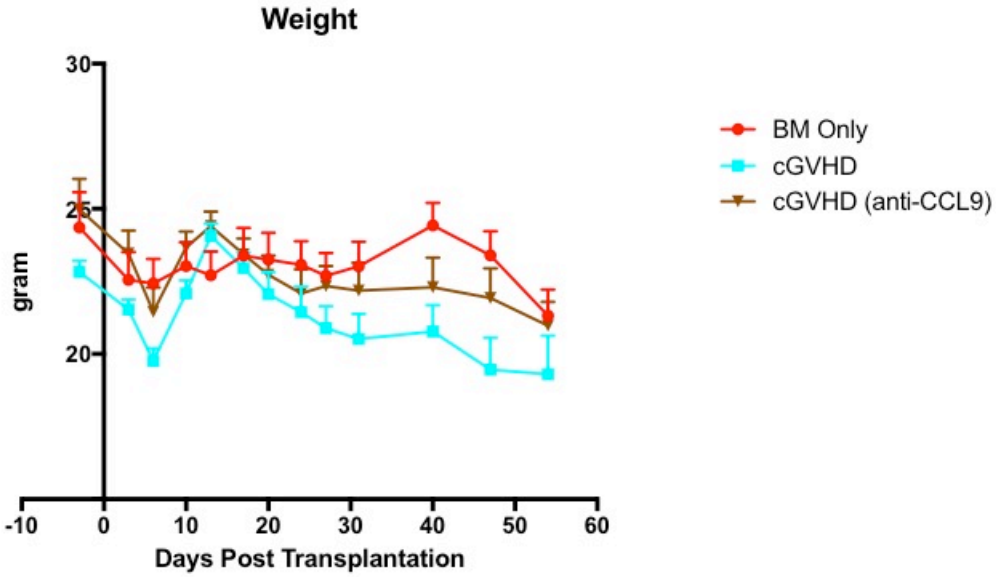

Supplementary Figure 3

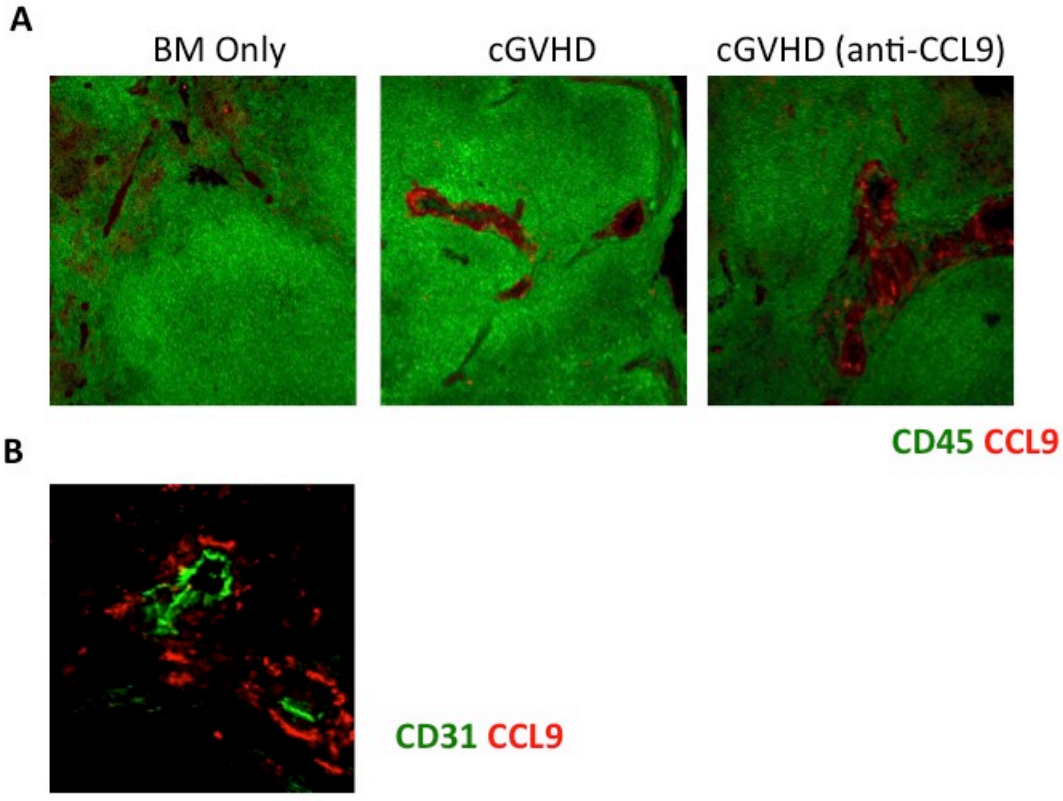

Supplementary Figure 4

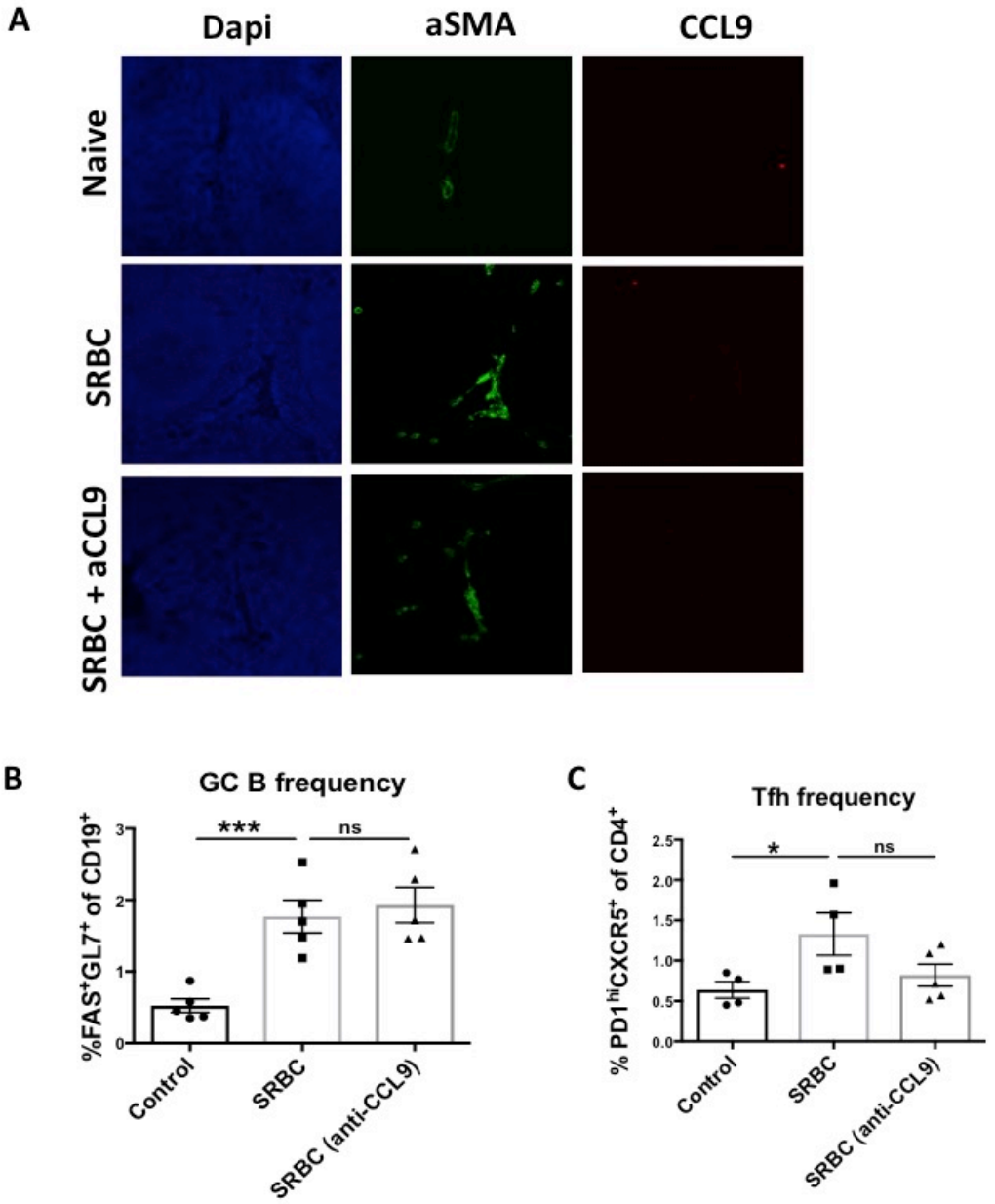

Supplementary Figure 5

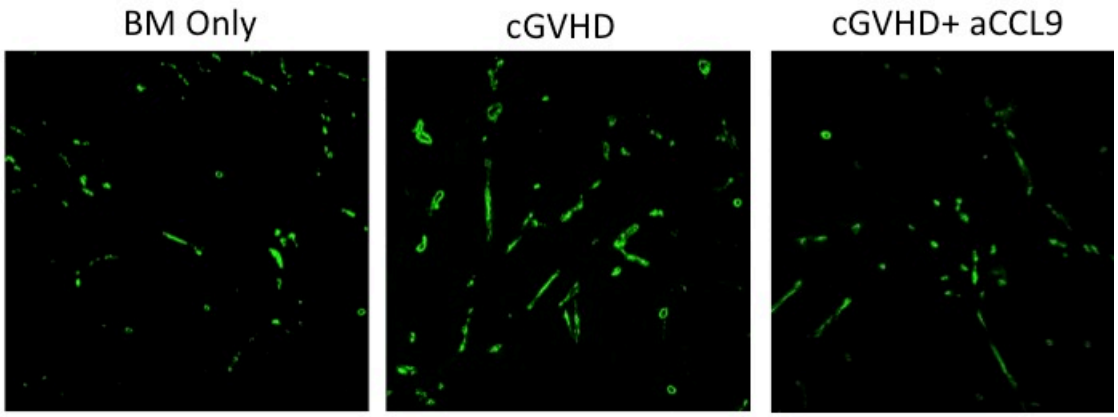

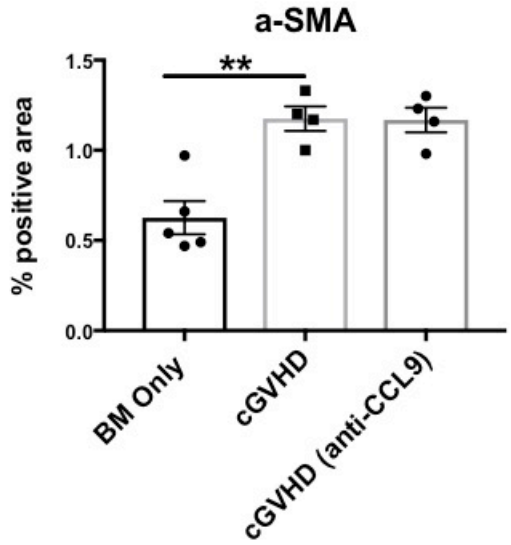

Supplementary Figure 6

Chapter 6 Concluding Statements

The application of aHSCT is mainly hindered by GVHD in spite of advances in clinical practice. cGVHD in specific remains the prevailing cause of nonrelapse mortality in long-term survivors of aHSCT. The current standard therapy for cGVHD is broad immune suppressive agents that may contribute to infection and relapse. New therapies are needed although there have been relatively few advances in the clinical management over several decades. With the development of several newer murine models of cGVHD that mimic different aspects of human cGVHD, the understanding of the pathogenesis of cGVHD has been significantly increased. In this study, we built on the current known knowledge of cGVHD mechanisms and evaluated several mechanistic approaches in preventing and treating cGVHD. Using different pre-clinical murine models of cGVHD we have identified new mechanisms of cGVHD and several potential therapeutic targets that might be brought into the clinic.

cGVHD is known to be a complex immune reaction rather than an extension of acute GVHD that was previously thought. A 3 phase model has been proposed that involved inflammation and tissue injury leading to donor T cell activation and effector function (phase 1), dysregulated immunity with auto immune phenotype (phase 2), and aberrant tissue repair often with fibrosis (phase 3). In the second chapter of this study, we described targeting a Ca^{2+} dependent inositol triphosphate kinase Itpkb using both genetic deletion and pharmaceutical inhibition could block cGVHD. This study suggested Itpkb is important in T cell alloresponse as $Itpkb^{-/-}$ donor T cells could not cause cGVHD. Interestingly, lack of this enzyme in BM did not seem to affect the development of

cGVHD. From the previously published studies, it is known that cGVHD is initiated by donor T cells in the graft and sustained by donor BM derived T cells and B cells. The different outcomes of Itpkb depletion on donor T cells and BM suggested Itpkb function is specifically required during allo-responses. Pharmaceutical inhibition of Itpkb using a selective low molecular weight compound GNF362 led to decrease of cGVHD in both the BO model and the scleroderma model. This study highlighted that blocking T cell function using LMW inhibitors early after aHSCT might be promising in ameliorating cGVHD. The initiating stages of acute and chronic GVHD have overlapping mechanism and depend largely on donor T cells. It is of interest to know whether blocking Itpkb has a role in aGVHD. In addition, future study should address the effect of GNF362 on infection and tumor.

The second stage of cGVHD is characterized by disrupted immune effector/regulatory balances thus the autoimmune phenotype in patients. Lack of regulatory subsets of immune cells such as Treg has been implicated in cGVHD. In the third chapter of this study, we reported an inadequate iNKT pool in cGVHD mice and the disrupted immune balance in cGVHD can be corrected by infusing iNKT- a small subset of T lymphocytes with potent immune regulatory functions. Therapeutic effect of iNKT is associated with an increased Treg density in the GC areas. Infused iNKT expand Treg through an IL-4 and CXCR5 dependent mechanism. This is of significant clinical relevance as iNKT has been show to reduce aGVHD, which is a risk factor for cGVHD. The shared effect of iNKT in both acute and chronic offers the possibility for optimal treatment of patients

with dual acute and chronic GVHD components. Compared to Treg, iNKT infusion offers several clinical advantages such as that iNKT can reach similar therapeutic effect with much fewer cells and that iNKT is more stable in function. We further demonstrated the efficacy of RGI2001, a peptide that activate iNKT cells in vivo after administration in preventing and treating cGVHD. This study offered an alternate immune regulation strategy to cGVHD patients.

Disrupted immune balance leads to antibody mediated tissue fibrosis, which often marks the end stage of cGVHD biology. Fibrosis in lung and skin leads to progressive BO and scleroderma and are the most detrimental and treatment refractory forms of cGHVD. Thus, in the fourth chapter of the study, we evaluated an anti-fibrosis agent that has been approved by FDA for the treatment of idiopathic pulmonary fibrosis. We discovered that pirfenidone reversed cGVHD though inhibition of macrophage infiltration and TGF-β production. Using an intravascular staining technique, we showed that the both macrophages and alveolar macrophages have increased production TGF-β – a pivotal cytokine for fibrotic responses. This study highlight the role of macrophage in cGVHD pathogenesis. Pirfenidone inhibited GC reaction in cGVHD but had no effect on GC responses in SRBC immunized mice. This suggests that pirfenidone reduces cGVHD GC responses by reducting the autoangen – collagen. We hypothesize a feedback loop may exist in cGVHD pathogenesis where GC reaction lead to Ig and collagen deposition, and collagen can serve as autoangen to fuel GC reactions. In addtion, we show that that pirfenidone administration at a later stage of disease is still very effective at reducing BO.

This novel finding is extremely important as there is an option of administering pirfenidone intermittently for patients who cannot tolerate continuous dosing without compromising drug efficacy. These data support the use of pirfenidone as a new agent in early-phase clinical trials for cGVHD treatment.

In the last part of this study, we focused on discovery and validation of novel druggable biomarkers for cGVHD. Using a whole serum proteomics analysis of a well-established murine multi-organ system cGVHD model, we discovered 4 up-regulated proteins during cGVHD that are targetable by genetic ablation or blocking antibodies, including the RAS and JUN kinase activator, CRKL, and CXCL7, CCL8 and CCL9 chemokines. Donor T cells lacking CRK/CRKL prevented the generation of cGVHD, germinal center reactions and macrophage infiltration seen with wild-type T cells. Whereas antibody blockade of CCL8 or CXCL7 was ineffective in treating cGVHD, CCL9 blockade reversed cGVHD clinical manifestations, histopathological changes and immunopathological hallmarks. Mechanistically, elevated CCL9 expression was present predominantly in spleen vascular smooth muscle cells and uniquely seen in cGVHD mice. Importantly, plasma concentrations of CCL15, the human homologue of mouse CCL9, were elevated when analyzed in a previously published, well-defined cohort of 211 cGVHD patients compared to controls. High CCL15 levels were associated with high NRM. These findings demonstrate for the first time the utility of preclinical proteomics screening to identify potential new targets for cGVHD and specifically CCL15 as a marker for cGVHD diagnosis.

In summary, this dissertation addressis the fundamental questions about cGVHD therapies and identified several potential therapeutic targets including Itpkb enzyme, CRKL/CRK adaptor proteins and CCL15, several componds with therapeutic efficacy including GNF362, RGI2001 and pirfenidone, and a potential biomarker – CCL9. This study also shed light on several previously unknown mechanisms of cGVHD pathogenesis.

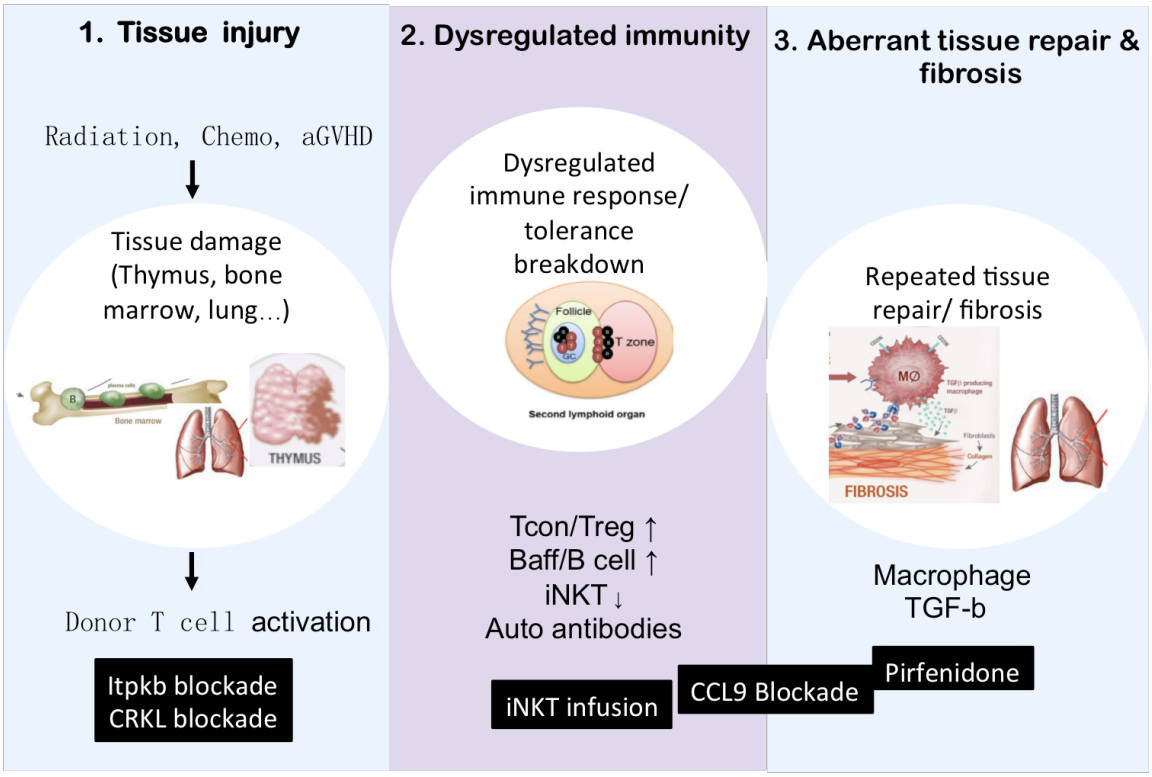

Figure 1. Blocking cGVHD at different biological stages

A 3-step model for the initiation and development of chronic GVHD is proposed that involves tissue injury (phase 1), dysregulated immunity (phase 2), and aberrant tissue repair and fibrosis (phase 3). In phase 1, factors such as irradiation, chemotherapy and previous aGVHD result in tissue damage and release of inflammatory cytokines – leading to the activation of donor T cells. Depletion of Itpkb or CRKL in donor T cells completely blocked aGVHD (Chapter 2&5). Phase 2 is characterized by lost of tolerance mechanism and autoimmune reactions. This stage is characterized by increased GC responses as a result of disturbed Tfh/Tfr, increased BAFF/B ratio, and an inadequate iNKT role. These factors lead to Ig deposition in cGVHD target organs. The balance of effector and regulatory function can be restored by iNKT infusion and CCL9 blockade (Chapter 3&5). In Phase 3, tissue damage caused in phase 1 and Ig deposition caused in phase 2 trigger tissue repair and pro-fibrotic pathways such as M2 macrophage activation and TGF-β production, leading to uncontrolled tissue repair and organ fibrosis. This can be reversed by anti-fibrotic treatment such as Pirfenidone (Chapter 4).

Bibliography

1. LORENZ E, UPHOFF D, REID TR, SHELTON E. Modification of irradiation injury in mice and guinea pigs by bone marrow injections. *J. Natl. Cancer Inst.* 1951;12(1):197–201.
2. FORD CE, HAMERTON JL, BARNES DWH, LOUTIT JF. Cytological Identification of Radiation-Chimæras. *Nature*. 1956;177(4506):452–454.
3. NOWELL PC, COLE LJ, HABERMEYER JG, ROAN PL. Growth and continued function of rat marrow cells in x-radiated mice. *Cancer Res.* 1956;16(3):258–61.
4. THOMAS ED, LOCHTE HL, LU WC, FERREBEE JW. Intravenous infusion of bone marrow in patients receiving radiation and chemotherapy. *N. Engl. J. Med.* 1957;257(11):491–6.
5. THOMAS ED, LOCHTE HL, CANNON JH, SAHLER OD, FERREBEE JW. Supralethal whole body irradiation and isologous marrow transplantation in man. *J. Clin. Invest.* 1959;38(10 Pt 1-2):1709–16.
6. Billingham RE, Brent L. Quantitative Studies on Tissue Transplantation Immunity. IV. Induction of Tolerance in Newborn Mice and Studies on the Phenomenon of Runt Disease. *Philos. Trans. R. Soc. B Biol. Sci.* 1959;242(694):439–477.
7. Gatti R, Meuwissen H, Allen H, Hong R, Good R. Immunological reconstitution of sex-linked lymphopenic immunological deficiency. *Lancet*. 1968;292:1366–1369.
8. Speck B, Zwann FE, van Rood JJ, Ernisse JG. Allogeneic bone marrow transplantation in a patient with aplastic anemia using a phenotypically HLA-identical unrelated donor. *Transplantation*. 1973;16(1):24–28.
9. Little M, Storb R. History of haematopoietic stem-cell transplantation. *Nat. Rev. Cancer*. 2002;2(3):231–238.
10. Thomas ED. A history of haemopoietic cell transplantation. *Br. J. Haematol.* 1999;105(2):330–339.
11. Henig I, Zuckerman T. Hematopoietic Stem Cell Transplantation—50 Years of Evolution and Future Perspectives. *Rambam Maimonides Med. J.* 2014;5(4):e0028.
12. Singh AK, McGuirk JP. Allogeneic stem cell transplantation: A historical and scientific overview. *Cancer Res.* 2016;76(22):6445–6451.
13. Juric MK, Ghimire S, Ogonek J, et al. Milestones of hematopoietic stem cell transplantation - From first human studies to current developments. *Front. Immunol.* 2016;7(NOV):1–16.
14. Pidala J, Kurland B, Chai X, et al. Patient-reported quality of life is associated with severity of chronic graft-versus-host disease as measured by NIH criteria: report on baseline data from the Chronic GVHD Consortium. *Blood*. 2011;117(17):4651–7.
15. Stem Cell Trialists' Collaborative Group. Allogeneic peripheral blood stem-cell compared with bone marrow transplantation in the management of hematologic malignancies: an individual patient data meta-analysis of nine randomized trials. *J. Clin. Oncol.* 2005;23(22):5074–87.

16. Markey K a, Macdonald KP a, Hill GR. The biology of graft-versus-host disease : experimental systems instructing clinical practice The biology of graft-versus-host disease : experimental systems instructing clinical practice. *Hematology*. 2014;124(3):354–362.
17. Hamilton BL, Parkman R. Acute and chronic graft-versus-host disease induced by minor histocompatibility antigens in mice. *Transplantation*. 1983;36(2):150–5.
18. Portanova JP, Claman HN, Kotzin BL. Autoimmunization in murine graft-vs-host disease. I. Selective production of antibodies to histones and DNA. *J. Immunol.* 1985;135(6):3850–6.
19. Ka S-M, Rifai A, Chen J-H, et al. Glomerular crescent-related biomarkers in a murine model of chronic graft versus host disease. *Nephrol Dial Transpl.* 2006;21(2):288–298.
20. Bruijn J a., van Elven EH, Hogendoorn PC, et al. Murine chronic graft-versus-host disease as a model for lupus nephritis. *Am. J. Pathol.* 1988;130(3):639–641.
21. Chu Y-W, Gress RE. Murine Models of Chronic Graft-versus-Host Disease: Insights and Unresolved Issues. *Biol. Blood Marrow Transplant.* 2008;14(4):365–378.
22. Radojcic V, Pletneva MA, Yen H-R, et al. STAT3 Signaling in CD4+ T Cells Is Critical for the Pathogenesis of Chronic Sclerodermatous Graft-Versus-Host Disease in a Murine Model. *J. Immunol.* 2010;184(2):764–774.
23. McCormick LL, Zhang Y, Tootell E, Gilliam a C. Anti-TGF-beta treatment prevents skin and lung fibrosis in murine sclerodermatous graft-versus-host disease: a model for human scleroderma. *J. Immunol.* 1999;163(10):5693–9.
24. Du J, Paz K, Flynn R, et al. Pirfenidone ameliorates murine chronic GVHD through inhibition of macrophage infiltration and TGF-β production. *Blood*. 2017;129(18):2570–2580.
25. Zhang Y, McCormick LL, Desai SR, Wu C, Gilliam AC. Murine Sclerodermatous Graft-Versus-Host Disease, a Model for Human Scleroderma: Cutaneous Cytokines, Chemokines, and Immune Cell Activation. *J. Immunol.* 2002;168(6):3088–3098.
26. Alexander K a, Flynn R, Lineburg KE, et al. CSF-1-dependant donor-derived macrophages mediate chronic graft-versus-host disease. *J. Clin. Invest.* 2014;13(8):1–15.
27. Skert C, Patriarca F, Sperotto A, et al. Sclerodermatous chronic graft-versus-host disease after allogeneic hematopoietic stem cell transplantation: incidence, predictors and outcome. *Haematologica*. 2006;91(2):258–61.
28. Panoskaltsis-Mortari A, Tram K V, Price AP, Wendt CH, Blazar BR. A new murine model for bronchiolitis obliterans post-bone marrow transplant. *Am. J. Respir. Crit. Care Med.* 2007;176(7):713–23.
29. Srinivasan M, Flynn R, Price A, et al. Donor B-cell alloantibody deposition and germinal center formation are required for the development of murine chronic GVHD and bronchiolitis obliterans. *Blood*. 2012;119(6):1570–80.
30. Ziegler TR, Panoskaltsus-Mortari A, Gu LH, et al. REGULATION OF GLUTATHIONE REDOX STATUS IN LUNG AND LIVER BY

CONDITIONING REGIMENS AND KERATINOCYTE GROWTH FACTOR IN MURINE ALLOGENEIC BONE MARROW TRANSPLANTATION1. *Transplantation*. 2001;72(8):1354–1362.
31. Cooke KR, Luznik L, Sarantopoulos S, et al. The Biology of Chronic Graft-Versus-Host Disease: a Task Force Report From the National Institutes of Health Consensus Development Project on Criteria for Clinical Trials in Chronic Graft-Versus-Host Disease. *Biol. Blood Marrow Transplant.* 2016;23(2):1–24.
32. Socie G, Schmoor C, Bethge WA, et al. Chronic graft-versus-host disease: long-term results from a randomized trial on graft-versus-host disease prophylaxis with or without anti–T-cell globulin. *Transpl. Int.* 2011;117(23):6375–6383.
33. Cutler CS, Koreth J, Ritz J. Mechanistic approaches for the prevention and treatment of chronic GVHD. *Blood*. 2017;129(1):22–29.
34. Luznik L, Donnell PVO, Fuchs EJ. Tolerance Induction in HLA-Haploidentical Bone. *YSONC*. 2012;39(6):683–693.
35. Dubovsky J a, Flynn R, Du J, et al. Ibrutinib treatment ameliorates murine chronic graft-versus-host disease. *J. Clin. Invest.* 2014;124(11):4867–4876.
36. Zeiser R, Burchert A, Lengerke C, et al. Ruxolitinib in corticosteroid-refractory graft-versus-host disease after allogeneic stem cell transplantation: a multicenter survey. *Leukemia*. 2015;29(10):2062–8.
37. Flynn R, Paz K, Du J, et al. Targeted Rho-associated kinase 2 (ROCK2) inhibition decreases clinical and immune pathology of murine and human chronic GVHD through Stat3-dependent mechanism. *Blood*. 2016;127(17):2144–2155.
38. Serody JS, Hill GR. The IL-17 Differentiation Pathway and Its Role in Transplant Outcome. *Biol Blood Marrow Transpl.* 2012;100(2):130–134.
39. Murataa M, Fujimotoa M, Komurab K, et al. Clinical association of serum interleukin 17 levels in systemic sclerosis: Is systemic sclerosis a Th17 disease? *JDermatol Sci*. 2008;50(3):240–242.
40. Malard F, Bossard C, Brissot E, et al. Increased Th17/Treg ratio in chronic liver GVHD. *Bone Marrow Transplant.* 2014;49(4):539–544.
41. Forcade E, Paz K, Flynn R, et al. An activated Th17-prone T cell subset involved in chronic graft-versus-host disease sensitive to pharmacological inhibition. *JCI insight*. 2017;2(12):1–15.
42. Rouquette-Gally AM, Boyeldieu D, Prost AC, Gluckman E. Autoimmunity after allogeneic bone marrow transplantation. A study of 53 long-term-surviving patients. *Transplantation*. 1988;46(2):238–40.
43. Tsoi MS, Storb R, Jones E, et al. Deposition of IgM and complement at the dermoepidermal junction in acute and chronic cutaneous graft-vs-host disease in man. *J. Immunol.* 1978;120(5):1485–92.
44. Miklos DB, Kim HT, Miller KH, et al. Antibody responses to H-Y minor histocompatibility antigens correlate with chronic graft-versus-host disease and disease remission. *Blood*. 2005;105(7):2973–2978.
45. Sarantopoulos S, Blazar BR, Cutler C, Ritz J. B Cells in Chronic Graft-versus-Host Disease. *Biol. Blood Marrow Transplant.* 2014;1–8.

46. Canninga-van Dijk MR, van der Straaten HM, Fijnheer R, et al. Anti-CD20 monoclonal antibody treatment in 6 patients with therapy-refractory chronic graft-versus-host disease. *Blood*. 2004;104(8):2603–6.
47. Cutler C, Miklos D, Kim HT, et al. Rituximab for steroid-refractory chronic graft-versus-host disease. *Blood*. 2006;108(2):756–62.
48. Clavert a, Chevallier P, Guillaume T, et al. Safety and efficacy of rituximab in steroid-refractory chronic GVHD. *Bone Marrow Transplant.* 2012;48(5):734–736.
49. Cutler C, Kim HT, Bindra B, et al. Rituximab prophylaxis prevents corticosteroid-requiring chronic GVHD after allogeneic peripheral blood stem cell transplantation : results of a phase 2 trial. *Transplantation*. 2013;122(8):1510–1517.
50. Kuzmina Z, Gounden V, Curtis L, et al. Clinical significance of autoantibodies in a large cohort of patients with chronic graft-versus-host disease defined by NIH criteria. *Am. J. Hematol.* 2015;90(2):114–119.
51. Taur Y, Xavier JB, Lipuma L, et al. Intestinal domination and the risk of bacteremia in patients undergoing allogeneic hematopoietic stem cell transplantation. *Clin. Infect. Dis.* 2012;55:905–914.
52. Jin H, Ni X, Deng R, et al. Antibodies from donor B cells perpetuate cutaneous chronic graft-versus-host disease in mice. *Blood*. 2016;127(18):2249–2260.
53. Pelanda R, Torres RM. Central B-cell tolerance: where selection begins. *Cold Spring Harb. Perspect. Biol.* 2012;4(4):1–16.
54. Wardemann H, Yurasov S, Schaefer A, et al. Predominant autoantibody production by early human B cell precursors. *Science*. 2003;301(5638):1374–1377.
55. Sarantopoulos S, Stevenson KE, Kim HT, et al. High Levels of B-Cell Activating Factor in Patients with Active Chronic Graft-Versus-Host Disease. *Clin. Cancer Res.* 2007;13(20):6107–6114.
56. Sarantopoulos S, Stevenson KE, Kim HT, et al. High levels of B-cell activating factor in patients with active chronic graft-versus-host disease. *Clin. Cancer Res.* 2007;13(20):6107–14.
57. Allen JL, Wooten J, Fore M, et al. Oral Presentations: B Cells from Patients with Chronic GVHD Signal Via the Akt-Driven Survival and Metabolic Fitness Pathway. *Biol. Blood Marrow Transplant.* 2012;18(Supplement):S207–S208.
58. Allen J, Tata P, Fore M, et al. Increased BCR responsiveness in B cells from patients with chronic GVHD. *Blood*. 2014;123(13):2108–2116.
59. Flynn R, Allen JL, Luznik L, et al. Targeting Syk-activated B cells in murine and human chronic graft-versus-host disease. *Blood*. 2015;125(26):4085–4094.
60. Khoder A, Sarvaria A, Alsuliman A, et al. Regulatory B cells are enriched within the IgM memory and transitional subsets in healthy donors but are deficient in chronic GVHD. *Blood*. 2014;124(13):2034–2045.
61. Masson D, Bouaziz J, Buanec L, et al. CD24 hi CD27 1 and plasmablast-like regulatory B cells in human chronic graft-versus-host disease. *Blood*. 2015;125(11):1830–1840.
62. Yang M, Rui K, Wang S, Lu L. Regulatory B cells in autoimmune diseases. *Cell. Mol. Immunol.* 2013;10(2):122–132.

63. Tedder TF. B10 cells: a functionally defined regulatory B cell subset. *J. Immunol.* 2015;194(4):1395–401.
64. De Silva NS, Klein U. Dynamics of B cells in germinal centres. *Nat. Rev. Immunol.* 2015;15(3):137–148.
65. Forcade E, Kim HT, Cutler C, et al. Circulating T follicular helper cells with increased function during chronic graft-versus-host disease. *Blood*. 2016;127(20):2489–2497.
66. Flynn R, Du J, Veenstra RG, et al. Increased T follicular helper cells and germinal center B cells are required for cGVHD and bronchiolitis obliterans. *Blood*. 2014;123(25):3988–3998.
67. Porcheray F, Miklos DB, Floyd BH, et al. Combined CD4 T-Cell and Antibody Response to Human Minor Histocompatibility Antigen DBY After Allogeneic Stem-Cell Transplantation. *Transplantation*. 2011;92(3):359–365.
68. Zorn E, Miklos DB, Floyd BH, et al. Minor histocompatibility antigen DBY elicits a coordinated B and T cell response after allogeneic stem cell transplantation. *J. Exp. Med.* 2004;199(8):1133–1142.
69. Sage PT, Sharpe AH. T follicular regulatory cells in the regulation of B cell responses. *Trends Immunol.* 2015;36(7):410–418.
70. McDonald-Hyman C, Flynn R, Panoskaltsis-Mortari A, et al. Therapeutic regulatory T-cell adoptive transfer ameliorates established murine chronic GVHD in a CXCR5-dependent manner. *Blood*. 2016;128(7):1013–1017.
71. Du J, Paz K, Thangavelu G, et al. Invariant natural killer T cells ameliorate murine chronic GVHD by expanding donor regulatory T cells. *Blood*. 2017;129(23):3121–3125.
72. Nishiwaki S, Terakura S, Ito M, et al. Impact of macrophage infiltration of skin lesions on survival after allogeneic stem cell transplantation: A clue to refractory graft-versus-host disease. *Blood*. 2009;114(14):3113–3116.
73. Bensinger WI, Martin PJ, Storer B, et al. Transplantation of Bone Marrow as Compared with Peripheral-Blood Cells from HLA-Identical Relatives in Patients with Hematologic Cancers. *N. Engl. J. Med.* 2001;344(3):175–181.
74. Hill GR, Olver SD, Kuns RD, et al. Stem cell mobilization with G-CSF induces type 17 differentiation and promotes scleroderma. *Blood*. 2010;116(5):819–828.
75. Fujii H, Luo Z, Kim HJ, et al. Increased CD68+ Macrophages Are Associated with Liver Fibrosis in a Humanized Chronic Graft-Versus-Host Disease Mouse Model. *Biol. Blood Marrow Transplant.* 2015;21(2):S283–S284.
76. Wu JM, Thoburn CJ, Wisell J, Farmer ER, Hess AD. CD20, AIF-1, and TGF-beta in graft-versus-host disease: a study of mRNA expression in histologically matched skin biopsies. *Mod. Pathol.* 2010;23(5):720–8.
77. Blank U, Karlsson S. TGF-β signaling in the control of hematopoietic stem cells. *Blood*. 2015;125(23):3542–50.
78. Massagué J. TGFβ signalling in context. *Nat. Rev. Mol. Cell Biol.* 2012;13(10):616–30.
79. Fernandez IE, Eickelberg O. The impact of TGF-β on lung fibrosis: from targeting to biomarkers. *Proc. Am. Thorac. Soc.* 2012;9(3):111–6.

80. Kubiczkova L, Sedlarikova L, Hajek R, Sevcikova S. TGF-β - an excellent servant but a bad master. *J. Transl. Med.* 2012;10:183.
81. Akhurst RJ, Hata A. Targeting the TGFβ signalling pathway in disease. *Nat. Rev. Drug Discov.* 2012;11(10):790–811.
82. Banovic T, MacDonald KP a, Morris ES, et al. TGF-beta in allogeneic stem cell transplantation: friend or foe? *Blood*. 2005;106(6):2206–14.
83. Pines M, Snyder D, Yarkoni S, Nagler A. Halofuginone to treat fibrosis in chronic graft-versus-host disease and scleroderma. *Biol. Blood Marrow Transplant.* 2003;9(7):417–425.
84. Baron C, Somogyi R, Greller LD, et al. Prediction of graft-versus-host disease in humans by donor gene-expression profiling. *PLoS Med.* 2007;4(1):e23.
85. Anderson BE, McNiff JM, Matte C, et al. Recipient CD4+ T cells that survive irradiation regulate chronic graft-versus-host disease. *Blood*. 2004;104(5):1565–1573.
86. Fahlén L, Read S, Gorelik L, et al. T cells that cannot respond to TGF-β escape control by CD4 + CD25 + regulatory T cells. *J. Exp. Med.* 2005;201(5):737–746.
87. Socie G, Ritz J. Current issues in chronic graft-versus-host disease. *Blood*. 2014;124(3):374–384.
88. Feske S. Calcium signalling in lymphocyte activation and disease. *Nat. Rev. Immunol.* 2007;7(9):690–702.
89. Sauer K, Cooke MP. Regulation of immune cell development through soluble inositol-1,3,4,5-tetrakisphosphate. *Nat. Rev. Immunol.* 2010;10(4):257–271.
90. Miller AT, Chamberlain PP, Cooke MP. Beyond IP3: Roles for higher order inositol phosphates in immune cell signaling. *Cell Cycle*. 2008;7(4):463–467.
91. Miller AT, Beisner DR, Liu D, Cooke MP. Inositol 1,4,5-trisphosphate 3-kinase B is a negative regulator of BCR signaling that controls B cell selection and tolerance induction. *J. Immunol.* 2009;182(8):4696–704.
92. Miller AT, Sandberg M, Huang YH, et al. Production of Ins(1,3,4,5)P4 mediated by the kinase Itpkb inhibits store-operated calcium channels and regulates B cell selection and activation. *Nat. Immunol.* 2007;8(5):514–521.
93. Miller AT, Dahlberg C, Sandberg ML, et al. Inhibition of the Inositol Kinase Itpkb Augments Calcium Signaling in Lymphocytes and Reveals a Novel Strategy to Treat Autoimmune Disease. *PLoS One*. 2015;10(6):e0131071.
94. Jia Y, Loison F, Hattori H, et al. Inositol trisphosphate 3-kinase B (InsP3KB) as a physiological modulator of myelopoiesis. *Proc. Natl. Acad. Sci. U. S. A.* 2008;105(12):4739–4744.
95. Siegemund S, Rigaud S, Conche C, et al. IP<inf>3</inf> 3-kinase B controls hematopoietic stem cell homeostasis and prevents lethal hematopoietic failure in mice. *Blood*. 2015;125(18):2786–2797.
96. Zeng D, Lewis D, Dejbakhsh-jones S, et al. Bone Marrow NK1.1- and NK1.1+ T Cells Reciprocally Regulate Acute Graft versus Host Disease. *J. Exp. Med.* 1999;189(7):.

97. Schneidawind D, Pierini A, Alvarez M, et al. CD4+ invariant natural killer T cells protect from murine GVHD lethality through expansion of donor CD4+ CD25+ FoxP3+ regulatory T cells. *Blood*. 2014;124(22):3320–3329.
98. Schneidawind D, Baker J, Pierini A, et al. Third-party CD4+ invariant natural killer T cells protect from murine GVHD lethality. *Blood*. 2015;125(22):3491–3500.
99. Rossjohn J, Pellicci DG, Patel O, Gapin L, Godfrey DI. Recognition of CD1d-restricted antigens by natural killer T cells. *Nat. Rev. Immunol.* 2012;12(12):845–57.
100. Wilson SB, Delovitch TL. Janus-like role of regulatory iNKT cells in autoimmune disease and tumour immunity. *Nat. Rev. Immunol.* 2003;3(3):211–222.
101. Sag D, Krause P, Hedrick CC, Kronenberg M, Wingender G. IL-10-producing NKT10 cells are a distinct regulatory invariant NKT cell subset. *J. Clin. Invest.* 2014;124(9):3725–40.
102. van der Merwe M, Abdelsamed HA, Seth A, et al. Recipient Myeloid-Derived Immunomodulatory Cells Induce PD-1 Ligand-Dependent Donor CD4+Foxp3+ Regulatory T Cell Proliferation and Donor-Recipient Immune Tolerance after Murine Nonmyeloablative Bone Marrow Transplantation. *J. Immunol.* 2013;191(11):5764–5776.
103. Mansour S, Tocheva AS, Sanderson JP, et al. Structural and Functional Changes of the Invariant NKT Clonal Repertoire in Early Rheumatoid Arthritis. *J. Immunol.* 2015;195(12):5582–91.
104. Van der Vliet HJ, von Blomberg BM, Nishi N, et al. Circulating V(alpha24+) Vbeta11+ NKT cell numbers are decreased in a wide variety of diseases that are characterized by autoreactive tissue damage. *Clin. Immunol.* 2001;100(2):144–8.
105. Berzins SP, Smyth MJ, Baxter AG. Presumed guilty: natural killer T cell defects and human disease. *Nat. Rev. Immunol.* 2011;11(2):131–42.
106. Chaidos A, Patterson S, Szydlo R, et al. Graft invariant natural killer T-cell dose predicts risk of acute graft-versus-host disease in allogeneic hematopoietic stem cell transplantation. *Blood*. 2012;119(21):5030–5036.
107. Malard F, Labopin M, Chevallier P, et al. Larger number of invariant natural killer T cells in PBSC allografts correlates with improved GVHD-free and progression-free survival. *Blood*. 2016;127(14):1828–1835.
108. Rubio M-T, Moreira-Teixeira L, Bachy E, et al. Early posttransplantation donor-derived invariant natural killer T-cell recovery predicts the occurrence of acute graft-versus-host disease and overall survival. *Blood*. 2012;120(10):2144–2154.
109. Lowsky R, Takahashi T, Liu Y, Dejbakhsh-Jones S. Protective Conditioning for Acute Graft-versus-Host Disease. *N. Engl. J. Med.* 2005;353(13):1045–1057.
110. Lan F, Zeng D, Higuchi M, et al. Predominance of NK1.1+TCR alpha beta+ or DX5+TCR alpha beta+ T cells in mice conditioned with fractionated lymphoid irradiation protects against graft-versus-host disease: “natural suppressor” cells. *J. Immunol.* 2001;167(4):2087–2096.

111. Zorn E, Kim HT, Lee SJ, et al. Reduced frequency of FOXP3 ⁄ CD4 ⁄ CD25 ⁄ regulatory T cells in patients with chronic graft-versus-host disease. *Transplantation*. 2005;106(8):2903–2911.
112. Suffner J, Hochweller K, Kühnle M-C, et al. Dendritic cells support homeostatic expansion of Foxp3+ regulatory T cells in Foxp3.LuciDTR mice. *J. Immunol.* 2010;184(4):1810–1820.
113. Rieger K, Loddenkemper C, Maul J. Mucosal FOXP3+ regulatory T cells are numerically deficient in acute and chronic GvHD. *Blood*. 2006;107(4):1717–1724.
114. Pidala J, Vogelsang G, Martin P, et al. Overlap subtype of chronic graft-versus-host disease is associated with an adverse prognosis, functional impairment, and inferior patient-reported outcomes: A Chronic Graft-versus-Host Disease Consortium study. *Haematologica*. 2012;97(3):451–458.
115. Guan P, Bassiri H, Patel NP. Invariant natural killer T cells in hematopoietic stem cell transplantation: killer choice for natural suppression. *Bone Marrow Transplant.* 2016;(November 2015):1–9.
116. Brennan PJ, Brigl M, Brenner MB. Invariant natural killer T cells: an innate activation scheme linked to diverse effector functions. *Nat. Rev. Immunol.* 2013;13(2):101–17.
117. McDonald-Hyman C, Turka LA, Blazar BR. Advances and challenges in immunotherapy for solid organ and hematopoietic stem cell transplantation. *Sci. Transl. Med.* 2015;7(280):280rv2-280rv2.
118. Wolff D, Gerbitz A, Ayuk F, et al. Consensus conference on clinical practice in chronic graft-versus-host disease (GVHD): First-line and topical treatment of chronic GVHD. *Biol. Blood Marrow Transplant.* 2010;16(12):1611–1628.
119. Schroeder MA, DiPersio JF. Mouse models of graft-versus-host disease: advances and limitations. *Dis. Model. Mech.* 2011;4(3):318–33.
120. MacDonald KPA, Hill GR, Blazar BR. Chronic graft-versus-host disease: biological insights from pre-clinical and clinical studies. *Blood*. 2016;1–29.
121. Zeiser R, Blazar BR. Preclinical models of acute and chronic graft-versus-host disease : how predictive are they for a successful clinical translation ? *Blood*. 2016;127(25):3117–3127.
122. Iyer SN, Hyde DM, Giri SN. Anti-inflammatory effect of pirfenidone in the bleomycin-hamster model of lung inflammation. *Inflammation*. 2000;24(5):477–491.
123. Iyer SN, Gurujeyalakshmi G, Giri SN. Effects of pirfenidone on transforming growth factor-beta gene expression at the transcriptional level in bleomycin hamster model of lung fibrosis. *J. Pharmacol. Exp. Ther.* 1999;291(1):367–373.
124. Iyer SN, Gurujeyalakshmi G, Giri SN. Effects of Pirfenidone on Procollagen Gene Expression at the Transcriptional Level in Bleomycin Hamster Model of Lung Fibrosis1. *J. Pharmacol. Exp. Ther.* 1999;289(1):211–218.
125. Schelegle ES, Mansoor JK, Giri S. Pirfenidone Attenuates Bleomycin-Induced Changes in Pulmonary Functions in Hamsters. *Exp. Biol. Med.* 1997;216(3):392–397.

126. Abdollahi A, Li M, Ping G, et al. Inhibition of platelet-derived growth factor signaling attenuates pulmonary fibrosis. *J. Exp. Med.* 2005;201(6):925–35.
127. Zhou C, Liu F, Gallo PH, et al. Anti-fibrotic action of pirfenidone in Dupuytren's disease-derived fibroblasts. *BMC Musculoskelet. Disord.* 2016;17(1):469.
128. Zhou H, Latham CW, Zander DS, Margolin SB, Visner G a. Pirfenidone inhibits obliterative airway disease in mouse tracheal allografts. *J. Hear. lung Transplant.* 2005;24(10):1577–85.
129. Liu H, Drew P, Gaugler AC, Cheng Y, Visner G a. Pirfenidone inhibits lung allograft fibrosis through L-arginine-arginase pathway. *Am. J. Transplant*. 2005;5(6):1256–63.
130. Gurujeyalakshmi G, Hollinger M a, Giri SN. Pirfenidone inhibits PDGF isoforms in bleomycin hamster model of lung fibrosis at the translational level. *Am. J. Physiol.* 1999;276(2 Pt 1):L311-8.
131. Misra HP, Rabideau C. Pirfenidone inhibits NADPH-dependent microsomal lipid peroxidation and scavenges hydroxyl radicals. *Mol. Cell. Biochem.* 2000;204(1–2):119–26.
132. Oku H, Shimizu T, Kawabata T, et al. Antifibrotic action of pirfenidone and prednisolone: different effects on pulmonary cytokines and growth factors in bleomycin-induced murine pulmonary fibrosis. *Eur. J. Pharmacol.* 2008;590(1–3):400–8.
133. Grattendick KJ, Nakashima JM, Feng L, Giri SN, Margolin SB. Effects of three anti-TNF-a drugs: Etanercept, infliximab and pirfenidone on release of TNF-a in medium and TNF-a associated with the cell in vitro. *Int. Immunopharmacol.* 2008;8(5):679–687.
134. King TE, Bradford WZ, Castro-Bernardini S, et al. A Phase 3 Trial of Pirfenidone in Patients with Idiopathic Pulmonary Fibrosis. *N. Engl. J. Med.* 2014;1–10.
135. Rodríguez-Castellanos M, Tlacuilo-Parra A, Sánchez-Enríquez S, Vélez-Gómez E, Guevara-Gutiérrez E. Pirfenidone gel in patients with localized scleroderma: a phase II study. *Arthritis Res. Ther.* 2015;16(6):1–8.
136. Williams KM. How I treat bronchiolitis obliterans syndrome after hematopoietic stem cell transplantation. *Blood*. 2017;129(4):448–455.
137. Anderson B, McNiff J, Yan J. Memory CD4+ T cells do not induce graft-versus-host disease. *J. Clin. Invest.* 2003;112(1):101–108.
138. Estes JD, Reilly C, Trubey CM, et al. Antifibrotic Therapy in Simian Immunodeficiency Virus Infection Preserves CD4+ T-Cell Populations and Improves Immune Reconstitution With Antiretroviral Therapy. *J. Infect. Dis.* 2015;211(5):744–754.
139. Green TD, Park J, Yin Q, et al. Directed migration of mouse macrophages in vitro involves myristoylated alanine-rich C-kinase substrate (MARCKS) protein. *J Leukoc Biol*. 2012;92(3):633–639.
140. Glaab T, Taube C, Braun A, Mitzner W. Invasive and noninvasive methods for studying pulmonary function in mice. *Respir. Res.* 2007;8(1):63.

141. Dosanjh a, Ikonen T, Wan B, Morris RE. Pirfenidone: A novel anti-fibrotic agent and progressive chronic allograft rejection. *Pulm. Pharmacol. Ther.* 2002;15(5):433–437.
142. Anderson KG, Sung H, Skon CN, et al. Cutting Edge: Intravascular Staining Redefines Lung CD8 T Cell Responses. *J. Immunol.* 2012;189(6):2702–2706.
143. Anderson KG, Mayer-barber K, Sung H, et al. Intravascular staining for discrimination of vascular and tissue leukocytes. *Nat. protocals*. 2015;9(1):209–222.
144. Bedoret D, Wallemacq H, Marichal T, et al. Lung interstitial macrophages alter dendritic cell functions to prevent airway allergy in mice. *J. Clin. Invest.* 2009;119(12):3723–3738.
145. Doherty TA, Soroosh P, Khorram N, et al. The tumor necrosis factor family member LIGHT is a target for asthmatic airway remodeling. *Nat Med*. 2011;17(5):596–603.
146. Chen J-F, Ni H-F, Pan M-M, et al. Pirfenidone inhibits macrophage infiltration in 5/6 nephrectomized rats. *Am. J. Physiol. Renal Physiol.* 2013;304(6):F676-85.
147. Erbel C, Akhavanpoor M, Okuyucu D, et al. IL-17A influences essential functions of the monocyte/macrophage lineage and is involved in advanced murine and human atherosclerosis. *J. Immunol.* 2014;193(9):4344–55.
148. Hildebrandt GC, Duffner UA, Olkiewicz KM, et al. A critical role for CCR2 / MCP-1 interactions in the development of idiopathic pneumonia syndrome after allogeneic bone marrow transplantation. *Blood*. 2004;103(6):2417–2427.
149. Yoshizaki A, Yanaba K, Iwata Y, et al. Cell Adhesion Molecules Regulate Fibrotic Process via Th1/Th2/Th17 Cell Balance in a Bleomycin-Induced Scleroderma Model. *J. Immunol.* 2010;185(4):2502–2515.
150. Li W, Liu L, Gomez A, et al. Proteomics analysis reveals a Th17-prone cell population in presymptomatic graft-versus-host disease. *JCI Insight*. 2016;1(6):1–17.
151. van der Waart AB, van der Velden WJFM, van Halteren AGS, et al. Decreased Levels of Circulating IL17-Producing CD161+CCR6+ T Cells Are Associated with Graft-versus-Host Disease after Allogeneic Stem Cell Transplantation. *PLoS One*. 2012;7(12):1–13.
152. Baumjohann D, Preite S, Reboldi A, et al. Persistent Antigen and Germinal Center B Cells Sustain T Follicular Helper Cell Responses and Phenotype. *Immunity*. 2013;38(3):596–605.
153. Visner GA, Liu F, Bizargity P, et al. Pirfenidone Inhibits T-Cell Activation, Proliferation, Cytokine and Chemokine Production, and Host Alloresponses. *Transplantation*. 2009;88(3):330–338.
154. Zhang Y, McCormick LL, Desai SR, Wu C, Gilliam AC. Murine sclerodermatous graft-versus-host disease, a model for human scleroderma: cutaneous cytokines, chemokines, and immune cell activation. *J. Immunol.* 2002;168(6):3088–98.
155. Kitko CL, White ES, Baird K. Fibrotic and Sclerotic Manifestations of Chronic Graft-versus-Host Disease. *Ybbmt*. 2012;18(1):S46–S52.

156. Inomata M, Kamio K, Azuma A, et al. Pirfenidone inhibits fibrocyte accumulation in the lungs in bleomycin-induced murine pulmonary fibrosis. *Respir. Res.* 2014;15(1):16.
157. Togami K, Kanehira Y. Possible Involvement of Pirfenidone Metabolites in the Antifibrotic Action of a Therapy for Idiopathic Pulmonary Fibrosis. *Biol Pharm Bull*. 2013;36(October):1525–1527.
158. Giri SN, Wang Q, Xie Y, et al. Pharmacokinetics and metabolism of a novel antifibrotic drug pirfenidone, in mice following intravenous administration. *Biopharm. Drug Dispos.* 2002;23(5):203–211.
159. Armendariz-Borunda J. A Controlled Clinical Trial With Pirfenidone in the Treatment of Pathological Skin Scarring Caused by Burns in Pediatric Patients. *Ann. Plast. Surg.* 2012;69(1):111–112.
160. Wechalekar a, Cranfield T, Sinclair D, Ganzckowski M. Occurrence of autoantibodies in chronic graft vs. host disease after allogeneic stem cell transplantation. *Clin. Lab. Haematol.* 2005;27(4):247–9.
161. Visner GA, Liu F, Bizargity P, et al. Pirfenidone Inhibits T-Cell Activation, Proliferation, Cytokine and Chemokine Production, and Host Alloresponses. *Transplantation*. 2009;88(3):330–338.
162. Yasufuku K, Heidler KM, Woods KA, et al. Prevention of bronchiolitis obliterans in rat lung allografts by type V collagen-induced oral tolerance1. *Transplantation*. 2002;73(4):500–505.
163. Burlingham WJ, Love RB, Jankowska-Gan E, et al. IL-17–dependent cellular immunity to collagen type V predisposes to obliterative bronchiolitis in human lung transplants. *J. Clin. Invest.* 2007;117(11):3498–3506.
164. Vittal R, Fan L, Greenspan DS, et al. IL-17 induces type V collagen overexpression and EMT via TGF-β-dependent pathways in obliterative bronchiolitis. *Am. J. Physiol. Lung Cell. Mol. Physiol.* 2013;304(6):L401-14.
165. Zhou L, Askew D, Wu C, Gilliam AC. Cutaneous gene expression by DNA microarray in murine sclerodermatous graft-versus-host disease, a model for human scleroderma. *J. Invest. Dermatol.* 2007;127(2):281–292.
166. Yoon H-K, Lim J-Y, Kim T-J, Cho C-S, Min C-K. Effects of pravastatin on murine chronic graft-versus-host disease. *Transplantation*. 2010;90(8):853–60.
167. Belperio J a, Keane MP, Burdick MD, et al. Critical role for the chemokine MCP-1/CCR2 in the pathogenesis of bronchiolitis obliterans syndrome. *J. Clin. Invest.* 2001;108(4):547–56.
168. Gooley TA, Chien JW, Pergam SA, et al. Reduced mortality after allogeneic hematopoietic-cell transplantation. *N. Engl. J. Med.* 2010;363(22):2091–101.
169. Socié G, Stone JV, Wingard JR, et al. Long-Term Survival and Late Deaths after Allogeneic Bone Marrow Transplantation. *N. Engl. J. Med.* 1999;341(1):14–21.
170. Fraser CJ, Bhatia S, Ness K, et al. Impact of chronic graft-versus-host disease on the health status of hematopoietic cell transplantation survivors: a report from the Bone Marrow Transplant Survivor Study. *Blood*. 2006;108(8):2867–73.
171. Pidala J, Kurland B, Chai X, et al. Patient-reported quality of life is associated with severity of chronic graft-versus-host disease as measured by NIH criteria: Report

on baseline data from the Chronic GVHD Consortium. *Blood*. 2011;117(17):4651–4657.
172. Bhatia S, Francisco L, Carter A, et al. Late mortality after allogeneic hematopoietic cell transplantation and functional status of long-term survivors: report from the Bone Marrow Transplant Survivor Study. *Blood*. 2007;110(10):3784–92.
173. MacDonald KPA, Hill GR, Blazar BR. Chronic graft-versus-host disease: biological insights from preclinical and clinical studies. *Blood*. 2017;129(1):13–21.
174. Filipovich AH, Weisdorf D, Pavletic S, et al. National Institutes of Health consensus development project on criteria for clinical trials in chronic graft-versus-host disease: I. Diagnosis and staging working group report. *Biol. Blood Marrow Transplant.* 2005;11(12):945–56.
175. Jagasia MH, Greinix HT, Arora M, et al. National Institutes of Health Consensus Development Project on Criteria for Clinical Trials in Chronic Graft-versus-Host Disease: I. The 2014 Diagnosis and Staging Working Group Report. *Biol. Blood Marrow Transplant.* 2015;21(3):389–401.
176. Paczesny S, Hakim FT, Pidala J, et al. National institutes of health consensus development project on criteria for clinical trials in chronic graft-versus-host disease: III: The 2014 biomarker working group report. *Biol. Blood Marrow Transplant.* 2015;21(5):780–792.
177. Paczesny S. Discovery and validation of graft-versus-host disease biomarkers. *Blood*. 2013;121(4):585–94.
178. Pidala J, Sarwal M, Roedder S, Lee SJ. Biologic markers of chronic GVHD. *Bone Marrow Transplant.* 2014;49(3):324–31.
179. Saliba RM, Sarantopoulos S, Kitko CL, et al. B-cell activating factor (BAFF) plasma level at the time of chronic GvHD diagnosis is a potential predictor of non-relapse mortality. *Bone Marrow Transplant.* 2017;(August 2016):1–6.
180. Thoburn C, Miura Y, Miura Y, et al. Association of Foxp3 regulatory gene expression with graft-versus-host disease. *Blood*. 2004;104(7):2187–2193.
181. Matsuoka K, Kim HT, Mcdonough S, et al. Altered regulatory T cell homeostasis in patients with CD4+ lymphopenia following allogeneic hematopoietic stem cell transplantation. *J Clin Invest*. 2010;120(5):1479–1493.
182. Li Q, Zhai Z, Xu X, et al. Decrease of CD4(+)CD25(+) regulatory T cells and TGF-beta at early immune reconstitution is associated to the onset and severity of graft-versus-host disease following allogeneic haematogenesis stem cell transplantation. *Leuk. Res.* 2010;34(9):1158–68.
183. Peccatori J, Forcina a, Clerici D, et al. Sirolimus-based graft-versus-host disease prophylaxis promotes the in vivo expansion of regulatory T cells and permits peripheral blood stem cell transplantation from haploidentical donors. *Leukemia*. 2014;29(April):1–10.
184. Bassim CW, Ambatipudi KS, Mays JW, et al. Quantitative salivary proteomic differences in oral chronic graft-versus-host disease. *J. Clin. Immunol.* 2012;32(6):1390–1399.

185. Liu X, Yue Z, Yu J, et al. Proteomic Characterization Reveals That MMP-3 Correlates With Bronchiolitis Obliterans Syndrome Following Allogeneic Hematopoietic Cell and Lung Transplantation. *Am. J. Transplant.* 2016;16(8):2342–2351.
186. Weissinger EM, Human C, Metzger J, et al. The proteome pattern cGvHD_MS14 allows early and accurate prediction of chronic GvHD after allogeneic stem cell transplantation. *Leukemia*. 2016;(November 2016):654–662.
187. Park T-J, Curran T. Crk and Crk-like play essential overlapping roles downstream of disabled-1 in the Reelin pathway. *J. Neurosci.* 2008;28(50):13551–62.
188. Huang Y, Clarke F, Karimi M, et al. CRK proteins selectively regulate T cell migration into inflamed tissues. *J. Clin. Invest.* 2015;125(3):1019–1032.
189. Licklider LJ, Thoreen CC, Peng J, Gygi SP. Automation of nanoscale microcapillary liquid chromatography-tandem mass spectrometry with a vented column. *Anal. Chem.* 2002;74(13):3076–3083.
190. Eng JK, Mccormack AL, Yates JR. An Approach to Correlate Tandem Mass Spectral Data of Peptides with Amino Acid Sequences in a Protein Database. *Am. Soc. Mass Spectrom.* 1994;5:976–989.
191. Käll L, Canterbury JD, Weston J, Noble WS, MacCoss MJ. Semi-supervised learning for peptide identification from shotgun proteomics datasets. *Nat. Methods*. 2007;4(11):923–925.
192. Vizcaíno J, Deutsch EEW, Wang R, et al. ProteomeXchange provides globally coordinated proteomics data submission and dissemination. *Nat Biotech*. 2014;32(3):223–226.
193. Yu J, Storer BE, Kushekhar K, et al. Biomarker panel for chronic graft-versus-host disease. *J. Clin. Oncol.* 2016;34(22):2583–2590.
194. Cato MH, Yau IW, Rickert RC. Magnetic-based purification of untouched mouse germinal center B cells for ex vivo manipulation and biochemical analysis. *Nat. Protoc.* 2011;6(7):953–60.
195. Kitko CL, Levine JE, Storer BE, et al. Plasma CXCL9 elevations correlate with chronic GVHD diagnosis. *Blood*. 2014;123(5):786–793.
196. Paczesny S, Krijanovski OI, Braun TM, et al. A biomarker panel for acute graft-versus-host disease. *Blood*. 2009;113(2):273–278.
197. Vander Lugt MT, Braun TM, Hanash S, et al. ST2 as a marker for risk of therapy-resistant graft-versus-host disease and death. *N. Engl. J. Med.* 2013;369(6):529–39.
198. Fiema B, Harris AC, Gomez A, et al. High throughput sequential ELISA for validation of biomarkers of acute graft-versus-host disease. *J. Vis. Exp.* 2012;(68):6–11.
199. Bell ES, Park M. Models of Crk Adaptor Proteins in Cancer. *Genes Cancer*. 2012;3(5–6):341–352.
200. Luo LY, Hahn WC. Oncogenic Signaling Adaptor Proteins. *J. Genet. Genomics*. 2015;42(10):521–529.
201. Mintz PJ, Cardó-Vila M, Ozawa MG, et al. An unrecognized extracellular function for an intracellular adapter protein released from the cytoplasm into the tumor microenvironment. *Proc. Natl. Acad. Sci. U. S. A.* 2009;106(7):2182–7.

202. Kagawa S, Matsuo A, Yagi Y, et al. The time-course analysis of gene expression during wound healing in mouse skin. *Leg. Med.* 2009;11(2):70–75.
203. Itatani Y, Kawada K, Fujishita T, et al. Loss of SMAD4 from colorectal cancer cells promotes CCL15 expression to recruit CCR1+ myeloid cells and facilitate liver metastasis. *Gastroenterology*. 2013;145(5):1064–1075.e11.
204. Kitamura T, Fujishita T, Loetscher P, et al. Inactivation of chemokine (C-C motif) receptor 1 (CCR1) suppresses colon cancer liver metastasis by blocking accumulation of immature myeloid cells in a mouse model. *Proc. Natl. Acad. Sci. U. S. A.* 2010;107(29):13063–8.
205. Yamamoto T, Kawada K, Itatani Y, et al. Loss of SMAD4 Promotes Lung Metastasis of Colorectal Cancer by Accumulation of CCR1+ Tumor-associated Neutrophils through CCL15-CCR1 Axis. *Clin. Cancer Res.* 2016;833–845.
206. Mohamadzadeh M, Poltorak a N, Bergstressor PR, Beutler B, Takashima A. Dendritic cells produce macrophage inflammatory protein-1 gamma, a new member of the CC chemokine family. *J. Immunol.* 1996;156(9):3102–6.
207. Zhao X, Sato A, Dela Cruz CS, et al. CCL9 is secreted by the follicle-associated epithelium and recruits dome region Peyer's patch CD11b+ dendritic cells. *J. Immunol.* 2003;171:2797–2803.
208. Hara T, Bacon KB, Cho LC, et al. Molecular cloning and functional characterization of a novel member of the C-C chemokine family. *J. Immunol.* 1995;155(11):5352–8.
209. Riesner K, Shi Y, Jacobi A, et al. Initiation of acute graft-versus-host disease by angiogenesis. *Blood*. 2017;129(14):2021–2032.
210. Hildebrandt GC, Olkiewicz KM, Choi S, et al. Donor T-cell production of RANTES significantly contributes to the development of idiopathic pneumonia syndrome after allogeneic stem cell transplantation. *Blood*. 2005;105(6):2249–2257.
211. Choi SW, Hildebrandt GC, Olkiewicz KM, et al. CCR1/CCL5 (RANTES) receptor-ligand interactions modulate allogeneic T-cell responses and graft-versus-host disease following stem-cell transplantation. *Blood*. 2007;110(9):3447–3455.
212. Coulin F, Power CA, Alouani S, et al. Characterisation of macrophage inflammatory protein-5/human CC cytokine-2, a member of the macrophage-inflammatory-protein family of chemokines. *Eur. J. Biochem.* 1997;248(2):507–515.
213. Berahovich RD, Miao Z, Wang Y, et al. Proteolytic Activation of Alternative CCR1 Ligands in Inflammation. *J. Immunol.* 2005;174(11):7341–7351.
214. Shimizu Y, Dobashi K. CC-Chemokine CCL15 Expression and Possible Implications for the Pathogenesis of IgE-Related Severe Asthma. *Mediators Inflamm.* 2012;2012:1–7.
215. Joubert P, Lajoie-Kadoch S, Wellemans V, et al. Expression and regulation of CCL15 by human airway smooth muscle cells. *Clin. Exp. Allergy*. 2012;42(1):85–94.

216. Leach HG, Chrobak I, Han R, Trojanowska M. Endothelial cells recruit macrophages and contribute to a fibrotic milieu in bleomycin lung injury. *Am. J. Respir. Cell Mol. Biol.* 2013;49(6):1093–1101.
217. Guedj K, Khallou-Laschet J, Clement M, et al. Inflammatory micro-environmental cues of human atherothrombotic arteries confer to vascular smooth muscle cells the capacity to trigger lymphoid neogenesis. *PLoS One*. 2014;9(12):1–17.
218. Kanellis J, Watanabe S, Li JH, et al. Uric acid stimulates monocyte chemoattractant protein-1 production in vascular smooth muscle cells via mitogen-activated protein kinase and cyclooxygenase-2. *Hypertension*. 2003;41(6):1287–1293.
219. Schenk BI, Petersen F, Flad H-D, Brandt E. Platelet-Derived Chemokines CXC Chemokine Ligand (CXCL)7, Connective Tissue-Activating Peptide III, and CXCL4 Differentially Affect and Cross-Regulate Neutrophil Adhesion and Transendothelial Migration. *J. Immunol.* 2002;169(5):2602–2610.
220. Islam SA, Chang DS, Colvin RA, et al. Mouse CCL8, a CCR8 agonist, promotes atopic dermatitis by recruiting IL-5+ T(H)2 cells. *Nat. Immunol.* 2011;12(2):167–77.
221. Liu D. The adaptor protein Crk in immune response. *Immunol. Cell Biol.* 2014;92(1):80–9.